Improving Deterministic Reserve Requirements for Security Constrained Unit Commitment and Scheduling Problems in Power Systems

by

Fengyu Wang

A Dissertation Presented in Partial Fulfillment
of the Requirements for the Degree
Doctor of Philosophy

Approved January 2015 by the
Graduate Supervisory Committee:

Kory W. Hedman, Chair
Muhong Zhang
Daniel J. Tylavsky
Raja Ayyanar

ARIZONA STATE UNIVERSITY

May 2015

ABSTRACT

Traditional deterministic reserve requirements rely on ad-hoc, rule of thumb methods to determine adequate reserve in order to ensure a reliable unit commitment. Since congestion and uncertainties exist in the system, both the quantity and the location of reserves are essential to ensure system reliability and market efficiency. The modeling of operating reserves in the existing deterministic reserve requirements acquire the operating reserves on a zonal basis and do not fully capture the impact of congestion. The purpose of a reserve zone is to ensure that operating reserves are spread across the network. Operating reserves are shared inside each reserve zone, but intra zonal congestion may block the deliverability of operating reserves within a zone. Thus, improving reserve policies such as reserve zones may improve the location and deliverability of reserve.

As more non-dispatchable renewable resources are integrated into the grid, it will become increasingly difficult to predict the transfer capabilities and the network congestion. At the same time, renewable resources require operators to acquire more operating reserves. With existing deterministic reserve requirements unable to ensure optimal reserve locations, the importance of reserve location and reserve deliverability will increase. While stochastic programming can be used to determine reserve by explicitly modelling uncertainties, there are still scalability as well as pricing issues. Therefore, new methods to improve existing deterministic reserve requirements are desired.

One key barrier of improving existing deterministic reserve requirements is its potential market impacts. A metric, quality of service, is proposed in this thesis to evaluate the price signal and market impacts of proposed hourly reserve zones.

Three main goals of this thesis are: 1) to develop a theoretical and mathematical model to better locate reserve while maintaining the deterministic unit commitment and economic dispatch structure, especially with the consideration of renewables, 2) to develop a market settlement scheme of proposed dynamic reserve policies such that the market efficiency is improved, 3) to evaluate the market impacts and price signal of the proposed dynamic reserve policies.

ACKNOWLEDGEMENTS

First and foremost, my gratitude goes to my advisor, Dr. Kory W. Hedman, from whom I was firstly educated in this professional field during my Ph.D. study at Arizona State University. Dr. Hedman is an outstanding mentor, who not only taught me the professional knowledge but also transmitted the way of dealing with things and ethics to me. During my Ph.D. study, Dr. Hedman also supported me to attend conference meetings, which are very beneficial to my Ph.D. research.

Second, I would like to thank Dr. Muhong Zhang, Dr. Daniel Tylavsky, and Dr. Raja Ayyanar to be the members of my committee for their time and insightful comments.

I would also like to thank my colleagues and friends at Arizona State University, especially to Dr. Hedman's group, who continuously support me and give me invaluable suggestions.

I also appreciate Midcontinent Independent System Operator (MISO) and my mentor at MISO, Dr. Yonghong Chen, for providing me the internship. Dr. Chen also provided me some valuable guidance on my research and introduced me to the real-world system.

I would like to thank the Power Systems Engineering Research Center (PSERC) and Department of Energy (DOE) for funding this research. Without them, this thesis is impossible.

I also enjoyed the life at Arizona State University with my friends, especially to Xianjun Zhang, Di Shi, and Qing Zhang. You brought me a lot of joy.

Last but not least, I would also like to express my love to my parents, Guanglin Wang and Xuzhi Liu, and my fiancé, Chao Fan, who encourage and support me all the time. I will be always with you.

TABLE OF CONTENTS

Page

CHAPTER Page

CHAPTER Page

Page

LIST OF TABLES

Table Page

Table Page

LIST OF FIGURES

Figure Page

Figure Page

Figure Page

LIST OF PUBLICATIONS

1. F. Wang, and K. W. Hedman, “A Statistical Study of Dynamic Reserve Policies with Consideration of Renewables,” IEEE Transactions on Sustainable Energy, Under Review.
2. F. Wang, K. W. Hedman, and Y. Chen, “A Nodal Reserve Formulation for Systems with Renewable Resources,” Special Issue of IEEE Transactions on Sustainable Energy, Under Review.
3. J. Lyon, F. Wang, K. W. Hedman, and M. Zhang, “Market Implications and Pricing of Dynamic Reserve Policies for Systems with Renewables,” IEEE Transactions on Power Systems, Accepted for Publication, 2014.
4. F. Wang, K. W. Hedman, “Dynamic Reserve Zone for Day-Ahead Unit Commitment with Renewable Energy,” IEEE Transactions on Power System, vol. 30, no. 2, pp. 612-620, Mar. 2015.
5. F. Wang, K. W. Hedman, “Reserve Zone Determination Based on Statistical Clustering Method,” in Proceedings of North American Power Symposium, 2012.

NOMENCLATURE

Indices and Sets

c	Contingency Scenario
G	Set of Conventional Generators, $g, \gamma \in G$
$G(n)$	Set of Conventional Generators at Node n
$G(z)$	Set of Conventional Generators in the Reserve Zone Z
K	Set of Transmission Lines; $k \in K$
$K^+(n)$	Set of Transmission Lines with Node *n* as the "to" Node
$K^-(n)$	Set of Transmission Lines with Node *n* as the "from" Node
N	Set of Buses (Nodes), $n, m \in N$
$N(z)$	Set of Nodes in the Reserve Zone n
R	Reference Node
T	Set of Time Periods, $t \in T$
$VOLL$	Value of Lost Load
W	Set of Wind Generators, $w \in W$
$W(z)$	Set of Wind Generators in the Reserve Zone Z
$W(n)$	Set of Wind Generators at Node n

Z	Set of Reserve Zones, $z \in Z$
Parameters	
B_k	Susceptance of Transmission Line k
C_g	Fuel Cost of Generator g
C_g^{NL}	No Load Cost of Generator g
C_g^{SD}	Shut-Down Cost of Generator g
C_g^{SU}	Start-Up Cost of Generator g
C_g^{REG}	Resource g Available Offer Price for Regulation Reserve, in \$/MWh
C_g^{SPIN}	Resource g Available Offer Price for Spinning Reserve, in \$/MWh
C_g^{SUPP}	Resource g Available Offer Price for Supplemental Reserve, in \$/MWh
D_{nt}	System Demand at Node n in Period t
D_n^{max}	Peak Demand at Node n
D^{max}	System-Wide Peak Demand
DF_z^{SPIN}	Spinning Reserve Deployment Factor under the Largest Contingency Event in Zone z.

DF_z^{SUPP}	Supplemental Reserve Deployment Factor under the Largest Contingency Event in Zone z.
DT_g	Minimum Down-Time of Generator g, *hour*
$E_{z,t}$	Largest Contingency Event Size in Zone z in Period t
$EENS_{ct}$	Expected Energy Not Served During Event c in Period t
F_k^{max}	Normal Line Rating of Transmission Line k
$\bar{F}_k^{max}$	Contingency Line Rating of Transmission Line k
I_{nct}	Net Injection at Node n After Contingency c but Prior to Re-Dispatch in Period t
$N_{g,c}$	Generator's Contingency Status Indicator, 1 If $g \neq c$, *0* If $g = c$
P_g^{max}	Maximum Production Level of Generator g
P_g^{min}	Minimum Production Level of Generator g
P_{wt}	Forecasted Output of Wind Unit w in Period t
$PTDF_{k,n}^R$	The Power Transfer Distribution Factor of Transmission Line k from Bus n to Reference Bus R
$PTDF_{l,n,c}^R$	The Power Transfer Distribution Factor of Zonal Link l from Bus n to Reference Bus R During Contingency c

$PTDF_{k,LC}^{R}$	The Power Transfer Distribution Factor of Transmission Line k from Load Center to Reference Bus R
QOS_{gct}	Proportion of Reserve from Generator g Cleared in the Day-Ahead Market That Is Deliverable in Real- Time for Contingency c in Period t
R_g^{10}	Ten-Minutes Ramp-Rate Generator g
R_g^{HR}	Hourly Ramp-Rate Generator g in Period t
R_{gt}^{+}	Available Up Reserve from Generator g in Period t
R_{gt}^{-}	Available Down Reserve From Generator g in Period t
$\overline{R}_{gt}^{REG}$	The Regulation Reserve Capacity of Generator g in Period t
$\overline{R}_{gt}^{SPIN}$	The Spinning Reserve Capacity of Generator g in Period t
$\overline{R}_{gt}^{SUPP}$	The Supplemental Reserve Capacity of Generator g in Period t
$R_{MKT,t}^{REG}$	Market-Wide Requirement for Regulation Reserve in Period t
$R_{MKT,t}^{SPIN}$	Market-Wide Requirement for Spinning Reserve in Period t
$R_{MKT,t}^{SUPP}$	Market-Wide Requirement for Supplemental Reserve in Period t
$R_{z,t}^{REG}$	Base Zonal Requirement of Zone z for Regulation Reserve from Offline Study

$R_{z,t}^{SPIN}$	Base Zonal Requirement of Zone z for Spinning Reserve from Offline Study
$R_{z,t}^{SUPP}$	Base Zonal Requirement of Zone z for Supplemental Reserve from Offline Study
$\bar{U}_{gt}$	Determined Commitment Status of Generation g in Period t
UT_g	Minimum Up-Time of Generator g, *hour*
π_k	Weighted Factor of PTDF Differences for Transmission Line k
τ	Response Time Available for the Spinning Reserves to Ramp-Up Their Output, *hour*
η_z	Reserve Level at Zone z (Percentage of Load)
Γ_{gct}	Reserve Disqualification Indicator for Generator g ($\Gamma_{gt}^{c} = 0$ Means g is Disqualified for Contingency c) in Period t
Δ_{gct}	Reserve from Generator g Cleared for Contingency c in Period t
ρ_c	Probability of Contingency c
ϕ_{gct}	Reserve Payment to Generator g in Period t

Decision Variables

i_{nct}	Net Injection at Node n After Contingency c Following Re-dispatch

ls_{nct}	Load Shedding Due to Contingency *c* at Node *n* in Period *t*
p_{gt}	Power Produced by Generator g in Period *t*
p_{gct}	Power Produced by Generator g in Period *t* During Contingency *c*, MW
f_{kt}	Power Flow Variable of Transmission Line *k* in Period *t*
f_{lct}	Power Flow of Zonal Link *l* in Period *t* During Contingency *c*
r_{gt}^{REG}	Regulation Reserve Provided by Generator g in Period *t*
r_{zt}^{REG}	Solved Zone *z* Requirement for Regulation Reserve in Period *t*
r_{zt}^{SPIN}	Solved Zone *z* Requirement for Spinning Reserve in Period *t*
r_{zt}^{SUPP}	Solved Zone *z* Requirement for Supplemental Reserve in Period *t*
r_{gt}^{SPIN}	Spinning Reserve Provided by Generator g in Period *t*
r_{gt}^{SUPP}	Supplemental Reserve Provided by Generator g in Period *t*
r_{gct}	Output Change by Generator g in Period *t* During Contingency *c*
$\tilde{r}_{zct}^{SPIN}$	Spinning Reserve Designated as Deliverable from Zone *z* to Contingency *c* in Period *t*
s_{gct}	Cleared Reserve from Generator g That Cannot Be Dispatched for Contingency *c*

S_{zjt}	Reserve Import Capability from Zone z to Zone j
sd_{gt}	Shut-Down Variable of Generator g in Period t
su_{gt}	Start-Up Variable of Generator g in Period t
u_{gt}	Unit Commitment Variable of Generator g in Period t,(1: Committed, 0: Decommitted)
x^{+}_{gct}	Dispatched Up Reserve from Generator g for Contingency c in Period t
x^{-}_{gct}	Dispatched Down Reserve from Generator g for Contingency c in Period t
θ_{nt}	Bus Angle Variable at Node n in Period t

Shadow Prices

λ_t	Shadow Price of Power Balance Equation.
γ_t^{MRR}	Shadow Prices of the Market-Wide Regulation Reserve Requirement Constraints in Period t
γ_t^{MRS}	Shadow Prices of the Market-Wide Regulation Plus Spinning Reserve Requirement Constraints in Period t
γ_t^{MOR}	Shadow Prices of the Market-Wide Operating Reserve Requirement Constraints in Period t

γ_t^{MRR}	Shadow Prices of the Market-Wide Regulation Reserve Requirement Constraints in Period *t*
γ_{zt}^{ZRR}	Shadow Prices of the Minimum Zonal Regulation Reserve Requirement Constraint *z* in Period *t*
γ_{zt}^{ZRS}	Shadow Prices of the Minimum Zonal Regulation Plus Spinning Reserve Requirement Constraint *z* in Period *t*
γ_{zt}^{ZOR}	Shadow Prices of the Minimum Zonal Operating Reserve Requirement Constraint *z* in Period *t*
$\gamma 0_{zt}^{ZRR}$	Shadow Prices of the Base Zonal Regulation Reserve Requirement Constraint *z* in Period *t*
$\gamma 0_{zt}^{ZRS}$	Shadow Prices of the Base Zonal Regulation Plus Spinning Reserve Requirement Constraint *z* in Period *t*
$\gamma 0_{zt}^{ZOR}$	Shadow Prices of the Base Zonal Operating Reserve Requirement Constraint *z* in Period *t*
μ_{kt}	Shadow Prices of Transmission Constraint *k* in Period *t*
μ_{kt}^{REGUP}	Shadow Prices of Transmission Constraint *k* under Post Regulation Reserve up Deployment in Period *t*
μ_{kt}^{REGDN}	Shadow Prices of Transmission Constraint *k* under Post Regulation Reserve Down Deployment in Period *t*

δ_{kt}^{REGUP} Shadow Prices of Transmission Constraint k Nodal Post Regulation Reserve Up Deployment in Period *t*

δ_{kt}^{REGDN} Shadow Prices of Transmission Constraint k Nodal Post Regulation Reserve Down Deployment in Period *t*

$\mu_{k,z,t}^{CR}$ Shadow Prices of Post-Zonal Contingency Event for Transmission Line *k* at Reserve Zone *z* in Period *t*

Market Clearing Price

LMP_{nt} Locational Marginal Price at Node *n* in Period *t*

$MCP_{z,t}^{REG}$ Zonal MCP for Regulation Reserve of Zone *z* in Period *t*

$MCP_{z,t}^{SPIN}$ Zonal MCP for Spinning Reserve of Zone *z* in Period *t*

$MCP_{z,t}^{SUPP}$ Zonal MCP for Supplemental Reserve of Zone *z* in Period *t*

1. INTRODUCTION

1.1 Background

Reliability standards are necessary in order to guarantee a continuous and high quality supply of energy. Uncertainties such as load, renewable, and contingencies, exist in the power system. Reserves are used as backup capacities to protect against these uncertainties. For instance, regulation reserve is used to follow load variations.

The North American Electric Reliability Corporation (NERC), which is the designated Electric Reliability Organization (ERO) by the Federal Energy Regulatory Commission (FERC), establishes and enforces the N-1 reliability standard, which requires the system to be able to survive any single generator or transmission contingency. Adequate operating reserves are essential to ensure reliable system operations when contingencies happen. Operating reserves ensure that there is sufficient generation capacity available in case there are load forecast errors, potential generator outages, or transmission outages, [1]. The definition of operating reserves may vary from the consideration of only spinning and non-spinning reserve to the inclusion of interruptible loads, voltage and frequency support, regulation, replacement reserve, [1]. For this research, the discussion of operating reserves will refer to regulation reserve, spinning reserve, and non-spinning reserve.

Regulation reserve is used to compensate the variability and uncertainty of the system load within the shortest scheduling interval. Spinning reserve is defined as the reserve capacity offered by generators that are already spinning, synchronized with the grid. Many ISOs specify a ten-minute spinning reserve requirement where the generator must be able to immediately change its output once called upon by the system operator and must be able to reach the desired level specified by the system operator within ten minutes. Non-

spinning reserve comes from generators that are offline but can respond quickly once called upon. Similar to the ten-minute spinning reserve requirement, many operators specify a ten-minute non-spinning reserve requirement where the offline generator must be able to reach the required output level within ten minutes; however, they are not required to inject their output immediately unlike spinning reserve since these generators are not currently online and synchronized with the grid.

Reserve requirements are typically based on a predefined set of rules. The California Independent System Operator (CAISO) states its requirement for its operating reserve (OR) in [2]. The operating reserve requirement in CAISO is the maximum of OR1 and OR2, then plus 100% of the non-firm (interruptible) imports. OR1 is calculated for each reserve zone and is equal to 5% of the demand met by hydro resources plus 7% of the demand from non-hydro resources. OR2 is based on the worst single contingency and it is calculated system wide. The worst contingency is based on the largest committed generator or the largest net tie-line import. The Western Electricity Coordinating Council (WECC) establishes its guidelines for contingency reserve, i.e., spinning and non-spinning reserve, in [3]. These rules vary from what is posted by CAISO, which raises the question as to which set of rules is more reliable and which set is more efficient. With more stringent reserve requirements, reliability should improve but this improvement in reliability may not be necessary if it goes beyond N-1, which may then result in unnecessary losses in economic efficiency. So there is a common tradeoff between reliability and economic efficiency. However, an even more pressing question is how they generate these prescribed rules and whether these rules can be improved.

Historically, ad-hoc methods or rule-of-thumb methods have been used to determine reserve requirements. The most basic rule-of-thumb is that the amount of reserves must be at least as great as the single worst contingency, as can be identified by the CAISO operating reserve requirement rule for OR2 above. It is often assumed that if a system acquires reserve equal to single largest contingency, then it has satisfied N-1 reliability. This is not always true, since most grids are congested or have voltage limitations. Simply having reserve equal to the single largest contingency may not suffice.

Historical information on system operating conditions may also be used to estimate the level of reserves required in order to avoid involuntary load shedding. The problem with the use of historical information is that wide-spread load shedding is not a common event and it is very difficult to determine the actual optimal amount of reserves to acquire based on historical information when the grid and resources are ever changing; there is not sufficient historical information to validate a choice in reserves. Moreover, historical information is inadequate to capture future grid conditions especially when the available resources are transitioning from primarily fossil-fuel based controllable generators to variable, uncertain renewable resources.

Such past ad-hoc or rule-of-thumb methods are archaic and will no longer suffice. First, there is a need for more systematic ways to determine the reserve levels and reserve zones. Many papers have proposed the use of probabilistic methods to determine reserve requirements by stochastic unit commitment; some of these papers are identified in the literature review section. Second, zones today come from ad-hoc methods. Furthermore, reserve zones are static and do not change with the market and operational conditions of the grid. Since the system operating condition is changing all the time, it is highly unlikely

that the optimal reserve zones would be static. Third, with the increasing penetration of variable generation, e.g., wind and solar, reserve requirements must be updated to accommodate for the intermittency and uncertainties of variable renewable generation. As a result, there are opportunities to greatly improve existing methods of determining reserve levels and reserve zones.

The rest of this chapter includes a discussion on spinning reserve requirements and different methods to determine the reserve requirements.

1.2 Reserve Procurement Methods

1.2.1 Deterministic Reserve Requirements

The most widely used deterministic criterion is to deploy the amount of spinning reserve greater or equal to the largest online generator and, in the unit commitment (UC) or economic dispatch (ED) formulation, it can be modeled by the following constraint [4]. Note that reserve quantity exceeding the largest contingency may not guarantee N-1 reliability due to the network congestion.

$$u_{gt}P_g^{max} - \sum_{g=1}^{|G|}(r_{gt}) \leq 0 \qquad (1—1)$$

Constraint (1—1) can be replaced by

$$SR_t - \sum_{g=1}^{|G|}(r_{gt}) \leq 0 \qquad (1—2)$$

where

$$SR_t = \max_g(u_{gt}p_{gt}) \qquad (1—3)$$

Another deterministic criterion is to set spinning reserve equal to a fraction of peak demand, i.e., $\sum_{g\in G(z)}(r_{gt}) \geq \eta_z \sum_{n\in N(z))} D_{nt}$. The Spanish system complies with this

deterministic criterion. Additional deterministic criterions are listed in the Table 1.1 [5]-[8].

Table 1.1 Operating Reserve Requirements in Different Countries and ISOs

Country or ISO	Criterion of spinning reserve
Australia and New Zealand	$\max_g u_{gt}p_{gt}$
BC Hydro	$\max_g u_{gt}p_{gt}$
CAISO	50% ×max(5% ×Hydro Generation+7% ×Non-Hydro Generation+ Interruptible Imports, Single Largest Contingency)
UCTE	$\sqrt{10 \times D^{max} - 150^2} - 150$
Spain	Between $3 \times (D^{max})^{1/2}$ and $6 \times (D^{max})^{1/2}$
Southern PJM	$\max_g u_{gt}p_{gt}$
Western PJM	1.5%× D^{max}
PJM (Other Zones)	1.1% ×Peak Load + probabilistic calculation based on typical day and hours
Yukon Electrical	$\max_g u_{gt}p_{gt}$ + 10% × D^{max}
NYCA	50% ×$\max_g u_{gt}p_{gt}$
Eastern New York	25% ×$\max_g u_{gt}p_{gt}$
Long Land	5% ×$\max_g u_{gt}p_{gt}$

In spite that different Independent System Operators (ISOs) or utilities apply different reserve requirements criterions, as shown in Figure 1.1, there is a tradeoff between the

reliability and efficiency. The EENS [1] is used to measure the reliability cost, which can be mathematically expressed as the following,

$$EENS_{ct} = \rho_c \sum_{n=1}^{|N|} ls_{nct}, t \in T, c \in C \quad (1—4)$$

where ρ_c represents the probability of contingency (or event) c occurring. The probability of contingency c can be estimated based on historical outage rates, which is generally assumed to be constant.

Insufficient reserve quantity may lower the system reliability, thereby increase the expected energy not served (EENS) cost. Excessive reserve quantity may incur more operating cost.

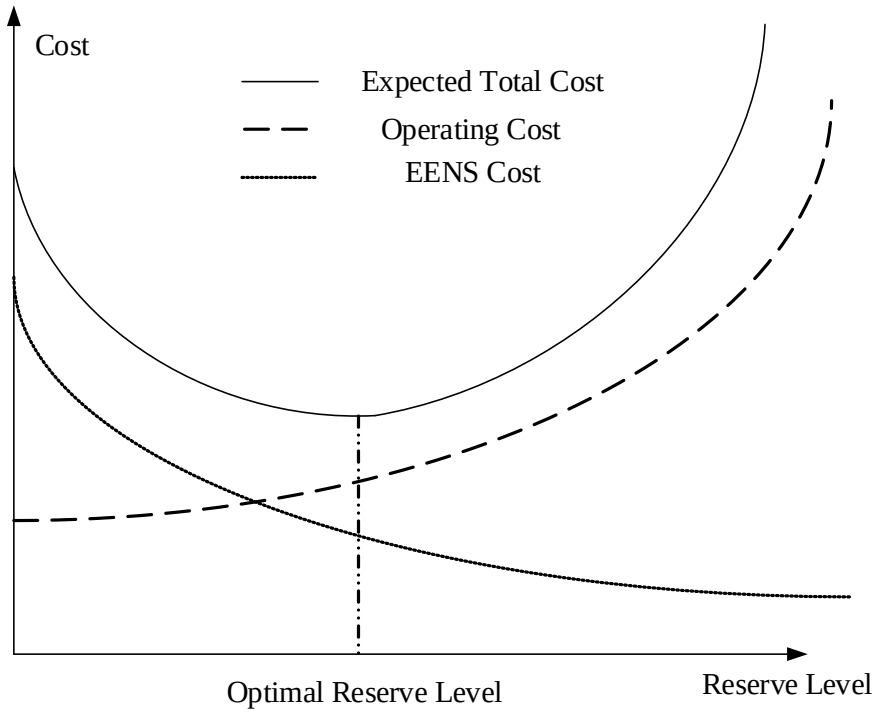

Figure 1.1 The Relationship Between Reserve Level and Total Cost

Due to the continuous change of system operating conditions and uncertainties, it is very complex to optimize the reserve level such that minimize the expected total cost (operating cost plus EENS cost) for each period. To improve system operating efficiency,

deterministic reserve requirements can also be determined through offline statistical studies with consideration of generators outage rates and system operating conditions.

1.2.2 Stochastic Programming to Procure Reserve

Deterministic reserve requirements are approximate methods to acquire reliable backup capacities and they "blindly" choose the location of reserve without taking into consideration operational limitations, such as congestion and voltage limitations. In other words, there is no direct scenario-based determination of reserve using deterministic reserve. As a result, traditional reserve requirements do not guarantee N-1 reliability or the reserve requirement rules are likely to be overly conservative such that market efficiency is compromised.

Due to the drawbacks of deterministic criterions, stochastic programming, which models uncertainties, has been proposed to overcome these challenges. By explicitly modeling credible contingencies in UC, there are three ways to balance the system efficiency and reliability. The first way is that no load shedding and transmission violation is allowed and all the uncertainties scenarios must be feasible. This way follows the N-1 reliability.

Second one is to set an upper bound of the EENS through all the periods of the optimization process [9] as shown in (1—5),

$$EENS_{ct} \leq EENS^{max}, t \in T \qquad (1—5)$$

The ceiling of EENS is difficult to come up with and an improper ceiling of EENS may result in infeasibilities, which implies that there are not sufficient reserve capacities in the system to meet the EENS constraint or the units are not very reliable.

Third approach is to penalize the EENS by placing it in the objective with an associated cost. The penalization of EENS is usually the value of lost load (*VOLL*). There are different ways of defining *VOLL*; recently, operators have quantified the cost of new entry (CONE) as a mechanism to place a lower bound on *VOLL*; CONE refers to the cost to build a new power plant. The expected cost of load shedding during contingency c is $EENS_{ct} \times VOLL$. In order to maximize social welfare, there should be a balance between ensuring a more reliable system versus the associated costs.

However, it is not practical to endogenously model all of the contingencies in the UC formulation because the number of constraints and variables increases dramatically. Since UC is a mixed integer linear programming (MILP), the solution time may increase exponentially with the number of endogenously modeled contingencies. As a result, a subset of contingencies is often modeled. Therefore, scenarios selection techniques of significant contingencies are essential to this penalization probabilistic method.

In [10], P. A. Ruiz *et al.* realized the significance of scenarios selection and the relationship between the reserve requirements and scenarios. Only the loss of the three largest units are considered in [10] with the philosophy that it is better to select a subset of significant contingencies rather than none at all. Unfortunately, [10] didn't provide a theoretical scenario selection technique.

Reference [8] pre-selected a set of random generators and line contingencies with probabilistic outage rates based on historical data and the model incorporates involuntary load shedding. With contingencies endogenously modeled in the UC problem, spinning reserve requirements are determined endogenously in the UC formulation. However, since the MIP cannot be solved in polynomial time, the complexity of the problem increases

exponentially with additional endogenously modeled contingencies and, thus, modeling a large set of the contingencies in the UC is unsolvable to date. If only a subset of contingencies is considered, there may not be sufficient available capacity to prevent expensive involuntary load shedding since many contingencies are not included.

As a result, there are still some limitations of stochastic programming to determine reserve, and they are not sophisticated enough to today's real world system. A gradual change from deterministic reserve requirements to stochastic or a hybrid of stochastic programming and deterministic reserve requirements may be an alternative way that is more applicable and acceptable.

1.3 Outline

Chapter 2: Literature Review

In this chapter, relevant literature will be reviewed. State of the art reserve policies will be investigated such as deterministic reserve requirements and stochastic programming. Comparisons between different reserve policies will be presented.

Chapter 3: Proposed Reserve Zones Determination Method

This chapter presents the proposed reserve zone determination method, which is based on the Power Transfer Distribution Factor Difference (PTDFD). The reserve zone is then partitioned by the K-means clustering algorithm. A different centrality measurement, electrical distance, is also evaluated. Furthermore, different clustering algorithms are also compared with the K-means clustering algorithm. Different results from the IEEE RTS96 system and IEEE 118-bus system are presented to show the effectiveness of proposed reserve zone partitioning method.

Chapter 4: Deterministic Unit Commitment

In this chapter, the mathematical formulation of a deterministic unit commitment problem is presented. The IEEE RTS96 system and IEEE 118-bus system are tested with deterministic unit commitment using proposed reserve zone partition method.

Chapter 5: Reserve Zone Determination with High Penetration of Wind

This chapter proposes a daily reserve zone determination procedure, which is able to reflect system operating conditions by utilizing probabilistic power flows. The proposed method is validated by testing it on a modified IEEE 118-bus system for multiple days; the proposed method is compared against existing reserve zone partitioning procedures. While the proposed reserve zone determination method is a heuristic, it is shown to be effective and it is a computationally tractable method. The proposed method can be used on its own and can be used along with stochastic programming techniques that implicitly determine reserves.

Chapter 6: Hourly Reserve Zone Determination and Its Market Implications

This chapter examines the market implications associated to implementing dynamic reserve zones, which change by the hour, in day-ahead SCUC for systems with intermittent renewable resources. Two case studies are performed in this chapter. For case study I, the proposed compensation mechanisms are more aligned with the services generators provide as dynamic zones are better equipped to identify a generator's ability to respond to random disturbances and events and the market impacts of the proposed hourly reserve zone determination method are studied. For case study II, the proposed hourly reserve zone determination method is examined with MISO's SCUC formulation with consideration MISO's manual reserve disqualifications and the market results confidence interval is also provided to improve the credibility of the test results.

Chapter 7: A Nodal Regulation Reserve Pricing Model

To improve the reserve deliverability, independent system operators (ISOs) acquire reserve on a zonal basis to ensure that reserve is at least zonally distributed across the grid. However, zonal reserve requirements cannot guarantee the reserve is deliverable on a nodal basis. In this chapter, a nodal regulation reserve pricing model is proposed with consideration of nodal post regulation reserve deployment constraints to balance the regulation reserve on a nodal basis.

Chapter 8: Conclusion

This chapter summarizes the main achievements of this thesis.

Chapter 9: Future Work

In this chapter, future research is suggested.

2. LITERATURE REVIEW

While existing procedures to determine reserve requirements may be archaic, the modeling of reserve requirements is not new and has been an interesting topic in the research community for many years. Even still, there is a growing need for more attention on the modeling of reserve requirements. Back in 1963, the authors from [11] developed a probabilistic method to determine reserve requirements. The authors evaluated the forced outage probabilities from historical data and defined a uniform level of risk. The reserve requirements can be adjusted to meet the required uniform level of risk. However, the challenge with this approach is getting the correct risk level; furthermore, the risk level is approximated and vague, which may incur extra cost.

In [12], the authors combined the determination of reserve requirements and unit commitment together and evaluated the system reliability based on various predefined risk levels. A two-stage UC model without optimal power flow (OPF) is solved based on Lagrangian Relaxation (LR). Each system risk level is evaluated in the first stage and the reserve requirements are adjusted in the second stage. The system risk level with the least expected total cost will be selected and the reserve requirement corresponding to the system risk is optimal.

Reference [9] developed a UC problem considering contingency states, which are preselected, and also incorporated an OPF. Instead of enforcing spinning reserve requirements, spinning reserve is determined inherently in the UC problem. The objective function is the expected total costs with a penalty for involuntary load shedding. Appropriate spinning reserve may reduce the chances of involuntary load shedding and, thus, reduce the total cost; however, excessive spinning reserve may increase operating

cost substantially. The advantage of this approach is that spinning reserve is endogenously determined, which ensures that there is no power flow violation. The drawback of this approach is that a large number of preselected contingencies may be too computationally burdensome whereas reducing the number of preselected contingences may provide an inaccurate solution. How to best determine a set of preselected contingencies is still a challenging problem today.

Ortega-Vazquez [13] discussed the tradeoff between the spinning reserve level and the expected outage costs. In [13], an approximate, linearized curve of expected outage cost with respect to spinning reserve is drawn and the optimal spinning reserve corresponding to the minimum total cost can be revealed in this curve. However, the drawback is that this UC formulation does not include an OPF. As a result, the location of spinning reserve may not be efficient; for instance, a contingency may cause expensive involuntary load shedding even though there is ample committed capacity in the power system if this available reserve cannot reach the desired locations due to power flow limitations, i.e., congestion.

A two-stage stochastic programming approach is applied to manage the uncertainty in the power system in [14]. The commitment decision is made in the first stage and the dispatch decision is made in the second stage. The proposed approach in [14] reduces the uncertainty of the system by adding the number of scenarios in the unit commitment formulation and reserve requirements, so more scenarios can reduce the reserve requirements; however, the drawback is a longer solution time.

Reference [15] proposed a long term stochastic programming unit commitment model with an upper bound on the loss of load expectation (LOLE). The total cost including the operating cost and expected load shedding cost depends on some uncertain factors such as

fuel cost, emission cost, and outages. Monte Carlo simulations are employed to simulate this stochastic UC model and calculate the expected load shedding cost. The spinning reserve is expected to meet the upper bounds of LOLE. However, the solutions may not be economically optimal if the LOLE bound is either too high, which would allow too much load shedding, or too low, which would cause operational costs to be higher than necessary.

Due to national goals to increase the penetration level of variable renewable resources, the importance of developing reliable and efficient reserve requirements escalates as intermittent resources add even more uncertainties to power system operations. Based on the weighted scenarios in [16], a two-stage stochastic UC model is used to obtain spinning reserve from both fast and slow generators in the first state and reserve from fast generators in the second stage. The authors develop a novel scenario reduction technique so that they are able to properly model the characteristics of the wind with limited scenarios in order to reduce the computational burden.

Reference [17] states that optimizing the energy and ancillary services (e.g., reserve) simultaneously is better than optimizing these services sequentially since co-optimization will result in a higher level of social welfare. Based on optimization theory, co-optimization will lead to a global optimal solution, whereas optimizing sequentially may lead to a suboptimal solution.

Table 2.1 provides an overview of the research literature on the topic of reserve requirements and stochastic unit commitment.

Table 2.1 Literature Review of Reserve Policies

Authors	Title	Year	Journal	OPF	Load shedding allowed[1]	Scenarios	Fast generators	Contingency	
								Generator[2]	Line
L. T. Anstine *et al.*	Application of probability methods to the determination of spinning reserve requirements for the Pennsylvania-New Jersey-Maryland interconnection [11]	1963	IEEE Trans on Power Systems	N	N	Y	N	N	N
H. B. Gooi *et al.*	Optimal scheduling of spinning reserve [12]	1999	IEEE Trans on Power Systems	N	N	N	N	N	N
F. Bouffard *et. al.*	Market-clearing with stochastic security—Part I: Formulation [9]	2005	IEEE Trans on Power Systems	Y	Y	Y	Y	Y	Y
M. A. Ortega-Vazquez *et. al.*	Optimizing the Spinning Reserve Requirements Using A Cost/Benefit Analysis [13]	2007	IEEE Trans on Power Systems	N	Y	N	N	N	N

Authors	Title	Year	Journal	OPF	Load shedding allowed[1]	Scenarios	Fast generators	Contingency	
								Generator[2]	Line
L. Wu *et. al.*	Stochastic security-constrained UC [16]	2007	IEEE Trans on Power Systems	Y	N	Y	N	Y	Y
L. Wu *et. al.*	Cost of reliability analysis based on stochastic UC [14]	2008	IEEE Trans on Power Systems	Y	Y	Y	N	Y	Y
T. Zheng *et. al.*	Contingency-based zonal reserve modeling and pricing in a co-optimized energy and reserve market [18]	2008	IEEE Trans on Power Systems	Y	N	Y	N	Y	N
P. Ruiz *et. al.*	Uncertainty management in the UC problem [10]	2009	IEEE Trans on Power Systems	N	Y	Y	Y	Y	N
A. Papavasiliou *et. al.*	Reserve requirements for wind power integration: a scenario-based stochastic programming framework [15]	2011	IEEE Trans on Power Systems	N	N	Y	Y	N	N

Authors	Title	Year	Journal	OPF	Load shedding allowed[1]	Scenarios	Fast generators	Contingency	
								Generator[2]	Line
A. Papavasiliou *et. al.*	Multi-area stochastic UC for high wind penetration in a transmission constrained network [19]	2011	Operations Research	Y	N	Y	Y	Y	Y

Y = Yes

N = No

[1] Load shedding / disruption allowed based on VOLL. Some papers allow load shedding if no feasible solution can be found.

[2] In general, scenario based stochastic models should be able to model continuous and discrete generation (negative load) disruptions. Some papers choose to only evaluate one or the other.

3. PROPOSED RESERVE ZONE DETERMINATION METHOD

3.1 Introduction

Nowadays, reserve zones are primarily divided by asset ownership or geographic locations and there is no systematic way to partition reserve zones; thus, it is highly unlikely that reserve zones today are economically optimal. With poorly designed reserve zones, involuntary load shedding may happen even though there is enough committed reserve capacity if the reserves cannot be delivered due to network congestion. To reduce the expected cost of involuntary load shedding, a theoretical and mathematical way of partitioning reserve zones is of crucial importance. Efficiency and reliability of power system operations will be improved with well-designed reserve zones.

Usually, existing reserve zones are treated as static; however, the operational conditions of power systems vary by hours, days, seasons, and years. As a result, it is not efficient to have static reserve zones when operating conditions constantly vary. Moreover, under the trend of more renewable energy in the grid, the location of reserves and their associated deliverability will increase in importance. New technologies to determine reserve requirements are needed to guarantee system reliability and market efficiency. While stochastic programming produces an optimal solution (with respect to the modeled uncertainties), the concerns are as below:

1) Limitation of stochastic information. Modelling all the continuous and discrete uncertainties in the UC formulation is impossible today and usually selected "scenario trees" are modelled. Including more branches in the optimization formulation will improve the representation of the uncertainties but this also

increases the computational time. The modelled uncertainties in the day-ahead may be quite different from true scenarios.

2) Scalability issue. Even though some alternative formulations or decomposition approaches are investigated [15], the computational times for most stochastic UC problems increases significantly (an order of 10 or more) compared to a deterministic UC problem, depending on the formulation structure, problem size, and the number of scenarios modelled.
3) Pricing issues. There is an ongoing debate as to how to design a market where the internal mathematical program is a stochastic program. Therefore, stochastic UC is being considered for problems such as residual unit commitments but there is still hesitation due to the market complexities it adds to existing markets.

An alternative way to improve reserve deliverability is by improving reserve zones. Thus, the development of a systematic way to determine reserve zones is one promising way to meet these future challenges.

Chapter 3 will propose a method of partitioning reserve zones using statistical clustering techniques and Chapter 3 also demonstrates a comparison of different clustering methods. Moreover, two different clustering centrality measurements, PTDF difference and electrical distance, will be analyzed.

3.2 Power Transfer Distribution Factor Difference and Electrical Distance

3.2.1 PTDF Difference

In the DC model, power transfer distribution factor, $PTDF_{k,i}^{R}$, is the flow on transmission line *k* when injecting one unit of active power at bus *i* and withdrawing the

unit of active power from reference bus *R*. Kumar *et al.* [20] used real and reactive transmission congestion distribution factors (TCDFs) based on an AC model to identify the congestion zones, which is a cluster of buses, selected based on the sensitivity of flow in the congested line. Buses with similar TCDFs to the congested lines are divided into the same congestion zones. To improve the market efficiency, the dispatch strategies of generators and capacitors are discussed with respect to various market models, including a pool model, a bilateral contract model, and a multilateral contract model.

Similarly, in [21], the Electric Reliability Council of Texas (ERCOT) defines the congestion zones based on PTDFs; generators and loads that have similar impacts on the zonal links, which are the inter-tie lines between different congestion zones, are grouped together. A set of commercially significant constraints (CSCs) are selected and updated in November annually based on the analysis of load flow data from the Steady State Working Group (SSWG) under the current topology of the ERCOT system. Typically, CSCs are the high voltage transmission lines that are frequently congested. A statistical clustering technique is applied to determine the congestion zones based on the PTDFs relative to all the CSCs.

To measure the difference of impact on all the power transmission lines by bus *m* and bus *n*, inspired by [20] and [21], PTDF differences (PTDFDs) are proposed in (3—1),

$$PTDFD_{mn} = \frac{\sum_{k=1}^{|K|} \left| PTDF_{k,m}^{R} - PTDF_{k,n}^{R} \right|}{|K|}. \quad (3—1)$$

$|K|$ represents the number of transmission lines and $\left| PTDF_{k,m}^{R} - PTDF_{k,n}^{R} \right|$ represents the difference between the flow on transmission line *k* due to a MW injection at bus *m* versus the flow on transmission line *k* due to a MW injection at bus *n*. The PTDFD is proposed as a metric that can be used to group buses together based on whether they have

similar impacts on the system. Smaller PTDFDs imply that two buses have relatively similar impacts on transmission lines. If the PTDFDs for bus *m* and bus *n* are zero, these two buses have the exact same impact on all of the transmission lines. Compared to [20] and [21], PTDFDs consider all the transmission lines instead of only considering congested transmission assets or CSCs. While the PTDFD takes all transmission lines into consideration equally, typically there are only a few critical transmission lines.

One simple way to focus on critical transmission lines is by adding weights. Suppose there are $|K|$ transmission lines, then the weighted PTDFD (WPTDFD), with weight π_k on transmission line *k* between bus *m* and bus *n*, is

$$WPTDFD_{mn} = \frac{\sum_{k=1}^{|K|} \pi_k |PTDF_{k,m}^{R} - PTDF_{k,n}^{R}|}{|K|}. \quad (3—2)$$

For the weighted PTDFD reserve zone determination method, weights are essential to creating dynamic reserve zones that reflect expected operating conditions. The difficulty lies in determining appropriate weights since the weights will influence the clustering results. The weights are associated with each transmission asset and can be based on many different factors including the expected flow, the variance of the line's flow, the probability of an outage, as well as other factors.

Without weights, all of the transmission lines are treated as the same and the determined reserve zones are incapable of reflecting current operating conditions. The goal of partitioning reserve zones is to improve the reserve deliverability in order to improve the system reliability and market efficiency. As a result, it is preferred to integrate system operating conditions into the determination process of reserve zones. Weights can involve system operating condition, such as load information, expected available transfer capability (ATC), and flowgate price, which can come from historical data and forecasted data. The

weights can also be used to incorporate the information of uncertainties, such as renewable resources, and this will be discussed in Chapter 5.

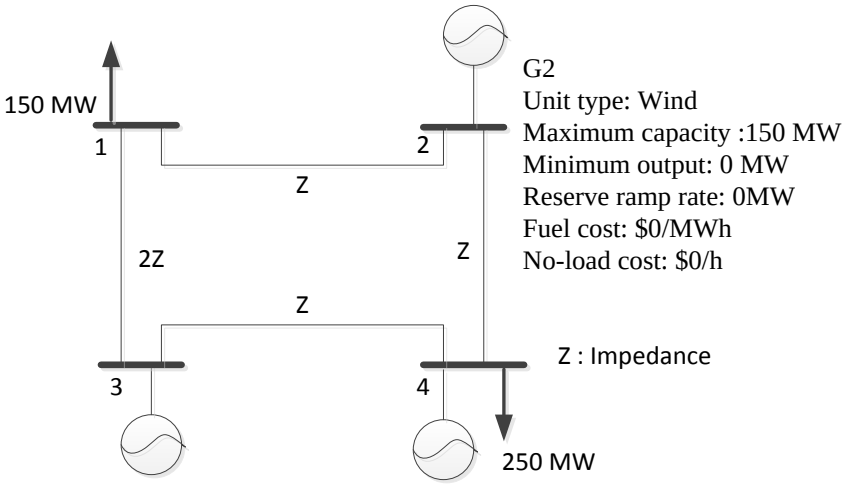

Figure 3.1 Four-bus Example

The rationale behind using PTDFDs as a metric stems from the fact that generators with similar PTDFs should be considered in the same reserve zone as their resulting impact on network flows will be relatively similar. The rationale behind using a weighted PTDFD scheme is due to the variation in operating conditions. With the advent of large levels of variable renewable resources, unexpected congestion may occur and, thus, the deliverability of operating reserve is critical in order to maintain system reliability. Figure 3.1 provides a simple four-bus example to illustrate this fact. In this four-bus system, three generators (a wind generator, G2, a nuclear generator, G3, and an oil generator, G4) are modeled and the wind penetration level is 23%. The PTDFs and the line ratings are listed

in Table 3.1; with bus 1 as the reference bus, the PTDF for line 3 to 1, for an injection at bus 3, is 3z/5z.

Table 3.1 PTDF Matrix and Line Rating

Branches	Bus 1	Bus 2	Bus 3	Bus 4	Line Rating
2 to 1	0	4/5	2/5	3/5	200MW
2 to 4	0	1/5	-2/5	-3/5	200MW
3 to 4	0	-1/5	2/5	-2/5	200MW
3 to 1	0	1/5	3/5	2/5	200MW

Suppose that the forecasted wind power output is 100MW. The NREL 3+5 rule is applied to this system; note that this example focuses on uncertainty regarding the renewables and not N-1. To minimize the operating cost, assuming no forecast error, the optimal solution of this four-bus system is $P_{G3} = 300\text{MW}, P_{G4} = 0\text{MW},$ and $P_{G2,forecasted} = 100\text{MW}$. Note that G4 is not committed and is not providing reserve. The power flows are P_{21}= 50MW, P_{24}= 50MW, P_{34}= 200MW, and P_{31}= 100MW. The only congested path is branch 3 to 4. If the actual wind power output is lower than the forecasted value, e.g., suppose the actual wind power output $P_{G3,actual} = 95\text{MW}$, then the drop in renewable production is compensated by G3. If G3 increases its output to 305 MW, P_{34} will increase to 203MW, which violates the line rating of branch 3 to 4. To avoid load shedding, the optimal solution is to increase P_{G4} to 25MW and decrease P_{G3} to 280MW, even though G4 is a more expensive generator. Such a change to the originally proposed dispatch solution can be considered an out of market corrections.

3.2.2 Electrical Distance

Electrical distance is widely used to analyze the electrical network, such as voltage control and reactive power management. There are different methods to define electrical distance, including sensitivity methods or impedance. A sensitivity method can be based on the sensitivity study between voltage and reactive power [22]. Since unit commitment is based on a DC model, only impedance is discussed in this thesis.

The impedance method is commonly based on examining the relationship between the voltage drop due to injecting a unit of current at one bus and withdrawing it at the receiving bus. The larger the voltage drop, the larger the electrical distance. To determine the electrical distance, the following equation is used: $\Delta V = Z_{Bus} \Delta I$, where Z_{Bus} is the matrix of impedances, ΔV is the change of nodal voltage, and ΔI is the change of nodal current. If the change of any injected current is zero except the injected current at node *m*, then

$$\begin{pmatrix} \Delta V_1 \\ \Delta V_2 \\ \dots \\ \Delta V_n \end{pmatrix} = \begin{pmatrix} Z_{1\mathrm{m}} \\ Z_{2\mathrm{m}} \\ \dots \\ Z_{nm} \end{pmatrix} \Delta I_m \qquad (3—3)$$

In general,

$$Z_{im} = \Delta V_i / \Delta I_m \qquad (3—4)$$

The electrical distance between node *i* and *j*, $D_{i,j}$, is defined as the voltage drop when a unit of current is injected at node *i* and withdrawn at node *j*, which can be stated as (3—5):

$$D_{i,j} = Z_{ii} + Z_{jj} - 2Z_{ij}. \qquad (3—5)$$

From equation (3—5), a smaller voltage drop between node *i* and node *j* implies a smaller electrical distance between node *i* and node *j*, which is consistent with the fact that power tends to flow between nodes with smaller electrical distance.

Blumsack *et al.* [23] defined power network zones based on electrical distance and they examine four electrical centrality measurements based on electrical distance. With the use of clustering techniques, they rank the importance of buses and transmission lines in [23] and provide a new way of studying the relationship between power grid topology and electrical parameters. However, the measure of electrical distance proposed in [23] is $\|Z^{bus}\|$, which is theoretically incorrect in comparison to equation (3—5). In [24], Wang *et al.* pointed out the mistake and corrected the definition of electrical distance given in [23].

Determining zones can be used for alternative purposes as well. Reference [24] employed clustering techniques, with electrical distance as the centrality measurement, in order to develop secondary voltage control zones. Developing secondary voltage control zones can help ensure voltage stability across the power grid.

3.2.3 Comparisons of PTDF Difference and Electrical Distance

Partitioning the power grid network into reserve zones based on electrical parameters instead of asset ownership or geographic location is more reasonable to guarantee load deliverability. Both PTDFDs and electrical distance include topology and electrical parameter information.

Based on the definition of electrical distance, the larger the electrical distance is, the more voltage drop there is. Compared to PTDFDs, electrical distance is usually applied to voltage reliability and control issues. However, the voltage in the DC model, which is

applied in our UC formulation, is assumed to be 1 per unit, i.e., voltage is not considered in the DC model. Therefore, the electrical distances may not be an appropriate measurement for reserve zones in a DC model.

One primary concern for developing reserve zones is the congestion throughout the network. Both PTDFDs and electrical distances without weights are independent of system operating conditions. Determining reserve zones without considering the operating status is not preferred. While neither PTDFDs nor electrical distances contain knowledge regarding line ratings and network flows, PTDFDs are still a better measurement because PTDFDs capture the impacts on transmission lines while electrical distance does not. The motivation to use PTDFDs is based on the fact that the spinning reserve provided by generators, which have similar PTDFDs and, thus, have similar impacts on transmission lines, should be clustered together. Generators and loads within the same zone will have similar reserve deliverability features. This increases the probability that the location of the reserves within a single zone is indistinguishable since the generators' impacts on transmission lines are relatively similar. Such an approach is, thus, more congruent with the mathematical structure of reserve requirement modeling within unit commitment, which does not differentiate reserve from one generator in a zone from another in the same zone. Consequently, it is expected that reserve zones, based on PTDFDs, will improve reserve deliverability. Compared to PTDFDs, there is no evidence showing that electrical distance may cluster the buses with similar impacts on the transmission lines. Numerical comparisons of PTDFDs and electrical distance are presented in Chapter 3 Section 3.4.

3.3 Clustering Methods

Clustering methods are used to extract useful information from huge amounts of data. Clustering methods are applied in many topics and fields, which become a very important tool for data analysis. In [25], various clustering methods, which are applied in power systems for electricity customer classification, are compared and evaluated. Similarly, clustering methods can also assist in partitioning reserve zones. Buses that have similar impacts on the power system tend to be viewed as one zone; in other words, buses with similar PTDFDs tend to be in the same zone. Therefore, reserve zones can be clustered based on PTDFDs or EDs. Four clustering methods, K-means algorithm, fuzzy c-means algorithm, self-organizing map (SOM), and hierachical clustering, will be discussed in this section.

3.3.1 K-means Clustering Algorithm

K-means is one elementary, but popular, clustering method that attempts to partition n observations into K clusters based on the closeness to the centers. In the K-means clustering algorithm, one observation can only belong to exactly one cluster and, for the power system, an observation represents a bus.

The K-means clustering algorithm starts by randomly choosing K centroids; centroids are used to represent the center of a cluster (zone). Based on the chosen centrality measurement (PTDFDs or EDs), each node has a distance to each centroid and each node is assigned to the cluster whose centroid is closest to that node. At the end of each iteration, new centroids are calculated, the clusters are again updated by reassigning each node to its closest centroid, and this algorithm is repeated until the centroids are stable.

Generally, the K-means algorithm converges fast, unless there is an extreme number of data points; the computational complexity of K-means is *O(mnKT)*, where *m* and *n* represent the dimension of data, *K* is the number of clusters, and *T* is the number of iterations. The number of clusters, *K*, is pre-determined and an inappropriate choice of *K* may cause poor results. Thus, it is important to run a diagnostic check to determine an appropriate number of clusters for the problem at hand. Reference [26] stated that one way to ensure a proper number of clusters is to maximize the stability of central points by selecting the optimal *K*. While this method to determine *K* may work for other applications, the motivation of determining reserve zones is not centered on ensuring a stable centroid for each zone.

One drawback of the K-means clustering algorithm is that the starting points are selected randomly. Different sets of starting points may result in different sets of terminal central points and, thus, different clusters. Since the clustering results can be sensitive to the starting points, the stability issue is one main drawback of the K-means algorithm. Kuncheva [27] evaluated the relationship of the stability of K-means and random starting points and an exprimental comparsion of differerent *K* value reveals that clustering with larger *K* values is more stable. Reference [28] proposed a clustering algorithm with refined starting points that are determined by the expected maximation (EM) clustering method, and the refined initial starting points can converge to a "better" local minimum. Another simple solution is to try a number of different starting points and select the most frequent set of terminal points. However, K-means is a heuristic method and, thus, there is no guarantee that a global optimial solution is found.

Due to these K-means limitations, some modified K-means methods are proposed. Reference [29] proposed a novel K-means clustering method that can generate variable weights automatically; by applying variable weights, the convergence speed of K-means method will be accerelated. This automatic variable weighted K-means clustering method is useful in dealing with large datasets.

3.3.2 Fuzzy C-means Clustering Algorithm

Fuzzy C-means clustering algorithm was first proposed by J. C. Bezdek [30]. In fuzzy clustering [30], a soft membership of clusters replaces the hard memberhsip in the K-means clustering algorithm. Each point is assigned a probability of belonging to one cluster, which can be viewed as weights. Various fuzzy clustering methods have been proposed in [31]. The widely used fuzzy c-means algorithm is as following:

1. Choose the number of clusters.
2. Set each point coefficent u_k randomly such $\sum_{k=1}^{N} u_k(i) = 1$, where N represents the number of clusters.
3. Compute the centroid $center_k = \frac{\sum_{i=1}^{N} u_k^m(i)x(i)}{\sum_{i=1}^{N} u_k^m(i)}$ for cluster k.
4. For each point, compute its coefficients of being in the clusters, $u_k(i) = \frac{1}{\sum_{k=1}^{Center_k} \left(\frac{\|x_i - Center_j\|}{\|x_i - Center_k\|}\right)^{2/(m-1)}}$.
5. Repeat until the algorithm has converged, i.e., the coefficients' change between two iterations is no more than a small number, ε.

As is the case with K-means, the number of clusters has to be pre-determined and an inappropriate choice of the number of zones may result in poor results. The results also

depend on the initial choice of weights and different weights may generate different clusters. The terminal weight may be a local optimum since the fuzzy c-means algorithm is a heuristic method.

3.3.3 Self-Organizing Map

A self-organzing map (SOM), which was first proposed by Teuvo Kohonen [32], is a type of unsupervised artificial neural network (ANN) and high-dimensional data can be presented in a lower dimensional space, which is typically two-dimentional. A SOM is comprised of nodes or neurons. Each node is corresponding to a weight vector with the same dimension as the input data vector u. The weight vector $w(t)$ is initialized randomly or evenly. Weight vectors of the neurons are adjusted close to the input vector u. The weight vector $w(t)$ can be updated by equation (3—6),

$$w(t+1)=w(t)+\theta(v,t)\,\eta(t)(u-w(t)) \qquad (3—6)$$

where $\eta(t)$ is a learning coefficient and $\theta(v,t)$ is the neighborhood function, which depends on the lattice distance between the neuron that is closest to the input vector u and neuron v [25]. The training process is a competing process, i.e., how close is the neuron to the input vector. The weight vector is updated during the training process based on the similarity that is obtained by caculating the Euclidean distance between the input vector and the neuron's weight vector and there is only one winning neuron, which is closest to the input vector u. This process will be repeated and it is guaranteed to converge within a finite interval. In the end, the map is similar to the original set.

The SOM can be used to visualize low-dimensional views of high-dimensional data. However, the clustering outcome cannot be obtained from SOM directly. Applying K-means in the reduced dimension space of the resulting map will be based on the low-

dimensional data and not the high-dimensional data since data is lost. Reference [33] proposed a new learing algorithm, which clsuters not only based on the winning weight vector but also the neighboring units' weights.

3.3.4 Hierarchical Clustering

Hierachical clustering takes a divisive or agglomerative approach to construct the hierarchy of clusters. At first, a similarity matrix can be obtained based on an appropriate metric such as Euclidean distance, squared Euclidean distance, or Manhattan distance. Differenct metrics may give different shape of clusters. Hierachical clustering starts from individual nodes and then clusters are merged (agglomerative) or split (divisive) iteratively based on the linkage criterion, which determines the distance between different sets of observations and the linkage criterion can be determined by similarity matrix.

A linkage criterion measures the distance of clusters and it includes single-linkage clustering, complete linkage clustering, average linkage clustering, and minimum energy clustering. A different choice of linkage criterion may give a different cluster size. For example, single linkage criterion may lead to clusters with big sizes and complete linkage criterion may lead to clusters with small sizes.

3.3.5 Comparisons of Different Clustering Methods

Altought K-means clustering method is sensitive to initialization and the number of clusters is pre-determined, it is simple and efficient. K-means clulstering method randomly selects K buses as the centroids and converges to *K* zones and each bus only belongs to one zone. Moreover, the clustering outcomes are sensitive to the weights. With more weights

on the congested transmission lines, reserve zones boundaries tend to cut the congested transmission lines thereby improving the load deliverability.

Compared to K-means, the fuzzy c-means clustering method assigns soft membership to the nodes. One problem of fuzzy c-means is the clustering centroids of two zones may overlap with each other. This problem will result in two overlaping reserve zones and, thus, the number of clusters may not be the number required and some undesired large reserve zones may be obtained.

SOM can be used to project high dimensional data into one or two dimensional spaces. The structure of neural network and the number of cluster need to be pre-specified for SOM, which is the same as for K-means and fuzzy c-means. When SOM is applied to determine reserve zones, the size of clusters may be unbalanced, i.e., some large long reserve zones are not preferred because low load deliverability and small reserve zones may not have enough capacity to provide sufficient reserve.

Hierachical clustering is simple to implement and the clustering result is more informative. Compared to other clustering methods, the number of clusters is not required to be pre-determined. The cutoff value is critical because once the clusters are merged or split, what has been done previously cannot be undone. Improper merge or split decisions may result in undesired clustering outcomes.

Even though all the metioned clusering methods have drawbacks, K-means clustering is still prefered because it is simple to implement, unbiased, and reliable.

3.4 Numerical Clustering Results

3.4.1 Test Cases without Weights

In this section, both the IEEE 118-bus system and the 73-bus reliablity test system (RTS) are studied. Three different clustering methods, K-means algorithm, fuzzy c-means algorithm, and SOM are applied to obtain the reserve zones and there is no weights involved, i.e., all of the transmission lines are treated as the same.

1) K-means algorithm

K-means clustering method is used to partition reserve zones based on PTDFDs and EDs with K equal to 3. From the test results, the reserve zones based on PTDFDs are partitioned equally; however, the reserve zones based on EDs are biased in size. The 73-bus RTS system is naturally a three-zone model because it is a replication of a 24-bus system, three times. The ED clustering results end up splitting zone three in half while combining the original zones one and two together. Without considering system operating conditions, equal reserve zones are prefered due to the symmetry of the system. The results are displayed by Figure 3.2.

Comparing PTDFDs with EDs, the outcomes based on PTDFDs present better load deliverability than the outcomes based on EDs. From Figure 3.3, in the second zone, two buses are completely isolated from all other buses in the same zone and, thus, there is the question as to how reliable such a zone would be and load deliverability cannot be guaranteed in this case.

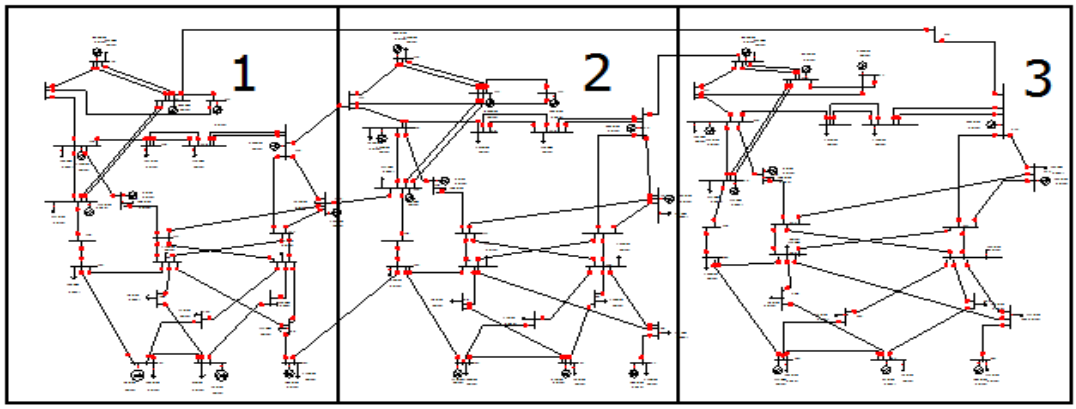

a) Clustering result based on PTDF difference

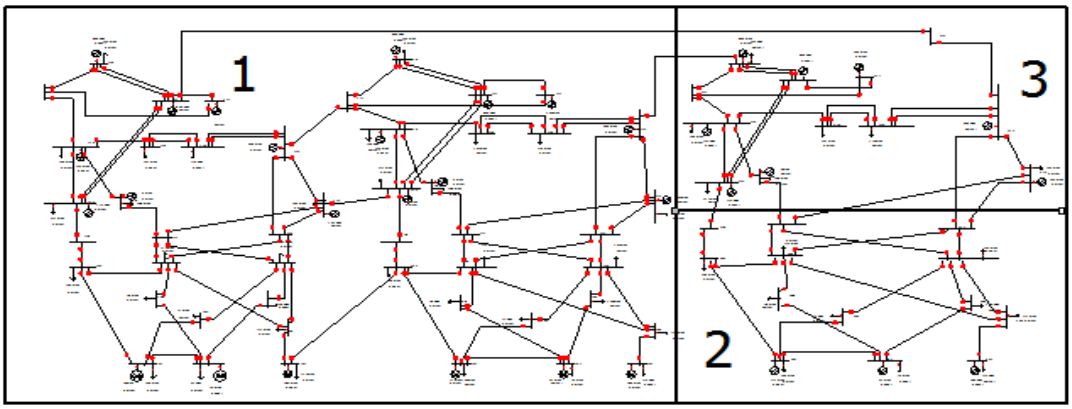

b) Clustering result based on Electrical Distance

Figure 3.2 Reliability Test System Clustering Results

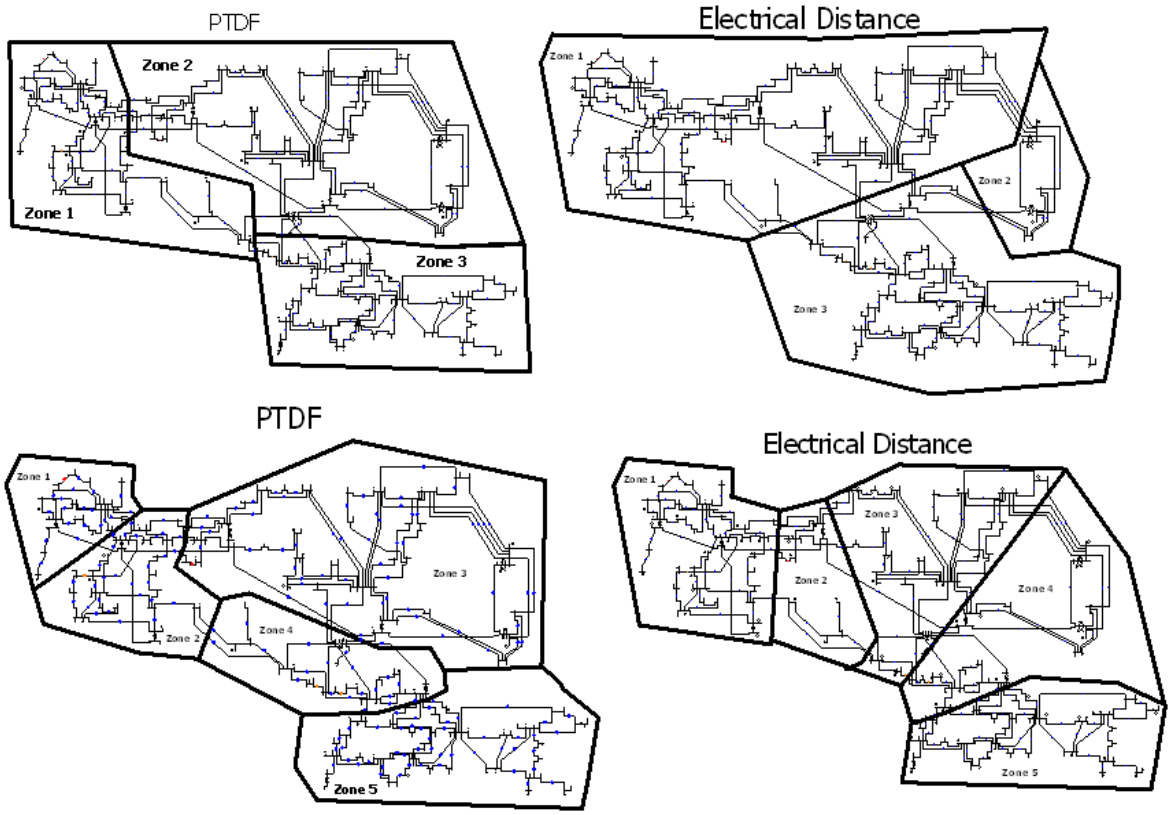

Figure 3.3 IEEE 118-Bus System Clustering Results with Different Number of Zones

2) Fuzzy c-means algorithm

The clustering result of fuzzy c-means is shown in Figure 3.4 for the RTS 96 system based on PTDFDs. Without weights considered, reserve zones are partitioned unevenly, which implies that fuzzy c-means algorithm may bias the clustering results. Compared to the numerical results of K-means for PTDFDs in Figure 3.2, the upper four buses of the original RTS 96 system's second zone are a part of zone one for the Fuzzy c-means result. These four buses are connected by only one transmission line to the rest of the buses in zone one whereas they are connected to the remaining buses in zone two by four

transmission lines. As a result, it is expected that the K-means reserve zones are more reliable than Fuzzy c-means reserve zones, and, thus, K-means is preferred.

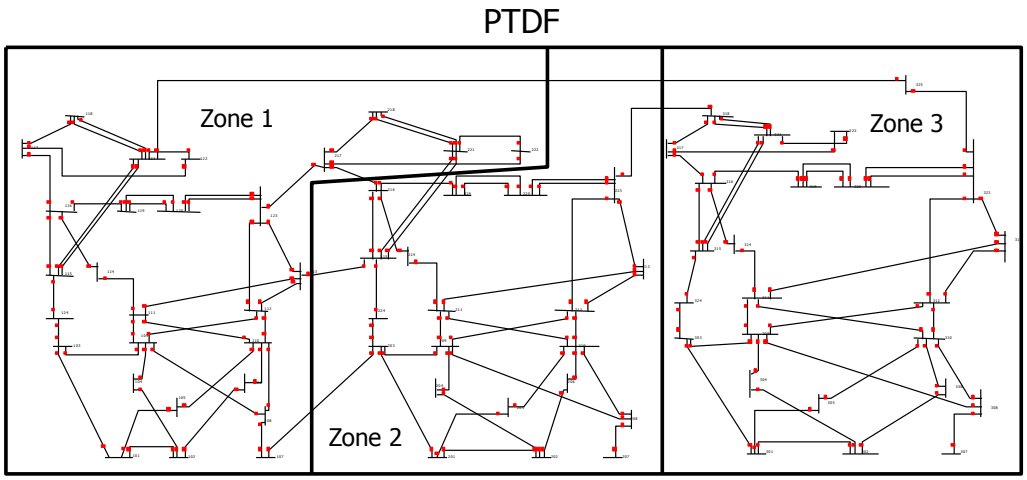

Figure 3.4 Reserve Zones without Weights Based on PTDFDs (*K*=3) for RTS96

3) SOM

The clustering results of SOM, applied to the IEEE 118-bus system, are shown in Figure 3.5. From the result, the first zone is much larger than the other two zones. Large reserve zones may degrade the reserve deliverability since reserve may not be deliverable across such a large zone if there is excess congestion. However, in comparison to the 3-zone K-means result for PTDFDs in Figure 3.3, it can be seen that the reserve zones are more similar in overall size. While it may not always be preferred to have zones of equivalent sizes, the inclusion of weighted factors can help correct for this by incorporating operational conditions into the statistical clustering techniques. Nonetheless, since these clustering results are currently only based on topological information, the results suggest that K-means is preferred over SOM.

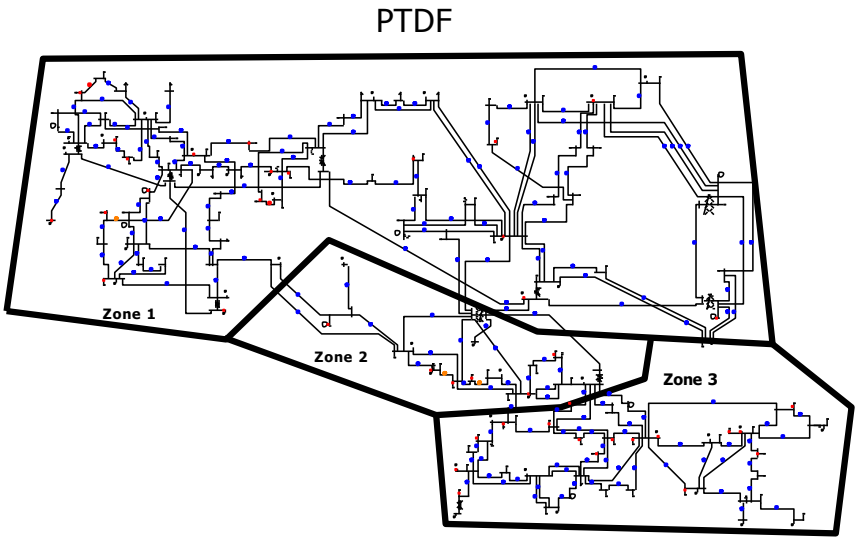

Figure 3.5 Reserve Zones without Weights Based on PTDFDs (*K*=3) for IEEE 118bus System

3.4.2 Test Cases with Weights

Since congestion can substantially influence the deliverability of reserves, weights are added to the transmission lines, which are proportional to the power flow divided by each line's rating. The motivation is to determine zones that have relatively minimal internal congestion such that the probability that the reserve internal to a zone can be delivered is higher. As a result, this should improve the deliverability of reserves system-wide and, hence, improve the systemy reliabilty and market efficiency. In Figures 3.6 and Figure 3.7, red represents heavy loading and blue represents light loading. Based on Figure 3.6 and Figure 3.7, reserve zones tend to have heavily loaded transmission lines as the inter-zonal links and, thus, the intra-zone congestion is lowered. Although system operating conditions may change with new reserve zones, these numerical results still present the benefits of involving the system operating conditions within the statistical clustering techniques.

However, to update system operating condition, the weights can be updated iteratively until the reserve zones partitioning is stable.

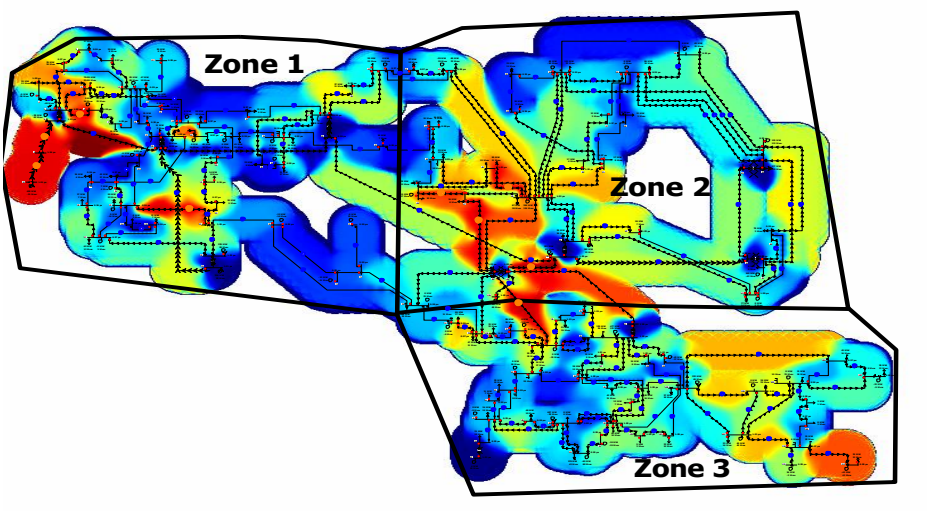

Figure 3.6 3-Zone 118-Bus with Weights

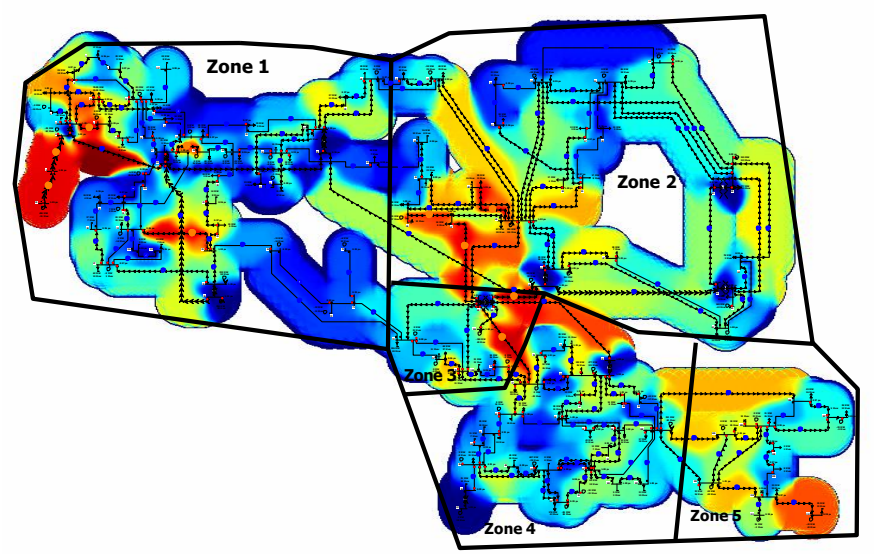

Figure 3.7 5-zone 118-Bus with Weights

4. SECURITY CONSTRAINED UNIT COMMITMENT AND SECURITY CONSTRAINED ECONOMIC DISPATCH

4.1 Security Constrained Unit Commitment

Security constrained unit commitment (SCUC) is the process of deciding the commitment status of generating units and the dispatch levels of the units to meet all the power constraints, such as generator output constraints, power flow constraints, power balance constraints, spinning reserve requirements, ramp rate constraints, and minimum-up and minimum-down time constraints. The objective is to minimize the total cost, which includes the variable operating costs, the no-load costs, the start-up costs, and the shut-down costs.

The SCUC problem is a complicated mixed integer programming (MIP) problem with a large number of constraints, continuous variables, and binary variables. The non-linear cost functions and start-up cost and shut-down cost also increase the complexity of the SCUC problem; thus, the SCUC problem is a difficult problem to solve. The formulation of the SCUC problem presented in this chapter includes a lossless DCOPF.

4.1.1 Objective Function

The objective function is to minimize the production cost, which includes fuel cost, start-up cost, shut-down cost, and no-load cost. Since the load is fixed, i.e., assumed to be perfectly inelastic, minimizing the total cost is the same as maximizing the social welfare. For energy markets, the objective is to maximize the market surplus. It can be formulated as follows:

$$\sum_{t\in T}\sum_{g\in G}[C_g p_{gt} + C_g^{SU} su_{gt} + C_g^{SD} sd_{gt} + C_g^{NL} u_{gt}] \quad (4—1)$$

The start-up cost refers to the cost the unit incurs due to the startup process it must undergo before it connects to the grid; similarly, there is the shut-down cost. In order to model the startup and shutdown costs, new binary variables are needed: a startup variable that equals one when the unit is turned on (and zero otherwise) and a shutdown binary variable that equals one when the unit is turned off (and zero otherwise). The modeling of these variables is shown by Equation (4—2) through Equation (4—4). While these variables represent binary states, they can be modeled as continuous variables. While the variables can take on any fractional value, it can be proven that, with the right minimum up and down time constraints, these variables will always take on a binary solution even if they are modeled as continuous variables. The no-load cost is a fixed cost that the generator incurs during any period that the unit is operating.

$$su_{gt} - sd_{gt} = u_{gt} - u_{g,t-1}, t \in T, g \in G \quad (4—2)$$

$$0 \leq su_{gt} \leq 1, t \in T, g \in G \quad (4—3)$$

$$0 \leq sd_{gt} \leq 1, t \in T, g \in G \quad (4—4)$$

4.1.2 Node Balance Constraints

At each period, the sum of power flow into bus *n*, the power flow out bus *n*, and the generation at but *n* must equal the demand at bus *n*. This is often referred to as the node balance constraint and the corresponding dual variable of the node balance constraint is the locational marginal price (LMP).

$$\sum_{k\in K^+(n)} f_{kt} - \sum_{k\in K^-(n)} f_{kt} + \sum_{g\in G(n)} p_{gt} = D_{nt}, t \in T, n \in N \quad (4—5)$$

4.1.3 Power Output Constraints

Every generator has its own operating constraints and usually there are minimum and maximum production limits. Hydro generating units are usually modeled with a minimum power output at 0MW while most thermal generating units have a positive minimum operating level. The power output constraint for unit g at period t can be written as follows:

$$u_{gt}P_g^{min} \leq p_{gt} \leq u_{gt}P_g^{max}, g \in G \quad (4—6)$$

where p_g^{min} and p_g^{max} are the lower and upper power output bound respectively and u_{gt} is the unit commitment binary variable. By multiplying lower and upper bound by the commitment variables u_{gt}, p_{gt} will be forced to 0 MW if generator g is not committed.

4.1.4 Spinning Reserve Requirements

To ensure the system reliability, a required amount of market wide spinning reserve requirements $R_{MKT,t}^{SPIN}$ should be satisfied for every period t:

$$\sum_{g=1}^{|G|}(r_{gt}^{SPIN}) \geq R_{MKT,t}^{SPIN},, t \in T \quad (4—7)$$

where r_{gt}^{SPIN} is the spinning reserve supplied by generator g at period t. For each generator,

$$r_{gt}^{SPIN} = \min(u_{gt}p_g^{max} - p_{gt}, R_g^{10}u_{gt}), t \in T, g \in G \quad (4—8)$$

where τ is the response time by which the generators must ramp up their output, which is 10 minutes in many systems, and R_g^{up} is the minute ramp up rate of generator g. Equation (4—8) can be rewritten into two inequalities as shown below by Equation (4—9) and Equation (4—10).

$$r_{gt}^{SPIN} \leq u_{gt}p_g^{max} - p_{gt}, t \in T, g \in G \quad (4—9)$$

$$r_{gt}^{SPIN} \leq R_g^{10}u_{gt}, t \in T, g \in G \quad (4—10)$$

SCUC also has regulation and supplemental reserve requirements and they have similar formulation as equation (4—7).

4.1.5 Minimum-Up and -Down Time Constraints

For thermal generating units, due to physical limitations, once a unit is turned off, it must stay off for a minimum length of time, which is called minimum down time. Similarly, there is the minimum up time. The minimum up and minimum down time constraints for unit g can be expressed as follows:

$$\sum_{t'=t-UT_g+1}^{t} su_{gt'} \leq u_{gt}\ , t \in \left(UT_g\ , .. , T\right), g \in G \qquad (4—11)$$

where UT_g is the minimum up time, and

$$\sum_{t'=t-DT_g+1}^{t} sd_{gt'} \leq 1 - u_{gt}\ , t \in \left(DT_g\ , .. , T\right), g \in G \qquad (4—12)$$

where DT_g is the minimum down time. There are many different ways to mathematically write the minimum up and down time constraints. The formulation of the minimum up and down time constraints can affect the solution time; an overview of various formulations is presented in [34]. This thesis chooses a formulation that provides the tightest possible representation for the UC problem.

4.1.6 Ramp Rate Constraints

Most generators have physical restrictions on how fast their output can change and such constraints are known as ramp rate constraints. For example, if the ramp up rate of a generator is 50MW/hour and if this unit is outputting 200MW during hour *t*, then it cannot operate at more than 250MW during hour *t*+1. The ramp rate constraints can be written as follows,

$$p_{gt} - p_{g,t-1} \leq R_g^{HR}, t \in T, g \in G \qquad (4—13)$$

$$p_{g,t-1} - p_{gt} \leq R_g^{HR}, t \in T, g \in G \qquad (4—14)$$

where R_g^{HR} is the hourly ramp up (down) rate. There are more complex ways to formulate ramp rate constraints; for instance, it is possible to incorporate startup and shutdown ramp restrictions, [34].

The complete deterministic unit commitment formulation is presented in Appendix A.

4.2 Security Constrained Economic Dispatch

The security constrained economic dispatch (SCED) is the process of deciding the dispatch levels of the units to balance generation and system demand while minimizing the production cost in real time operation. SCUC determines the most commitment decisions for day-ahead operation and SCED balances generation and demand in the real-time. Deterministic SCED is a linear programming problem when the objective is a piecewise linear formulation of the operating cost. Its formulation is similar as SCUC without some inter-temporal constraints, commitment variables, and start-up and shun-down variables. Below is the formulation of SCED.

Minimize $$\sum_{t\in T}\sum_{g\in G}[C_g p_{gt}] \quad (4—15)$$

Subject to:

$$\sum_{k\in K^+(n)} f_{kt} - \sum_{k\in K^-(n)} f_{kt} + \sum_{g\in G(n)} p_{gt} = D_{nt}, t \in T, n \in N \quad (4—16)$$

$$f_{kt} = B_k(\theta_{nt} - \theta_{mt}), t \in T, k = (n,m) \in \mathrm{K} \quad (4—17)$$

$$-F_k^{max} \le f_{kt} \le F_k^{max}, t \in T, k \in K \quad (4—18)$$

$$\overline{U}_{gt} P_g^{min} \le p_{gt} \le \overline{U}_{gt} P_g^{max}, t \in T, g \in G \quad (4—19)$$

$$p_{gt} - p_{g,t-1} \le R_g^{HR}, t \in T, g \in G \quad (4—20)$$

$$p_{g,t-1} - p_{gt} \le R_g^{HR}, t \in T, g \in G \quad (4—21)$$

$$r_{gt} \le R_g^{10} \overline{U}_{gt}, t \in T, g \in G \quad (4—22)$$

$$0 \leq r_{gt}^{SPIN} \leq \overline{U}_{gt} P_g^{max} - p_{gt} \quad (4—23)$$

$$\sum_{g \in G} (r_{gt}^{SPIN}) \geq \mathrm{R}_{\mathrm{MKT,t}}^{\mathrm{SPIN}} \quad (4—24)$$

4.3 Application of PTDFD Reserve Zone Determination on SCUC

4.3.1 Case Study Based on RTS96

To validate the concept of co-optimizing the reserve zones and reserve levels, numerical results are presented with four different reserve zone partitions based on K-means: a single zone, a 3-zone partition based on PTDFDs, a 3-zone partition based on EDs, and a weighted PTDFD based 3-zone partition. The weights for the weighed 3-zone results are based on the power flow results when using the PTDFDs 3-zone model; the weight equals the average absolute value of transmission line's power flow divided by its thermal capacity rating. Even though the process to determine the optimal weights is not straightforward and while there is no guarantee that using weights will produce better results, the use of weights is still beneficial since PTDFDs, by themselves, are incapable of reflecting grid operating conditions. One primary goal of reserve zones is to improve reserve deliverability, which is heavily dependent on grid operating conditions and congestion, not just the topological structure of the grid.

The security constrained unit commitment model is implemented with the RTS96 test case and the reserve requirements specify that each zone must meet a specific reserve level. The detailed RTS96 test case information can be obtained from Appendix C Section C.1. The reserve level is determined based on a percentage of the demand in the reserve zone, as shown by (6), where α represents the percent reserve level, D_{nt} represents the demand in period t at bus n, and $N(z)$ represents the set of buses in zone z. A 24 hour horizon is

tested and the system contains 18 hydro units, 6 nuclear units, and 72 thermal units with a total installed capacity of 10215MW. An offline N-1 contingency analysis is implemented with the value of lost load (VOLL) equal to $40,000/MWh, and the formulation of N-1 contingency analysis is presented in Appendix B. The expected load shedding and expected total cost will be compared and analyzed among these different zone partitions.

$$\sum_{g\in G(z)} r_{gt}^{SPIN} \geq \eta_z \sum_{n\in N(z)} D_{nt} \qquad (4—15)$$

These cases were solved using the mixed-integer linear programming solver CPLEX 12.2 version. The average solution time was 120 minutes with an average optimality gap of 0.7% on a Windows-based server with a 2.66-GHz processor and a 2-GB of RAM.

As depicted in Figure 4.1, the original 3-zone result improves the involuntary load shedding due to contingencies as compared to the single zone result. The weighted 3-zone and ED 3-zone results are better than the original 3-zone result and the single zone result, since, by including weights, the intra-zone reserve deliverability of the weighted 3-zone model and ED 3-zone model is improved. Improving the reserve deliverability then decreases the amount of load shedding. As the reserve level goes up, the involuntary load shedding due to contingencies of all three reserve zones model goes down and approaches zero.

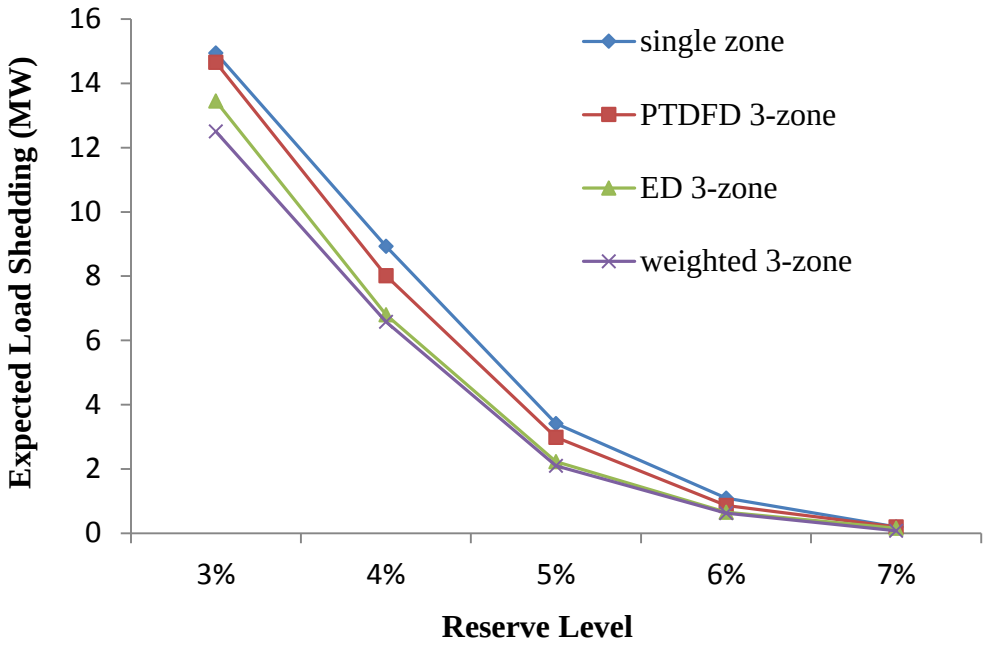

Figure 4.1 Expected Load Shedding (MW) from 3% to 7% of Peak Load with Single Zone, PTDFD 3-zone, ED 3-zone, and Weighted PTDFD 3-zone

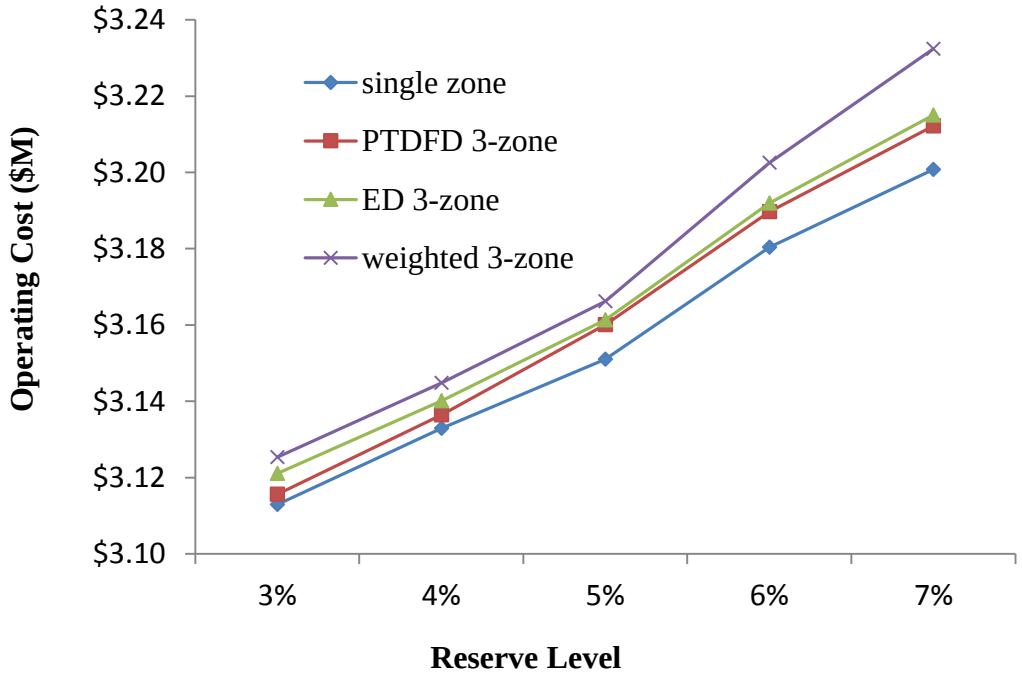

Figure 4.2 Operating Cost (Million dollars) from 3% to 7% of Peak Load with Single Zone, PTDFD 3-zone, ED 3-zone, and Weighted PTDFD 3-Zone

From Figure 4.2, as the reserve level goes up, the operating costs increase as well. The operating cost of the weighted 3-zone, ED 3-zone, and the original 3-zone is higher than the single zone because the network partitioning due to the reserve zones causes a different unit commitment solution to be chosen due to the zonal reserve requirements. Note that the operational costs in Figure 4.2 do not include the costs due to load shedding.

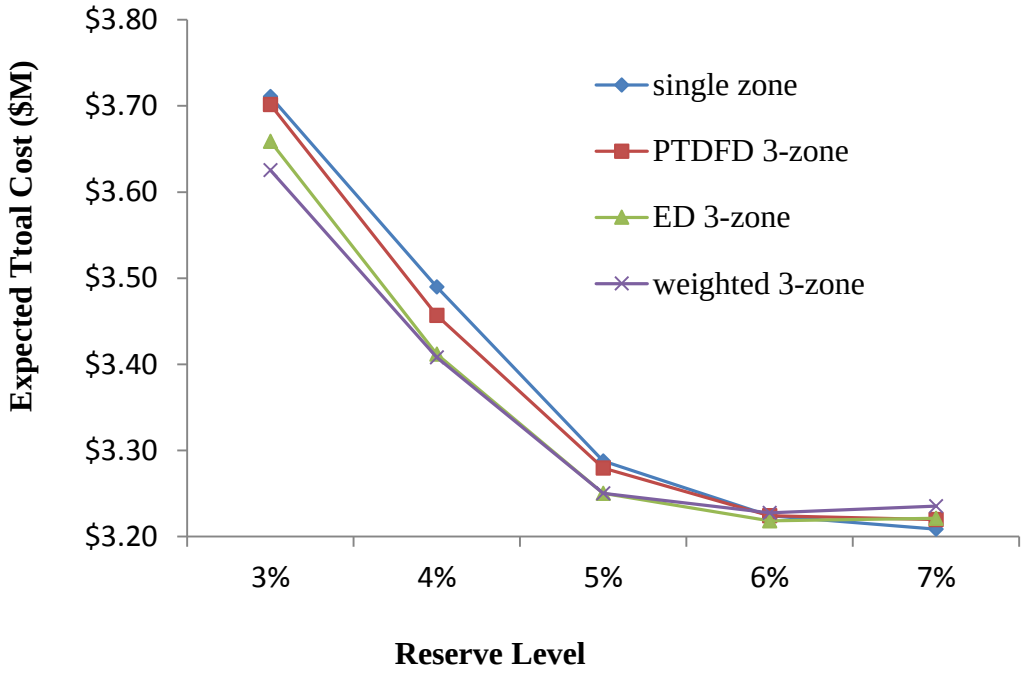

Figure 4.3 Expected Total Cost (Million dollars) from 3% to 7% of Peak Load with Single Zone, PTDFD 3-Zone, ED 3-Zone, and Weighted PTDFD 3-Zone with the Value of Lost Load at $40,000/MWh

From Figure 4.3, the minimum expected total cost is achieved at the 5% reserve level where the operating and total contingency costs is the lowest; the total contingency cost is determined by calculating the expected load shedding for N-1 contingencies and multiplying it by the VOLL. However, the expected total cost of these four zones are similar, since the RTS96 is a small system and the system was designed to be overbuilt and, hence, congestion is not a big issue in this system. The minimum expected total costs of

the original 3-zone model, the weighted 3-zone model, and the ED 3-zone model is not better than that of the single zone model and ED 3-zone for high reserve levels because the load shedding is primarily due to insufficient reserve and not congestion for these cases.

4.3.2 Case Study Based on IEEE 118-Bus System

Another case study is based on IEEE 118-bus system. Since the weighted PTDFD 2-zone is the same as PTDFD 2-zone, only three different zone partitions will be presented, which are single zone, PTDFD 2-zone, and ED 2-zone.

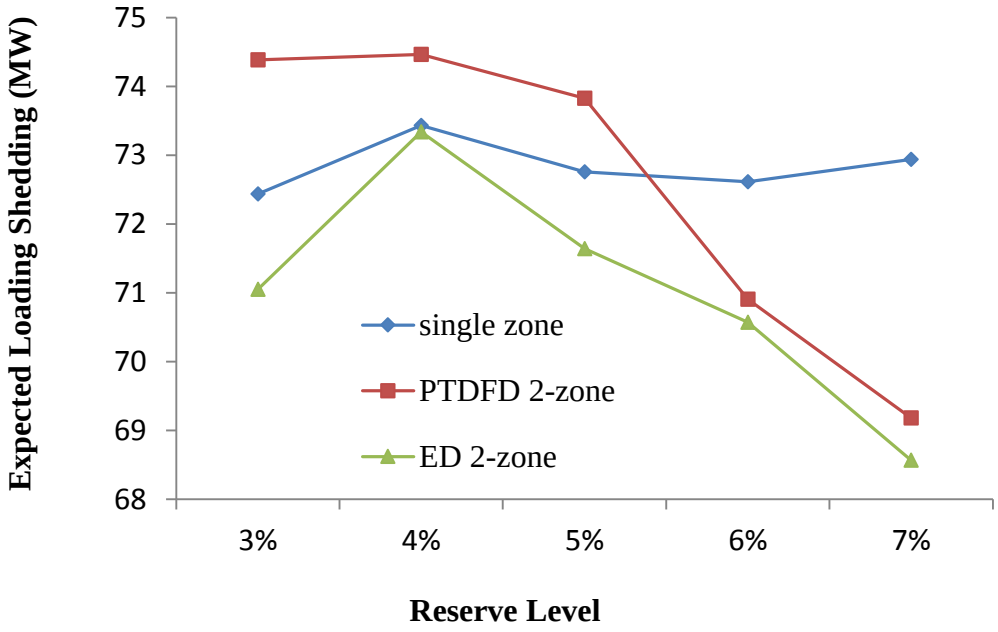

Figure 4.4 Expected Load Shedding (MW) from 3% to 7% of Peak Load with Single Zone, PTDFD 3-Zone, and ED 3-Zone

The result of expected load shedding is present in Figure 4.4. What makes the results interesting is that as the reserve level goes from 3% to 4%, the expected load shedding increases instead of decreasing, which implies increasing the reserve level does not necessarily improve the system reliability. The reason of this result is that increasing reserve level leads to committing a larger unit instead of several small units. Contrast to

losing a small unit, losing a large unit may cause more load shedding. However, based on the results of Figure 4.4, the load shedding typically decreases while the reserve level increases. The result of ED 2-zone is better than that of the single zone and the PTDFD 2-zone. Therefore, system reliability is improved by the ED 2-zone approach.

As depicted in Figure 4.5, as the reserve level goes up, the operating costs increase as well. The operating cost of the ED 2-zone and the PTDFD 2-zone is higher than that of single zone approach because the spinning reserve of the ED 2-zone and the PTDFD 2-zone approaches are more restricted.

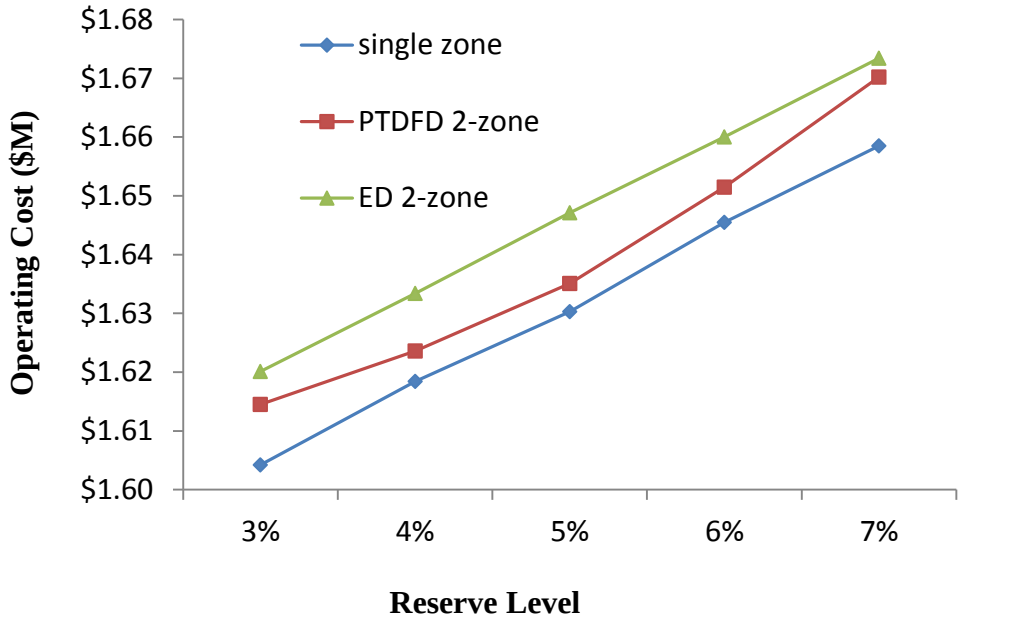

Figure 4.5 Operating Cost (Million dollars) from 3% to 7% of Peak Load with Single Zone, PTDFD 3-Zone, and ED 3-Zone

The expected total cost of three different zone partitions are displayed by Figure 4.6; the minimum expected total cost is achieved at the 7% reserve level by the ED 2-zone with the VOLL $40,000/MWh. While the expected costs of PTDFD 2-zone and ED-zone decrease steeply from 5% reserve level to 7% reserve level, the expected total cost for the

single zone result increases instead, which implies that the ED 2-zone and PTDFD 2-zone improve both market efficiency. Note that congestion for this IEEE 118-bus test system rarely happened, since the average line loading is only 20.97%, so the main reason of load shedding is insufficient reserve capacity.

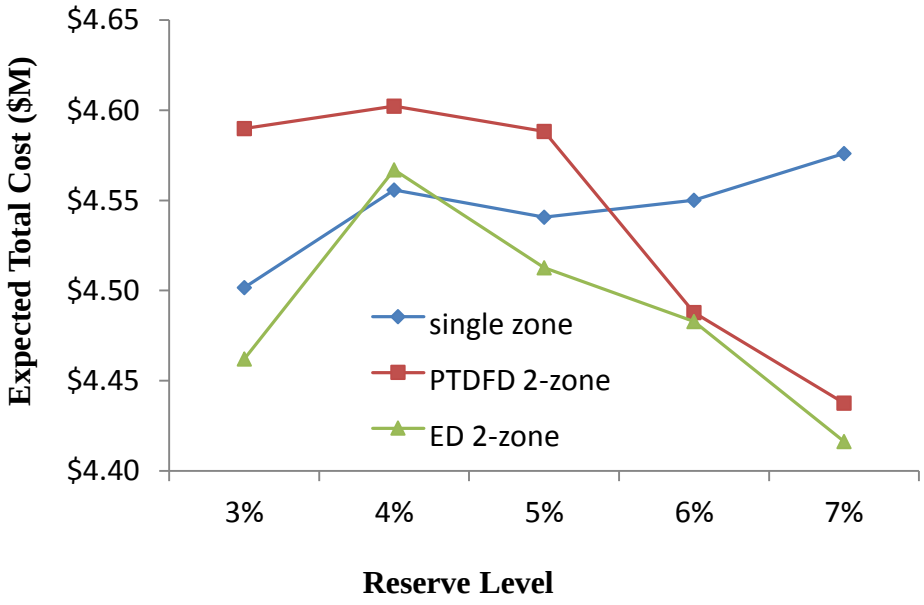

Figure 4.6 Expected Total Cost (Million dollars) from 3% to 7% of Peak Load with Single Zone, PTDFD 3-Zone, ED 3-Zone, and Weighted PTDFD 3-Zone with the Value of Lost Load at $40,000/MWh

5. DAILY RESERVE ZONE DETERMINATION WITH HIGH PENETRATION OF RENEWABLES

5.1 Introduction

The amount of renewable resources is expected to increase substantially in order to reduce the use of fossil fuel generators and reduce greenhouse gas emissions. For example, California's renewable portfolio standard (RPS) mandates that 33% of their electric energy production come from renewable resources by 2020 and beyond [35]. Most renewable resources (wind and solar) are semi-dispatchable (can only reduce power output) and their production is variable and uncertain. Due to the unpredictability and highly variable output of renewable generation, managing renewable resources while maintaining system reliability at least cost is a significant challenge. In order to manage the uncertainty and variability of renewable resources, adequate operating reserves must be acquired.

Prior research has investigated the impacts that renewable resources may have on reserve requirements, [37]-[42]. The New York Independent System Operator (NYISO) performed studies on the effects of wind energy production on transmission system planning, reliability, and operations [37] and also reported on the impacts on operating reserve. Another study, performed by Arizona Public Service (APS) in 2007, determined the amount of required reserve for wind penetration levels ranging from 1-10% for day-ahead scheduling [38]. In [39]-[40] the authors develop probabilistic metrics to determine the reserve requirements dynamically. The authors aimed to balance the operating costs with the outage costs by developing a probabilistic model, which accounts for renewable resources, generator outages, and transmission outages. M. A. Matos *et al.* [41] account for the probabilistic wind power forecasts, conventional generation outages, and load forecast

to determine the operating reserve level, and risk evaluation (e.g., risk of loss of load) is employed to determine the optimal level. [42] Short-term energy balancing with increasing levels of wind energy investigates the optimal short-term energy balancing to deal with the wind uncertainty, and it also states that dynamic reserve requirement can reduce the operating cost by decreasing excessive spinning reserve compared with static reserve policy, especially in the case of wind uncertainty.

In recent studies, the National Renewable Energy Laboratory (NREL) proposed a heuristic rule: the reserve should be no less than 3% of load and 5% of forecasted renewable generation [43]-[44]. While research has focused on the reserve quantity in response to renewable resources, few researchers have addressed the locational aspect of reserves, without the use of stochastic programming algorithms.

One method to address the locational aspect of reserves is to formulate a stochastic unit commitment framework; the imposed uncertainty of renewable resources can be implicitly modeled within the mathematical program, thereby allowing the optimal quantity and location of reserves to be determined, [15] [17] [45]. While stochastic programming produces an optimal solution (with respect to the modeled uncertainties), the concern is the computational burden.

Even today, there are many approximations that are built into deterministic day-ahead unit commitment (UC) models. For instance, even a full DC optimal power flow (DCOPF) model, which approximates the AC optimal power flow (ACOPF), is rarely solved with unit commitment for realistic systems today. Instead, nomograms are created that approximate transmission bottlenecks and a few key transmission corridor limits are explicitly enforced by including the power transfer distribution factors (PTDF) associated

with the generation. Once the UC solution is obtained, it is checked against the base case and select N-1 contingencies; the resulting constraint violations (line overloads) are then handled by either out of market corrections (i.e., based on the operator's discretion, the operator will modify the dispatch solution to obtain a reliable solution) or a feasibility cut is applied that enforces the previously violated constraints and the unit commitment model is solved again. While the process of applying feasibility cuts can be repeated (e.g., Benders' decomposition can be applied) in order to obtain the global optimal solution, such approaches are generally not used due to time limitations. Instead, system operators will directly modify the solution to obtain an N-1 reliable solution, i.e., implement out of market corrections.

Implementing stochastic programming will, therefore, be a greater challenge since stochastic programming relies on an accurate representation of power flow in order to obtain the optimal location for reserves. Thus, there is a need to improve the stochastic programming algorithms but there is also a need to enhance the approximations that exist today within unit commitment frameworks. Hence, there will be a need for better nomograms and dynamic reserve policies to complement stochastic unit commitment.

Existing reserve requirements within deterministic unit commitment models, formulations that do not have a stochastic programming framework, see (5—14) – (5—17), simply impose quantity requirements, not a locational aspect of the reserves. The underlying assumption is, thus, that the acquired reserve is assumed to be deliverable no matter the operational state of the network. This is, undoubtedly, an egregious assumption.

System operators address this issue by using reserve zones, producing nomograms that approximate transfer capabilities between regions and around key bottleneck areas, as well

as de-rating transmission lines. By specifying a partition of the network as a reserve zone, the operator is able to apply a regional reserve policy for that particular network partition. The motivation is to improve the deliverability of reserves by ensuring that the reserves are dispersed across the grid while not having to acquire more than is necessary in order to operate efficiently. However, there is still the assumption that there is no intra-zonal congestion that inhibits the deliverability of reserves.

Costs associated to manage intra-zonal congestion are already high even without high penetration levels of renewables. The California Independent System Operator (CAISO) and the Electric Reliability Council of Texas (ERCOT) incur significant costs to manage intra-zonal congestion [46]-[47]. For example, CAISO spent approximately $207 million in 2006 to mitigate intra-zonal congestion. In [48], CAISO describes what they refer to as Minimum Load Cost Compensation (MLCC), which they state, "these costs result from generating units that are committed to operate on a day-ahead basis under the provisions of the Must-Offer Obligation in order to mitigate anticipated intra-zonal congestion," [46]. The MLCC costs in 2006 were $109 million out of the total $207 million.

CAISO also describes in [46] that, if the market solution does not resolve the intra-zonal congestion, they may dispatch reliability must run (RMR) units, call energy bids out of sequence (OOS) (change their scheduled dispatch), or they may call units out of market (OOM) (turn on additional units). In this thesis, such procedures are referred to as out of market corrections. Note that CAISO has since made changes to their market structure through their market redesign and technology upgrade (MRTU) by having a more accurate grid model in order to reduce such costs.

With the trend towards higher levels of intermittent renewable resources, the location, i.e., deliverability, of reserves will increase in importance. Higher levels of renewables not only increase the reserve level but also increase the difficulty to predict the network flows and the resulting bottlenecks. Existing procedures will, thus, be even more inefficient at achieving system reliability at least cost. Additional reserves will need to be acquired, thereby forcing generators to operate at undesirable production levels for the sake of providing reserves; many conventional fossil-fuel based generators are not designed to operate at such low operating levels where their average costs and emissions are higher. While it is possible to rely on such ad-hoc reserve policies and out of market corrections to ensure reliable operations, such procedures drive up the costs. Thus, the creation of new, efficient reserve policies is paramount to ensure reliable system operations at least cost.

One way to improve reserve deliverability is by improving the reserve zones since the added computational complexities are minimal, if at all, and they are effective at imposing locational reserve requirements without incurring excessive operational costs. However, there is limited knowledge regarding how to optimally partition the network into reliable and efficient reserve zones while considering the system operational conditions and uncertainties, e.g., contingencies, load, area interchange, and renewable resources. For instance, one of the most common ways to determine reserve zones is based on asset ownership, instead of determining the reserve zones based on system operating conditions. Furthermore, existing reserve zones are treated as static even though the operational conditions widely vary. Such a static operational rule for such a dynamic and complex engineered system results in inefficiencies.

This chapter proposes a new method to determine reserve zones on a daily basis, which is capable of accounting for the variability and uncertainty in renewable resources and it is able to account for N-1 contingencies as well. First, due to the computational complexities of stochastic programming, limited renewable generation scenarios are modeled within dispatch optimization models (existing practices typically model one scenario, the forecasted wind, i.e., they solve deterministic unit commitment models). As a result, there will be unexpected congestion that operators will have to resolve (both at the day-ahead and real-time stages) for base-case (no-contingency) operations. Second, existing approaches also do not explicitly account for N-1 contingencies (while reserve rules are used, they do not optimally locate reserves). The proposed dynamic reserve zone model improves the locational aspect of reserves for the day-ahead scheduling process in an effort to reduce such out of market corrections.

5.2 Dynamic Zones Based on Probabilistic Flow

Day-ahead forecasting techniques for renewable resources are roughly 10% to 20% inaccurate [48]. While the accuracy of the forecast improves as the future period approaches, system operators must ensure a reliable solution at each look-ahead time stage (e.g., day-ahead, hour-ahead). Intermittent renewable resources impose added uncertainty to system operations, making it more challenging to guarantee that the acquired reserve will be deliverable, i.e., congestion will not impede the necessary reserve from reaching its destination. Inadequate procurement of reserves (quantity and location) forces operators to make costly out of market corrections. System operators may need to turn on additional local generation to compensate for deliverability issues. These actions, which are made outside of the optimization engine and based on operator knowledge (or lookup tables), are

costly. Furthermore, the probability that the system operator is able to determine a cost effective corrective solution is likely to decrease as resource uncertainty increases. Advanced reserve determination procedures can improve economic efficiency and reliability, by reducing costly out of market corrections and by reducing the probability of outages.

This section proposes a reserve zone partitioning framework that involves the variability and uncertainty of renewable resources (wind) by creating a zone partitioning method based on wind scenarios. The zone partitioning procedure is demonstrated below and the flowchart is illustrated in Figure 5.1.

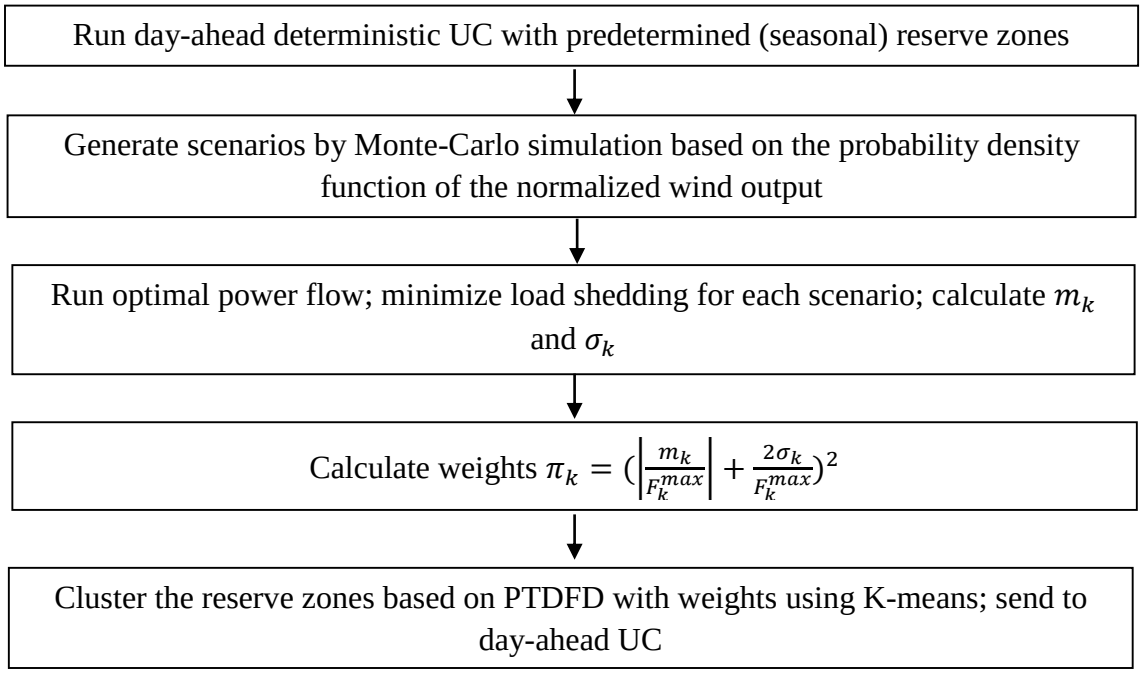

Figure 5.1 Flowchart for Daily Reserve Zones Based on Probabilistic Power Flows

Step 1 A deterministic unit commitment is solved based on predetermined (e.g., seasonal) zones. The unit commitment solution is then fixed for Step 3. The unit commitment formulation will be discussed in Chapter 5 Section 5.3.

Step 2 Generate the wind scenarios by Monte-Carlo simulation in order to characterize the potential wind power output. The wind scenario generation procedure is presented in Chapter 5 Section 5.6

Step 3 Solve the optimal power flow (OPF) with selected wind scenarios and record the power flows for the various wind scenarios. The expected power flow on transmission line k, represented by m_k, and the standard deviation of power flow of transmission line k, i.e., σ_k, are calculated.

Step 4 Calculate the weight, π_k, for each transmission line: $\pi_k = (\left|\frac{m_k}{F_k^{max}}\right| + \frac{2\sigma_k}{F_k^{max}})^2$; the term is squared in order to place more attention to the critical paths.

Step 5 Run the statistical clustering algorithm (K-means) to partition the reserve zones based on PTDF differences and the weights from Step 4.

The proposed method to determine the reserve zones is sensitive to the chosen weights. The first fraction of the weight, the expected line flow divided by the line's maximum capacity, is similar to the commonly known performance index (PI) [4] for one specific line. The second fraction of the weight is based on the standard deviation. The desire is to identify critical lines not only based on their expected line flow (for the following day) but also by the variability and uncertainty of the line's flow, which is caused by the intermittency of the renewable resources. This helps to ensure that critical transmission bottlenecks can be identified in order to determine better reserve zones. For the weight term that is used in this chapter, *n* (see [4], page 430) is equal to one.

The standard deviation part can be viewed as a confidence interval. Using only the mean value $\left|\frac{m_k}{F_k^{max}}\right|$ doesn't reflect the potential power flow uncertainty, which is caused by intermittent resources. For instance, transmission line A with lower average power flow uncertainty may have a higher possibility of getting congested than that of transmission

line B, which has a higher average power flow due to higher uncertainties of the probabilistic power flow on the transmission line A. This is why the mean value of the line plus its variation is considered. However, increasing the bias on the standard deviation to 4 seems to be too much, $(\left|\frac{m_k}{F_k^{max}}\right| + \frac{4\sigma_k}{F_k^{max}})^2$, as this puts too much bias on the power flow variation.

Table 5.1 Tested Weights and Resulting Congested Zonal Links

Weights	**Critical Transmission lines as zonal links (Total number 10)**
$\left\|\frac{m_k}{F_k^{max}}\right\|$	3
$(\left\|\frac{m_k}{F_k^{max}}\right\|)^2$	4
$\left\|\frac{m_k}{F_k^{max}}\right\| + \frac{2\sigma_k}{F_k^{max}}$	3
$(\left\|\frac{m_k}{F_k^{max}}\right\| + \frac{2\sigma_k}{F_k^{max}})^2$	5
$(\left\|\frac{m_k}{F_k^{max}}\right\| + \frac{2\sigma_k}{F_k^{max}})^4$	5
$(\left\|\frac{m_k}{F_k^{max}}\right\| + \frac{4\sigma_k}{F_k^{max}})^2$	3

Table 5.1 presents the number of critical lines cut by different reserve zone partition based on different weights. The metric that cuts most of the critical transmission lines (the line is not contained within any single zone) will be chosen.

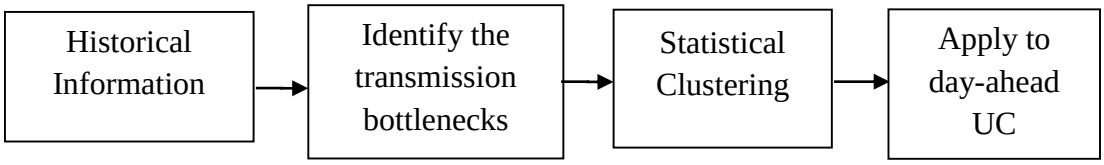

Figure 5.2 Traditional Seasonal Zone

From Figure 5.2, the traditional seasonal zone identifies the transmission bottleneck by historical information that does not take the advantage of the "newest" system operational conditions.

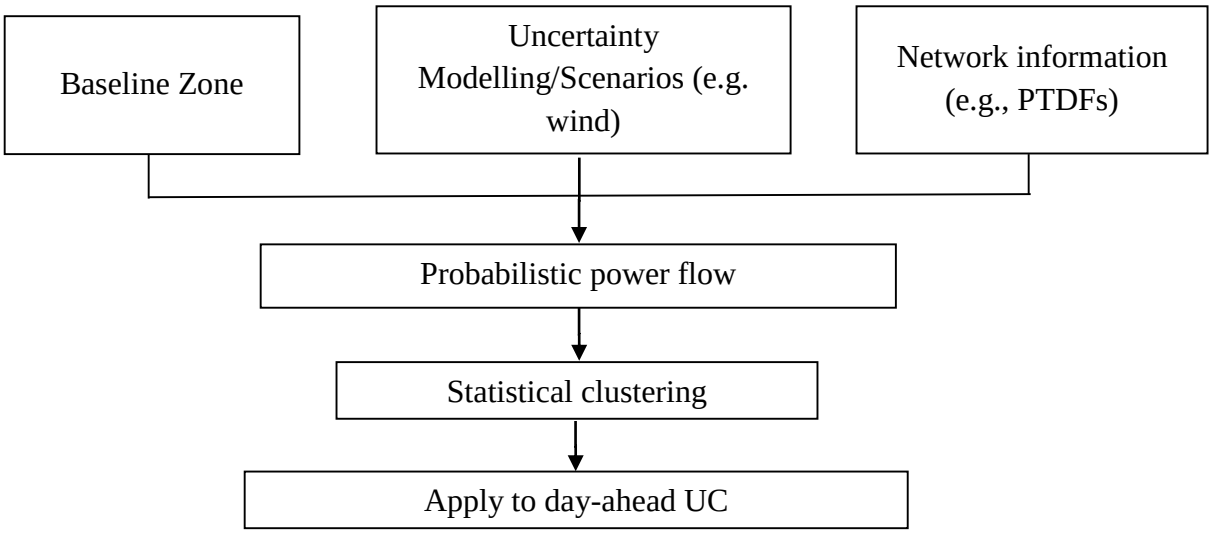

Figure 5.3 The Reserve Zone Determination Method Based on Probabilistic Power Flow

From Figure 5.3, the probabilistic flow has the information of baseline zone, uncertainties modeling (e.g., wind), and network information. The probabilistic flow can reflect the system operational conditions. For example, system operators will utilize the day-ahead wind forecast and potential forecast error to capture the wind output and its variation's impact on the power flow, which is not accounted for in the seasonal zone. The method can be easily extended to other uncertainties such as other intermittent resources and load.

Note that probabilistic flows are generated based on wind uncertainty and that the procedure can be easily extended to consider other uncertainties (load, N-1).

5.3 Security Constrained Unit Commitment

Security constrained unit commitment is formulated as a mixed integer programming (MIP) problem and is shown by (5—1) to (5—18).

Minimize: $$\sum_{t\in T}\sum_{g\in G}[C_g p_{gt} + C_g^{SU} su_{gt} + C_g^{SD} sd_{gt} + C_g^{NL} u_{gt}] \quad (5—1)$$

Subject to:

$$su_{gt} - sd_{gt} = u_{gt} - u_{g,t-1}, t \in T, g \in G \quad (5—2)$$

$$0 \le su_{gt} \le 1, t \in T, g \in G \quad (5—3)$$

$$0 \le sd_{gt} \le 1, t \in T, g \in G \quad (5—4)$$

$$\sum_{k\in K^+(n)} f_{kt} - \sum_{k\in K^-(n)} f_{kt} + \sum_{g\in G(n)} p_{gt} - \sum_{w\in W(n)} sp_{wt} = D_n^t - \sum_{w\in W(n)} P_{wt}, t \in T, n \in N \quad (5—5)$$

$$0 \le sp_{wt} \le P_{wt}, t \in T, w \in W \quad (5—6)$$

$$f_{kt} = B_k(\theta_{nt} - \theta_{mt}), t \in T, k = (n,m) \in K \quad (5—7)$$

$$-F_k^{max} \le f_{kt} \le F_k^{max}, t \in T, k \in K \quad (5—8)$$

$$u_{gt}P_g^{min} \le p_{gt} \le u_{gt}P_g^{max}, t \in T, g \in G \quad (5—9)$$

$$\sum_{t'=t-UT_g+1}^{t} su_{gt'} \le u_{gt}, t \in (UT_g, \ldots, T), g \in G \quad (5—10)$$

$$\sum_{t'=t-DT_g+1}^{t} sd_{gt'} \le 1 - u_{gt}, t \in (DT_g, \ldots, T), g \in G \quad (5—11)$$

$$p_{gt} - p_{g,t-1} \le R_g^{HR}, t \in T, g \in G \quad (5—12)$$

$$p_{g,t-1} - p_{gt} \le R_g^{HR}, t \in T, g \in G \quad (5—13)$$

$$r_{gt}^{SPIN} \le P_g^{max} u_{gt} - p_{gt}, t \in T, g \in G \quad (5—14)$$

$$r_{gt}^{SPIN} \le R_g^{10} u_{gt}, t \in T, g \in G \quad (5—15)$$

$$\sum_{\gamma\in G} r_{\gamma t}^{SPIN} \ge p_{gt} + r_{gt}^{SPIN}, t \in T, g \in G \quad (5—16)$$

$$\sum_{g\in \mathrm{G(z)}} r_{gt}^{SPIN} \ge 3\% \sum_{n\in N(z)} d_{nt}$$

$$+5\% \sum_{w \in W(z)} P_{wt}\,, t \in T, \mathrm{z} \in Z \qquad (5\text{—}17)$$

$$u_{gt} \in \{0,1\}, t \in T, g \in G \qquad (5\text{—}18)$$

The objective, (5—1), minimizes the operating cost, which includes start-up cost, shut-down cost, no-load cost, and the variable operating cost. The modeling of the start-up and shut-down variables is shown by constraints (5—2) – (5—4). Constraint (5—5) is the node balance constraint, which ensures that the net injection into a bus equals the net withdrawal. Constraint (5—6) is the wind curtailment (wind spillage) constraint. Equation (5—7) is the linearized real power line flow equation. Constraint (5—8) imposes the transmission line's rating (thermal or stability rating). Constraint (5—9) identifies the maximum and minimum operating capacity of each generator. Constraints (5—10) and (5—11) are the minimum-up and down time constraints, which are facet defining valid inequalities for the *u*, *v* restriction. Constraints (5—12) and (5—13) are the hourly ramp rate constraints. Constraints (5—14) – (5—15) are the spinning reserve constraints. Constraint (5—14) shows that the committed production plus spinning reserve offered by unit g cannot exceed its rated capacity. Note that the right hand side of (5—9) could be modified to capture (5—14); they are written separately simply for convenience. Constraint (5—15) represents that a unit's spinning reserve cannot be larger than its ten minute ramping capability. CAISO defines its operating reserve 2 (OR2) quantity as the maximum of the single largest generator outage, the largest net tie-line import, or based on an operator imposed value [5]. Constraint (5—16) is used to ensure that the amount of spinning reserve is no less than the single largest generator contingency; the formulation does not include restrictions related to tie-line imports or operator imposed quantities due to the chosen IEEE test system.

Constraint (5—17) shows that, for each zone *h*, the spinning reserve should not be less than 3% of the load and 5% of the forecasted renewable production (wind), [44].

5.4 N-1 and Wind Reliability Studies

To test the system reliability of the unit commitment solutions, two cases will be studied:

1) Only wind scenarios (this is the base-case, no-contingency case plus possible wind deviations – 1000 wind scenarios).

2) N-1 contingencies combined with wind scenarios (this is a post-contingency evaluation with, at most, 237 single contingencies combined with ten wind scenarios to create roughly 2370 N-1 plus wind scenarios).

Case 1 can be viewed as a normal operating condition without a generator or transmission contingency. Case 2 can be viewed as the contingency state with a single generator or transmission contingency; the simulation would represent the post-contingency operating condition within ten-minutes of the event. The N-1 and wind contingency studies are performed by solving an optimal power flow; the objective is to minimize the load shedding for each scenario with the commitment variables fixed to the original UC solution. Generation re-dispatch is allowed to the extent that a generator's output must be within its scheduled dispatch (from the original UC solution) plus or minus its ten-minute ramp rate, i.e., a generator can only move away from its scheduled dispatch level based on the amount of ten-minute reserve that it can provide. The probability of the normal operating condition is calculated to be 0.95 and the probability of any single N-1 contingency is 0.05, for any single hour; this is an outage replacement rate (ORR) for one hour [1]. This probability is calculated based on the mean time to failure (MTTF), [49]. The detailed calculation procedures are listed in the Appendix D.

5.5 Out of Market Corrections

There are many uncertainties in the power system today, such as load, renewables, generation and transmission contingencies, and are interchange. Unit commitment, which has thousands of transmission assets and generators with complex operating constraints, is a very computationally challenging problem. There are three main ways of managing those uncertainties:

1. Apply reserve requirements constrains to protect against uncertainties. For example, regulation reserve can be utilized to protect against load uncertainties and small forecast error of renewables, and operating reserve can be used to take care of contingencies.
2. Stochastic programming can be used to explicitly model uncertainties in the power system. However, the computational complexity in the large scale optimization is still a huge challenging and it is still not scalable enough to apply in the realistic power system.
3. Out of market corrections (OMCs) is an alternative to correct unreliable system solution such that reliable solutions are obtained.

Out of market corrections (OMC), also called out of market corrections by CAISO, occur when a dispatch solution must be corrected by the operator in order to satisfy a system requirement that was not implicitly or adequately modeled within the dispatch optimization problem. For instance, in current industry practice, nomograms (hyperplanes) are applied to approximate the feasible solution region. Inaccuracy of nomograms may require correction of the solution to ensure a feasible solution. Such procedures are taken to simplify the complex combinatorial dispatch problems that are solved daily and, in some locations, hourly. While such procedures are currently necessary in order to ensure a

solution is obtained within the required timeframe, the resulting out of market corrections that are necessary to correct for these approximations are extremely costly. The California Independent System Operator (CAISO) and the Electric Reliability Council of Texas (ERCOT) collectively spent roughly $80 million in 2006 on their out of market corrections [46] [47].

In [50] and [51], CAISO develops OMCs with lower price inconsistencies. OMCs will be used by CAISO unless no feasible solution is obtained. Regional Transmission Operators, such as SPP and ERCOT, also perform OMCs [52] and [53], if no feasible solution is found with economic bids. In [54], how system reliability is considered in day-ahead (DA) to real-time (RT) business processes of SPP integrated marketplace is discussed. System-wide and zonal requirement is evaluated based on system reliability and OMCs.

OMCs (out of market corrections) are employed by all energy providers: vertically integrated utilities or independent system operators (ISO). In particular, implementing OMCs under a deregulated market structure impact the market outcomes for its stakeholders. Performing an OMC changes the original solution, which is considered to be the most economical solution but is infeasible since it does not satisfy the reliability requirements.

5.6 Scenario Generation and Selection

There are many different approaches to generate wind scenarios. In [15], the wind speed is forecasted based on an autoregressive (AR) model, which is developed based on historical data, and the wind power production is mapped to the forecasted wind speed. AR models are accurate for short-term or mid-term wind power forecasting [54]; however, for

day-ahead wind power forecasting other techniques, such as numerical weather predictors (NWP) and artificial neural networks (ANN), are used to improve the accuracy of the forecast [54]. Since this chapter is focused on determining reserve zone partitions, determining new forecasting methods for day-ahead wind predictions is outside the scope of this thesis. Accurate wind scenarios are needed to examine the proposed dynamic reserve zone determination technique. Instead of forecasting wind speed, wind power scenarios are generated directly. Wind forecast data is taken from NREL and one thousand wind power scenarios are generated by Monte-Carlo simulations. For each period *t*, it is assumed that the probability distribution of the wind forecast error is Gaussian with a mean of zero and a standard deviation represented by σ_t. The folded Gaussian distribution can be used to determine the expected absolute error in order to calibrate the standard deviation to reflect typical forecasting errors, [48], for day-ahead wind forecasts. The expectation of the folded Gaussian distribution is shown by (21), where μ_t is the mean at time *t* and σ_t is the standard deviation at time *t*. Since the mean is zero, (21) becomes (22). σ_t is chosen to be 0.2 in order to create an expected absolute error of 16%, which is in the 10% to 20% range for day-ahead forecasting errors, [48].

$$E(error_t) = \sigma_t\sqrt{2/\pi}\, e^{(-\mu_t^2/2\sigma_t^2)} + \mu_t[1 - 2\Phi\left(\frac{-\mu_t}{\sigma_t}\right)] \qquad (5—19)$$

$$E(error_t) = \sigma_t\sqrt{2/\pi} \qquad (5—20)$$

Note that the distribution for the forecast error for a particular wind farm is not necessarily Gaussian; [55] uses a Rayleigh distributions for the forecast error while other distributions, Weibull and Beta, have been used as well [56]-[59]. However, as discussed in [58] and shown by the empirical studies from [59], with geographically diverse locations

for the wind farms, it is appropriate to apply the central limit theorem and, thus, assume a normal distribution for the forecast error. To account for the fact that the wind speed cannot be negative and that the wind turbine cannot produce more than its capacity, a truncated normal distribution has been suggested by CAISO, [60]. The proposed reserve zone determination approach is general enough to be compatible with any forecast error probability distribution.

Table 5.2 Selected Wind Scenario Probabilities

Scenario	Probabilities
1	0.593
2	0.08
3	0.025
4	0.06
5	0.043
6	0.072
7	0.043
8	0.011
9	0.02
10	0.053

A scenario reduction procedure is used to reduce the number of scenarios. Scenarios with low probabilities are eliminated and scenarios that are similar are combined. The scenario reduction techniques presented in [61] and [62] are applied to select ten wind scenarios out of the 1000 scenarios, which are used within the extensive form stochastic unit commitment problems. With the predetermined number of selected scenarios, scenarios will be selected such that the distance between the deleted scenarios is minimized. The probability of the deleted scenarios will be combined with the selected scenarios. The probabilities of selected wind scenarios are listed below.

5.7 Numerical Results

5.7.1 Data

A modified IEEE 118-bus test system is used to test the proposed zone partitioning method [49], the detailed information is listed in the Appendix C Section C.2. The system has 57 units (3 of which are wind), 186 transmission lines, and 91 loads; since the IEEE 118-bus test system is missing information, additional information is taken from the RTS 1996 test system [49] and from [45]. The generation capacity is 6982MW and the peak load is 4919MW. Three wind farms with 1200MW of capacity are placed at three buses, which is roughly 17% of the total installed generation capacity (total wind capacity divided by total system-wide generation capacity). Seasonal load information is taken from the RTS96 test system [49] for twelve days between January 1st and March 31st; the highest load day is January 9th, which is 90% of the yearly peak. Three of these days are weekend days and two of these days have a peak hour that is roughly 55% of the yearly peak load. The wind data is collected from the NREL 2006 western wind database from January 1st to March 31st. The original 10-minute data is averaged into hourly data, which is used as the forecasted wind output.

5.7.2 Numerical Results and Analysis

The proposed daily probabilistic-based dynamic zone partitioning method is used in combination with a deterministic unit commitment model and it is also combined with an extensive form stochastic unit commitment model. These two proposed frameworks are compared against two traditional zone partitioning models (a seasonal method and a daily method) and a stochastic programming framework that explicitly represents ten wind

scenarios, has only one reserve zone, and uses traditional reserve rules (reserve must exceed the single largest contingency). The only difference between the two stochastic models is that the first has its reserve zones determined by the proposed dynamic reserve zone method and the second has one reserve zone.

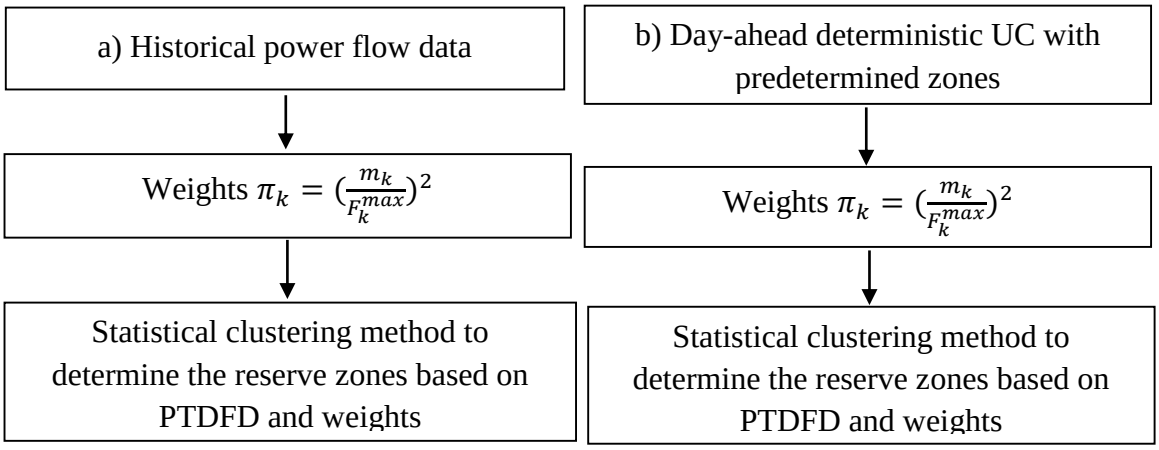

Figure 5.4 a) Flowchart for the Seasonal (Traditional) Method. b) Flowchart for the Daily (Traditional) Method

The seasonal and daily zone methods are determined as shown by Figure 5.4. The seasonal method is meant to mimic modern zone partitioning methods at ERCOT [21] and MISO [63]. Seasonal zone partitioning methods use historical information to identify key transmission bottlenecks. Generators that have similar impacts on these key transmission corridors are grouped together by utilizing a statistical clustering algorithm (K-Means). The traditional daily method builds on the seasonal method by using weights to adjust the zones on a daily basis, as shown by Figure 5.4.

The stochastic programming model is an extensive form scenario-based unit commitment formulation with ten scenarios modeled, which is similar to [9]. For all deterministic models, reserve requirements follow the NREL 3+5 rule as well as the largest contingency rule, which are constraints (5—16) and (5—17). For the stochastic models,

reserve requirements follow 3 percent of load in each reserve zone as well as the largest contingency rule; there is no reserve requirement imposed with respect to the forecasted wind output since that is handled by the explicit representation of the wind scenarios. The daily (probabilistic) zone model with stochastic UC follows the reserve rules used within the single-zone stochastic programming framework.

The five zonal models are applied to a day-ahead unit commitment problem and their resulting solutions are then tested against wind scenarios combined with N-1 contingency analysis. Table 5.3 presents the results for the expected load shedding for one thousand wind scenarios associated to the row labeled wind. The wind+N-1 row reports the expected load shedding when testing the solutions against N-1 (contingency analysis) simultaneously combined with ten wind scenarios (i.e., each contingency is simulated ten times for each wind scenario). The total overall expected load shedding is also presented along with the percent improvement for the various models.

When analyzing the proposed UC solutions against the 1000 wind scenarios, the expected involuntary load shedding for the seasonal (traditional) zone model is 3.522MW, with six days having involuntary load shedding, and the average load shedding of the daily (traditional) zone model is 2.55MW. This result demonstrates the advantage of updating reserve zones as operating conditions change since the load shedding reduced by 27.6%. The stochastic UC model with a single zone has 0.162MW of expected load shedding. Modeling all of the wind scenarios is computationally intractable; thus, ten scenarios are selected in this stochastic programming framework, which is why there is still load shedding. There is only 0.085MW of expected load shedding for the daily (probabilistic) zone model with a deterministic UC framework since it is better at ensuring reserve

deliverability. For this particular test case, the results show that the daily (probabilistic) zone model with stochastic UC is preferred over existing methods, since it has the lowest expected load shedding for the one thousand wind scenarios, with 0.01MW of expected load shedding. While the stochastic unit commitment framework only included ten wind scenarios out of the original one thousand, the expected load shedding is very close to zero, which shows the ability for the dynamic reserve zones to substantially improve the locational aspect of reserves.

Table 5.3 Expected Load Shedding (MW)

	Deterministic UC			Stochastic UC	
Zonal Model	Seasonal[1]	Daily[2]	Daily (Prob.)[3]	Single zone[4]	Daily (Prob.)[5]
Wind	3.522	2.55	0.085	0.162	0.01
Wind + N-1	13.5	13.13	10.45	20.37	9.62
Total	17.022	15.68	10.535	20.532	9.63
Improvement	-	7.88%	38.1%	-20.6%	43.42%

[1]Seaonal (traditional) zone model; [2]Daily (traditional) zone model; [3]The proposed daily (probabilistic) zone model with deterministic UC; [4]Stochastic UC model with a single zone; [5]The proposed daily (probabilistic) zone model with stochastic UC.

The five models are also tested against N-1 contingencies simultaneously with (plus) the selected ten wind scenarios; these methods against the N-1 contingencies plus the one thousand scenarios are not tested since it is computationally intense (more than 210k scenarios per hour per day). The involuntary load shedding of each case is presented in Table 5.3. The stochastic UC model with a single zone has the most involuntary load shedding, which is 20.37MW since the stochastic UC model with a single zone does not account for N-1 contingencies explicitly. The stochastic program only includes an explicit representation of the ten wind scenarios and traditional reserve requirements are used to protect against N-1 contingencies. The traditional (seasonal) zone model has 13.5MW of

expected involuntary load shedding, which is much better than the result of the stochastic program. This result is caused by the stochastic UC model including only one reserve zone whereas this seasonal model has three zones.

The load shedding of the daily traditional method is 13.13MW, which is lower than the seasonal approach since it predicts the next day's operating conditions better than the seasonal reserve zone model. The daily (probabilistic) zone model with deterministic UC has 10.45MW of expected load shedding, which demonstrates its ability to perform better than existing practices of using seasonal reserve zones. It also performs better than the daily (traditional) reserve zone procedure. The proposed daily (probabilistic) zone framework is able to identify congestion and reserve deliverability issues for the following day as it is based on probabilistic power flows related to the potential wind scenarios. Even though the daily (probabilistic) zone model with deterministic UC is a heuristic, the extensive empirical results demonstrate its superior ability to account for deliverability issues of reserves. The daily (probabilistic) zone model with stochastic UC performed the best with an expected load shedding of 9.62MW. However, while combining the dynamic reserve zone model with stochastic programming made an improvement, the solution time is much longer (see Table 5.9).

Table 5.3 also presents the total expected load shedding when adding up the expected load shedding for the base-case (no-contingency plus wind scenarios) with the contingency case (N-1 contingencies plus wind scenarios). The percent improvements are also shown, with respect to the seasonal reserve zone model. The daily traditional method improved the result by 7.88%. The daily (probabilistic) zone model with a deterministic UC formulation has 10.54MW of load shedding, a 38% improvement over existing reserve zone methods.

The daily (probabilistic) zone model with a stochastic UC formulation has the least expected load shedding, with 9.63MW of load shedding, but it also has the longest computational time (see Table 5.9). The stochastic UC with a single zone result performed worse than the seasonal zone model, primarily because there was only one zone imposed. While the stochastic programming (single-zone) approach can be improved by imposing a similar reserve zone rule within its formulation, the results show that, even though reserve policies are approximations, such reserve policies can be very effective. Even as computational advances are achieved with stochastic programming algorithms, there will continue to be a reliance on such reserve policies. It is critical to advance reserve policies and stochastic programming algorithms as well as design algorithms that rely on a balanced approach between these methods.

Note that the presented load shedding results come from contingency (or wind scenario) analysis; all solutions would be corrected via out of market corrections as the final day-ahead schedule must satisfy N-1 and the wind uncertainty. Detailed results for the expected load shedding can be found in Table 5.7 and 5.8, which reports the expected load shedding for each day (α), the number of scenarios that have a violation per one thousand scenarios (β), and the worst-case single violation for any single hour across the entire day (δ).

Table 5.4 Operating Cost and Expected Total Cost ($ Million)

	Deterministic UC			Stochastic UC	
Zonal Model	Seasonal	Daily	Daily (Prob.)	Single zone	Daily (Prob.)
Operating Cost	0.651	0.654	0.666	0.636	0.660
Expected Cost	0.702	0.701	0.698	0.698	0.689
Improvement	-	0.16%	0.64%	0.64%	1.82%

Based on the results in Table 5.4, the stochastic UC model with a single zone has the least average operating cost, which is $0.636 million. The average operating costs of the daily traditional and the seasonal zone methods are similar: $0.654 million and $0.651 million respectively. The daily (probabilistic) zone model with deterministic UC has the highest average operating cost, which is $0.666 million. The daily (probabilistic) zone model with stochastic UC has $0.660 million. Detailed results for the operating cost can be found in Table 5.9.

The reported average operating cost above does not account for the fact that the solutions are not reliable, i.e., they allow for load shedding. After the original day-ahead unit commitment solution is obtained, contingency analysis is performed and, if the solution does not satisfy N-1, then out of market corrections are necessary. It is difficult to quantify the costs of the out of market corrections relative to the quantity of load shedding as the out of market corrections are based on operator knowledge. Furthermore, the process of adjusting day-ahead unit commitment schedules to achieve reliable solutions will become more difficult and costly in the future with higher levels of intermittent renewables. If the load shedding costs are approximated with an adjustment cost of $3,000/MW, the stochastic plus dynamic reserve zone model have the lowest expected total cost. Such a result implies the method improves the economic efficiency by 1.82% comparing with the seasonal model. Note that the number of violations and/or the size of the single worst violation may be a better indicator in regards to the costs to perform the out of market corrections as compared to the expected load shedding. In regards to these other metrics, the proposed methods perform even better in comparison to existing techniques (see the detailed results in the Appendix). Future work will focus on applying out of market

corrections procedures in order to determine a more accurate cost assessment of these methods.

5.8 Computational Complexity

All problems were solved using CPLEX12.2 with a 3.6GHz processor and 48GB RAM; the optimality gap was set to 0.01% for the deterministic UC problems. From Table 5.5, the proposed method has a similar solution time as compared to the other deterministic approaches.

Table 5.5 Average Solution Time for Deterministic UC (s)

Zone model	Seasonal	Daily (Traditional)	**Daily (Probabilistic)**
Solution time	18	23	26

From Table 5.6, the extensive form stochastic UC problems take much longer time to solve in comparison to deterministic formulations. While Benders' decomposition can be used to improve the solution time of stochastic UC, the solution time is still not as good as deterministic formulations and there is also a problem with scalability for large-scale systems today. Larger optimality gaps may improve the solution time but then the solution quality is generally worse.

Note that there are a variety of decomposition algorithms that can be applied to try to improve the computational performance of stochastic unit commitment, e.g., Lagrange relaxation (LR), progressive hedging (PH), Benders' decomposition, as well as others. For this IEEE test case, Benders' decomposition did not improve the solution time dramatically.

Table 5.6 Average Solution Time for Extensive Form Stochastic UC (s)

Zone model	Single zone			**Daily (Probabilistic)**
Benders	No	Yes	Yes	No
Optimality gap	0.01%	0.01%	0.1%	0.01%

Solution time	339	321	90	505

For this particular stochastic unit commitment formulation, the subprolem for the Benders' decomposition approach is a feasibility problem and the subproblem formulation can be broken into ten independent subproblems that can be solved in parallel. This is possible as there are no constraints binding one scenario to another scenario; scenarios are only tied together through the first stage decisions, which are determined in the master problem and fixed within the subproblem formulation for Benders' decompsition. This allows for these independent subproblems to be solved in parallel but note that the reported solution times reflect a sequential procedure for solving the subproblems; with only ten subproblems, which are all linear programs, the improvement in solution time is minimal for this particular experiment as the majority of the time is spent solving the master problem. However, for larger systems and when there are more scenarios, it would be beneficial to solve the subproblems in parallel.

While Benders' decomposition did not dramatically improve the solution time over the extensive form stochastic unit commitment problem, it is expected that, for large-scale models, it will perform better than an extensive form formulation that will have a massive memory requirement. However, this still does not mean that Benders' decomposition will scale well. Benders' decomposition is known to have a bloat problem; at each iteration, additional cuts are applied to the master problem and it is possible for the master problem to grow in size such that it takes too long to solve or there can be a memory issue for the master problem as well. On the other hand, this work has demonstrated that better reserve rules can be used within a deterministic unit commitment problem formulation to improve the reliability of the proposed SCUC solution without substantial increases in costs;

furthermore, such deterministic SCUC formulations will not suffer from scalability issues like stochastic programming formulations.

More recent research has examined horizontal decomposition algorithms like progressive hedging (Benders' decomposition is a vertical decomposition approach), [64]-[66]. While PH cannot guarantee an optimal solution for mixed-integer programs, it has the advantage that it is trivial to parallelize and the problem structures at each iteration do not grow in complexity (suffer from bloating) like Benders decomposition. The drawback of PH is that it requires parameter tuning. PH may also struggle to converge. Overall, the preferred approach to handle stochastic unit commitment is not to rely fully on deterministic reserve policies or stochastic programming algorithms but to have a balanced approach; ongoing work is aimed at using the advances presented within this section to help improve the convergence of PH for stochastic unit commitment.

Table 5.7 Expected Load Shedding with Wind (MW)

	Deterministic UC			Stochastic UC	
Date	Seasonal	Daily	**Daily (Probabilistic)**	Single Zone	**Daily (Probabilistic)**
2-January	6.5 (4.7, 116)[1]	0.684 (2.1, 24)	0.36 (1.9, 14)	0.12 (0.6, 13)	0.09 (0.57, 10)
9-January	0	0	0	0	0
14-January	6.16 (3.5, 109)	0	0	0.31 (1.5, 15)	0
24-January	8.44 (4.6, 121)	0.16 (1.2, 11)	0	0.16 (0.9, 11)	0
5-February	0	0	0	0.1 (0.4, 11)	0
7-February	0	0	0	0.62 (1.0, 31)	0
14-February	0	0	0	0.64 (1.1, 30)	0
22-February	0	0	0	0	0
3-March	5.7 (3.3, 93)	8.55 (4.2, 132)	0	0	0
11-March	12.08 (6.5, 132)	7.52 (5.4, 87)	0.66 (1.3, 33)	0	0
14-March	0	0	0	0	0
26-March	3.38 (5.2, 41)	13.68 (8.5, 127)	0	0	0

[1] α (β, δ); α represents the expected load shedding (MW), β represents the number of scenarios that have a violation per one thousand scenarios, and δ represents the largest violation (MW) from any single hour across the entire day.

Table 5.8 Expected Load Shedding with Wind and N-1 Contingencies (MW)

	Deterministic UC			Stochastic UC	
Date	Seasonal	Daily	**Daily (Probabilistic)**	Single Zone	**Daily (Probabilistic)**
2-January	15 (2.5, 150)[2]	13.5 (3, 138)	10.7 (2.2, 109)	25.4 (3.2, 249)	9 (1.9, 117)
9-January	14.6 (2.4, 112)	12.2 (2.4, 90)	12.1 (2.3, 90)	21.6 (3, 235)	10.3 (2.6, 90)
14-January	11.7 (1.6, 142)	9.7 (1.5, 109)	7.7 (1.2, 90)	16.8 (2.6, 235)	5.4 (1.1, 84)
24-January	16.8 (3, 156)	20.2 (3.2, 212)	11.5 (2.6, 133)	30.2 (4.2, 270)	10.5 (2.3, 130)
5-February	15.6 (2.8, 183)	14 (2, 142)	13.1 (2.2, 118)	31.1 (3.8, 284)	12.5 (2, 121)
7-February	15.4 (3.4, 186)	14.4 (3.2, 187)	12.8 (3, 110)	30.3 (3.6, 280)	12.3 (2.5, 105)
14-February	15.4 (2.4, 193)	15.4 (2.4, 193)	9.6 (1.6, 111)	20.1 (3, 275)	9.3 (1.6, 107)
22-February	12.9 (2, 145)	13 (2, 148)	11.2 (1.6, 82)	20.8 (3, 287)	10.7 (0.6 , 90)
3-March	7.7 (1.2, 108)	8.5 (1.3, 158)	7.9 (1.4, 108)	8.9 (1.4, 132)	7.5 (1.2, 103)
11-March	11 (1.7, 157)	10.6 (1.6, 149)	7.2 (1.2, 87)	11.7 (1.8, 189)	8.3 (1.4, 87)
14-March	11.8 (2, 171)	12.1 (2, 183)	11.7 (2, 169)	12.7 (2, 90)	10.8 (2, 158)
26-March	14.1 (2.4, 142)	14 (2.4, 142)	9.9 (1.7, 120)	14.8 (2.4, 166)	8.8 (1.6, 124)

[2] α (β, δ); α represents the expected load shedding (MW), β represents the number of scenarios that have a violation per one thousand scenarios, and δ represents the largest violation (MW) from any single hour across the entire day.

Table 5.9 Operating Cost ($Million)

	Deterministic UC			Stochastic UC	
Date	Seasonal	Daily	**Daily (Probabilistic)**	Single Zone	**Daily (Probabilistic)**
2-January	0.8330	0.8510	0.8763	0.7707	0.8540
9-January	1.3884	1.3910	1.3936	1.3736	1.3927
14-January	0.4926	0.5000	0.5127	0.4829	0.5042
24-January	0.6587	0.6748	0.7000	0.6309	0.6840
5-February	0.7993	0.7977	0.8037	0.7873	0.8000
7-February	0.8610	0.8668	0.8700	0.8460	0.8677
14-Febuary	0.6352	0.6352	0.6724	0.6286	0.6631
22-February	0.7400	0.7370	0.7423	0.7251	0.7465
3-March	0.2153	0.2137	0.2240	0.2133	0.2161
11-March	0.1878	0. 1886	0.1980	0.1864	0.1960
14-March	0.6514	0.6505	0.6524	0.6480	0.6508
26-March	0.3446	0.3424	0.3510	0.3412	0.3499

6. HOURLY RESERVE ZONE DETERMINATION AND ITS MARKET IMPLICATIONS

6.1 Introduction

Independent system operators (ISOs) operate the power grid with the goal of maximizing the market surplus. Day-ahead market (DAM) and real-time market (RTM) models approximate physical and operational system constraints within security-constrained unit commitment (SCUC); generator capacity, ramping, and transmission constraints are important physical considerations that influence market decisions.

Several deterministic reserve policies have been proposed to address reserve deliverability. References [67], [68] constrain power flows based on participation factors that estimate how generators respond under different scenarios. Chen *at el*. [67] utilizes the zonal reserve requirements and contingency-constraint model, in which the largest post-contingency state is modelled, and the reserve price include market wide component, zonal component, and the contingency-constraint component. Their proposed model outperforms the original setting with operator manual disqualification in sending the correct price signal, which indicates that the contingency-constraint formulation reduce the distortion of reserve disqualification on reserve and energy price. Reference [69] proposes an algorithm for reserve disqualification that can be applied within the market model. MISO's current practice is to re-evaluate zones quarterly, unless there is an emergency [70], but MISO has also shown interest in updating zones daily or even hourly [71].

In Chapter 5, a reserve zone determination method is proposed to update the reserve zone on a daily basis. However, one barrier to updating zones more frequently is stakeholder opposition due to uncertainty in regards to their participating zone(s). However,

updating zones more frequently may improve market efficiency and reduce the need for out of market corrections, like reserve disqualification, which distort the market price signals and incur additional costs.

In this chapter, the market implications of implementing dynamic reserve zones in systems with wind generation will be examined. The focus is on how wind uncertainty affects the deliverability of contingency reserves. The proposed dynamic reserve model in Chapter 5 will be used to create hourly zones, at the day-ahead time stage, and the model of [69] is used to disqualify reserves so that the system is reliable in real-time. The primary hypothesis is that dynamic reserve zones will require fewer reserve disqualifications in order to acquire a reliable solution.

In order to carry out this analysis, a market settlement scheme is proposed for use with the reserve disqualification model of [69] for the test case I. Reserves are procured on a per-contingency basis, allowing reserves to be disqualified for a subset of contingencies. This settlement policy introduces a separate reserve product for each contingency, so that reserve providers cleared in the RTM are compensated only for contingencies for which they are qualified to provide ancillary service.

More importantly, Chapter 5 is not adequate to produce incentive for the industry application of the proposed hourly reserve determination method. This Chapter is also supposed to bridge the proposed method with real-world system operation by studying the feasibility of the proposed method's application based on real-life system operational rules and models. In the test case II, approximate MISO's SCUCmodel and look-ahead unit commitment model will be used to better approximate the MISO's market clearing process and to improve the quality and credibility of the numerical results.

In real-word operations, unreliable market solutions will be adjusted by operators. Evaluating the true operating cost using an assumed fixed value of lost load (VOLL) can be inaccurate. To obtain a better assessment of the cost of out-of-market corrections (reserve disqualifications) [72], unreliable solutions from the market SCUC are corrected based on similar procedures implemented today by ISOs. Reserve disqualifications occur after both the day-ahead SCUC and the look-ahead short-term SCUC. An accurate assessment of the actual costs to correct unreliable solutions is difficult to obtain and is generally overlooked as such ad-hoc practices are not well documented. This chapter utilizes an algorithm that mimics MISO's reserve disqualification process to accurately account for such reserve disqualification costs. Furthermore, a statistical technique (confidence intervals) is used to provide a proper statistical assessment of the benefits of the proposed reserve rule refinement.

6.2 Hourly Reserve Zone Determination

To determine the reserve zone on an hourly basis, the weight for each transmission line should be updated hourly by using WPTDFD metric. The proposed hourly reserve zone determination method is expected to involve the uncertainty and variability of renewable resources (e.g, wind) and load based on the probabilistic power flow, which involves the information of renewable resources.

To identify the critical transmission lines, two factors should be considered, the expected power flow and the deviation of power flow. To obtain the information of expected power flow and the deviation of power flow, simulations are needed to generate the sufficient power flow information based on different wind scenarios and contingencies. The procedures of generating weights and reserve zone are shown below,

Step 1 A deterministic unit commitment is solved based on predetermined zones. The unit commitment solution is then fixed for Step 3.

Step 2 Generate the uncertainty scenarios in order to characterize the uncertainty and variability of wind power output and load.

Step 3 Perform N-1 contingency analysis with generated wind scenarios while minimizing violations and record the power flows for the various wind scenarios. The expected power flow on transmission line k at hour t, represented by m_{kt}, and the standard deviation of power flow of transmission line k at period t, i.e., σ_{kt}, are calculated for each transmission line.

Step 4 Calculate each weight, π_{kt}, for transmission line k: $\pi_{kt} = (\left|\frac{m_{k,t}}{F_k^{max}}\right| + \frac{2\sigma_{k,t}}{F_k^{max}})^2$; the term is squared in order to place more attention to the critical paths.

Step 5 If there is any violation at period t for any wind scenario and contingency, perform the statistical clustering algorithm (K-means) to partition the reserve zones based on WPTDFD and the weights from Step 4. Otherwise, the reserve zone at period t will remain the same as pre-determined zone.

6.3 Reserve Disqualification

The electric power system is one of the most complex engineered systems to date. Power systems scheduling problems are very complex and challenging optimization problems. Due to the approximations of existing commercial grade SCUC and SCED models, such as uncertainties caused by forecasting errors or differences between the

linearized DC power flow and the actual AC power flow, there are various stages where the approximate market solutions are corrected by system operators. In such situations, corrections to the market solution will be needed to guarantee the system reliability when the original dispatch solution fails to satisfy system operating requirements. CAISO refer such out of market corrections (OMCs) as uneconomic adjustments or exceptional dispatches [21]-[22]. While CAISO states that such uneconomic adjustments are used to obtain feasible solution when using economic bids alone could not guarantee feasibility, note that this is not a complete description. SCUC and SCED models include many mathematical approximations, e.g., a linearized power flow, and no such economic bid can correct for such mathematical approximations. The Electric Reliability Council of Texas (ERCOT) refers to such OMCs as out of merit capacity and out of merit energy. CAISO and ERCOT collectively spent roughly $80 million in 2006 on the OMCs [20] [23].

Intra-zonal congestion may occur after contingency and cause undeliverability of reserve, which may harm the system reliability. One way to mitigate intra-zonal congestion is to acquire a reserve margin within each reserve zone and ATC margin of reserve sharing. For instance, PJM deploys operating reserve at least 1.5 times of the largest generation loss. The second way is that operators may improve system reliability by disqualifying reserves that are not deliverable for one contingency, and reserve disqualification is a potential out of market correction. Only qualified resources may then contribute towards the reserve requirements the next time the schedule is updated. The updated model with contingency-specific reserve disqualification is shown by (6—1)–(6—3) [69]. The binary parameter Γ_{gct} designates if resource g is qualified to provide reserve for contingency c in period t.

Note that the reserve sharing variable $\tilde{r}_{zct}^{SPIN}$ is indexed by destination contingency c instead of destination zone j.

$$\sum_{z\in Z} \tilde{r}_{zct}^{SPIN} \geq p_{ct} + r_{ct}^{SPIN}, \forall c \in \mathcal{G}(j), t \in T \quad (6—1)$$

$$\tilde{r}_{zct}^{SPIN} \leq \sum_{g\in \mathrm{G}(z)} \Gamma_{gct} r_{gt}^{SPIN}, \forall c \in C, z \in Z, t \in T \quad (6—2)$$

$$\tilde{r}_{zct}^{SPIN} \leq S_{z,z(c),t} \ \forall z \in Z, h \in Z, t \in T \quad (6—3)$$

Equations (6−1)–(6−3) enable finer management of reserve locations, provided that proper values for Γ_{gct}can be determined. MISO and ISO-NE manually disqualify reserves after the market model has cleared and there has been sufficient time to analyze reliability [73]–[75]. The DAM does not reflect these decisions because reserves are disqualified post hoc. The algorithm of reference [69] is used to simulate reserve disqualification decisions whenever the zonal reserve model provides a solution that is not N-1 reliable. In this thesis, this reserve disqualification algorithm is defined as Type I reserve disqualification algorithm.

MISO employs “manual dispatch” when it needs to adjust the dispatch solution to obtain a reliable solution [15]. During real-time operations, it is common that some allocated reserves may be undeliverable, which will harm the system reliability if they are deployed. To alleviate the potential risk to system reliability, operators will rank the nodes based on the sensitivities on the congested transmission lines and label the resources on the top ranked nodes as “not reserve qualified.” The process is defined as reserve disqualifications at MISO. Such rule of thumb manual correction procedures are decided outside the energy and ancillary service co-optimization process and lead to uneconomic solutions. In some circumstances, operators may disqualify a large number of reserves to guarantee sufficient amount of deliverable reserve, which may incur significant costs.

Furthermore, implementing reserve disqualifications will impact the market outcomes for its stakeholder due to price distortion. To reduce the need for manual reserve disqualifications determined by operators, it is important to improve existing reserve requirement formulations in order to enhance the market efficiency while maintaining reliability.

To mimic the reserve disqualification at MISO, for each period, resource with 1MW more power injection that aggravates most on binding transmission constraints will be disqualified. Reserve disqualification will be repeated until market solution is reliable. In this thesis, this reserve disqualification algorithm is defined as Type II reserve disqualification algorithm.

6.4 Case Study I

Note that this Section is collaborated with Joshua D. Lyon [76].

6.4.1 Proposed Market Clearing Process

The flowchart in Figure 6.1 summarizes the process used to analyze different reserve zone policies. Zones partition will be used as an input in this market clearing process. After reserve zones have been determined, SCUC is solved to produce the DAM solution based on the forecasted wind availability. The commitments decisions will be fixed for generators, whose minimum down time less or equal to four hours.

Several things occur between the DAM and RTM clearings. First, the wind forecast improves dramatically as operations move closer to real-time. Operators respond to forecast updates by re-dispatching the system and turning on additional generators if needed. Operators may also disqualify reserves, if congestion is found to threaten reliability,

and then procure additional reserves from available resources at preferred locations. All of these changes occur prior to the RTM, which is a spot market that is cleared near real-time.

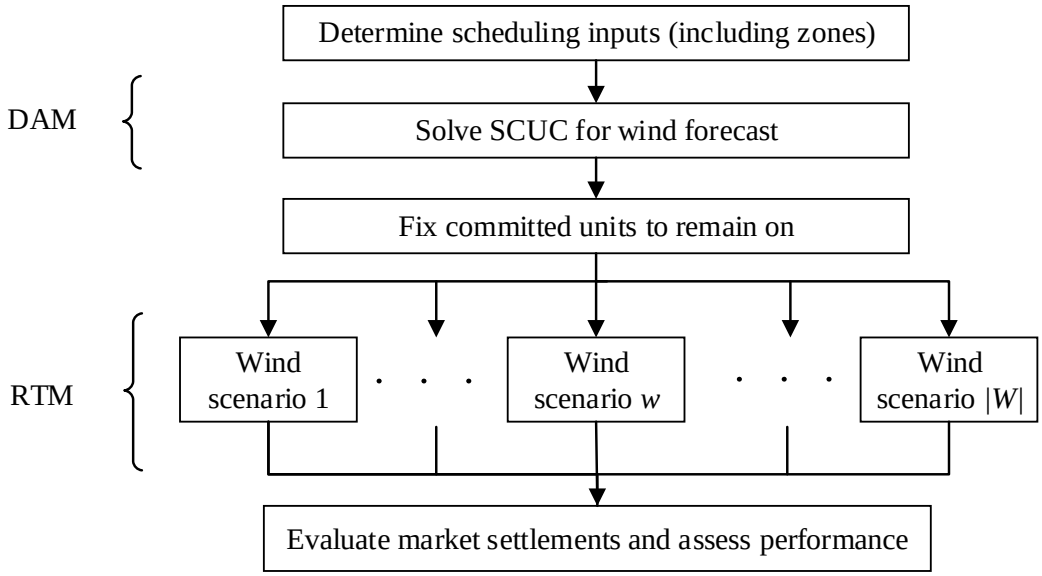

Figure 6.1 Summary of Analysis of Different Zonal Inputs for a Single Day

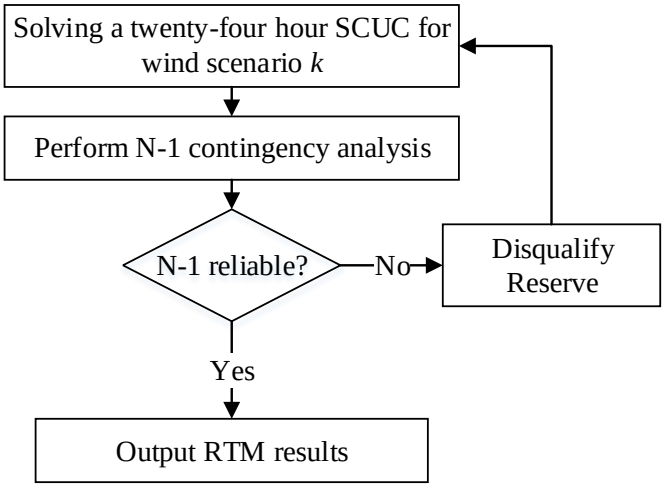

Figure 6.2 Dispatch and RTM Simulation for an Individual Wind Scenario

Figure 6.2 describes the simplified process used in this chapter to simulate actions that follow the DAM. It is assumed that wind uncertainty is revealed all at one time and a 24-hour SCUC is solved to dispatch the system. Additional commitments are allowed for generators that have minimum down times of less than five hours. The SCUC solution will

represent the RTM solution if it passes contingency analysis without violations. Otherwise, the algorithm of [17] is used to disqualify undeliverable reserves and the process is repeated until a reliable solution is found. This approach simplifies actual operations in that 1) the RTM is solved with an hourly time resolution instead of a five minute period and 2) the RTM is cleared with a 24 hour model instead of a series of shorter problems with a rolling horizon. This simplified process still approximates the effect of the real-time wind availability deviating from the day-ahead forecast.

6.4.2 Ancillary Services Market Settlements

Most ISOs clear energy and ancillary services simultaneously using optimization engine with consideration of both energy and reserve bids in the objective function [17]. The lowest bids that satisfy all physical and operational constraints will be cleared first.

Market clearing prices are calculated based on dual variables from the market model, which reflect shadow prices. Operators will solve the day-ahead unit commitment (scheduling) and fix all the commitment variables such that the dual variables can be derived from linear programming (pricing run) [77]. Service providers are compensated based on these dual variables, e.g., locational marginal prices (LMPs) are used to settle energy and reserve marginal prices (RMPs) are used to settle reserves. RMPs increase as reserve bids increase if locational reserves are scarce.

However, ancillary service settlements are complicated by reserve sharing model. For instance, ISO-NE has nested zones and uses a settlement policy that assumes reserve sharing constraints are always binding in the direction to a child zone, such as a load pocket, but never binding in the opposite direction [18]. In this situation, reserve providers are paid to provide ancillary service to outside zones because, by assumption, reserve exports are

never obstructed by transmission constraints since the reserves would produce a counter-flow. However, resources are not paid to provide ancillary service to inner zones because the binding reserve sharing constraint suggests that additional reserve may not be deliverable. However, this type of policy is based on operator's confidence of interface flow predictions. A more general mechanism is presented to acknowledge service provided to neighboring zones only when marginal reserves are deliverable. Such a payment scheme is provided by (6—4):

$$\phi_{gt} = -\sum_{c \in C} \Gamma_{gct} r_{gt}^{SPIN} \lambda_{z(g),c,t}, \quad (6—4)$$

$\Gamma_{gct} r_{gt}^{SPIN}$ is the amount of cleared spinning reserve and λ_{zct} is the dual variable of (6—2). Economic theory specifies that the dual variable λ_{zct} is a shadow price that reflects the marginal value of reserve in zone h providing ancillary service for contingency c [78]. Note that the payments in (6—4) compensate reserve service providers on an individual contingency basis.

Cleared reserve will have no marginal value when reserve exceeds the sharing capability since it is assumed that additional reserve of zonal model would not be deliverable. Equation (6—5) describes the quantity of cleared reserve that the model values for each contingency. In Chapter 6 Section 6.4.3, a proposed algorithm is used to measure how much of this cleared reserve is deliverable in real-time market.

$$\Delta_{gct} = \begin{cases} \Gamma_{gct} r_{gt}^{SPIN} & \text{if } \tilde{r}_{z(g),ct} < S_{z(g),z(c),t} \\ 0 & \text{otherwise} \end{cases} \quad (6—5)$$

6.4.3 Quality of Service

As an additional measure, an algorithm is proposed to assess the real-time performance of ancillary services procured in the DAM. To incentivize the supply of ancillary services,

generators should be compensated based on the quality of service provided, e.g., the deliverability of reserve. It is expected that the reserve would be deliverable in the event of a random disturbance. Model (6—6)–(6—12) is used to evaluate the deliverability of reserve with the respect of a single generator g following various generation contingencies. This model provides a basis for evaluating different reserve policies to measure how well the model anticipates the value of reserves in real-time. More precisely, (6—6)–(6—12) identify reserves that are not deliverable when the DAM anticipated they would be.

Let F_k^{max} be the rating of line k and let R_{gt}^{+} and R_{gt}^{-} be the available reserves in the up and down directions from resource g in period t. For contingency c, let $I_{n,c}^{t}$ represent the net injection (generation minus load) at node n prior to re-dispatch and $x_{gct}^{+} - x_{gct}^{-}$ be the amount of reserve exercised (dispatched) from resource g. Equations (6—7) and (6—8) impose flow balance and linear transmission constraints, (6—9) models locational injections, and (6—10) constrains reserve availability. The model considers spinning reserves but can be generalized to include other reserve products such as non-spinning reserve.

Ideally, a generator in zone z paid to provide Δ_{gct} of reserve for contingency c should be able to dispatch that amount. If this amount of reserve cannot be exercised during a coordinated re-dispatch, then the resource provides a lower quality of service than anticipated by the zonal reserve model. Equation (6—11) measures how much reserve is dispatched from generator g, where s_{gct} represents the shortfall below Δ_{gct}. The objective function (6—6) encourages a small shortfall: if the optimal solution is zero, then reserve from generator g can be dispatched up to the anticipated level. A large penalty M is included in the objective function to discourage down ramping. No generator may ramp

down during this process unless it is absolutely necessary to ensure reliability. Note that this assumption is not made to reflect actual operations; this model only estimates the quality of service provided by generator g by measuring its ability to deliver its procured reserve.

Minimize: $$\sum_{c\in C}\sum_{t\in T}\left(s_{gct}+M\sum_{\gamma\in G}x^{-}_{\gamma ct}\right) \quad (6—6)$$

Subject to: $$\sum_{n\in N} i_{nct}=0, \forall c\in C, t\in T \quad (6—7)$$

$$-\bar{F}_k^{max}\le\sum_{n\in N}PTDF_{nk}i_{nct}\le\bar{F}_k^{max}, \forall k\in K, c\in C, t\in T \quad (6—8)$$

$$i_{nct}=I_{nct}+\sum_{\gamma\in G(n)}\left(x^{+}_{\gamma ct}-x^{-}_{\gamma ct}\right), \forall n\in N, c\in C, t\in T \quad (6—9)$$

$$R^{-}_{gt}\le x^{+}_{gct}-x^{-}_{gct}\le R^{+}_{gt}, \forall g\in G, c\in C, t\in T \quad (6—10)$$

$$x^{+}_{gct}\ge \Delta_{gct}-s_{gct}, \forall\, c\in C\setminus g, t\in T \quad (6—11)$$

$$x^{+}_{gct}, x^{-}_{gct}\ge 0, \forall\, c\in C, g\in G, t\in T \quad (6—12)$$

An ideal market model would not pay generators for reserves that are unavailable. The proportion of reserve properly characterized as deliverable for each contingency is shown by QOS in (6—13), where $v_{gct}=1-s_{gct}$. Reserve policies that result in low values for $QOS^{t}_{g,c}$ poorly anticipate the quality of service provided by generator g. Equation (6—14) defines the average quality of service of reserves, $\overline{QOS}$, procured in the DAM. Efficient models should have $\overline{QOS}$ close to one, indicating that a large portion of reserves procured in the DAM are deliverable in real-time.

$$QOS^{t}_{g,c}=\frac{v_{gct}}{\Delta_{gct}} \quad (6—13)$$

$$\overline{QOS}=\frac{\sum_{t\in T}\sum_{g\in G}\sum_{c\in C}v_{gct}}{\sum_{t\in T}\sum_{g\in G}\sum_{c\in C}\Delta_{gct}} \quad (6—14)$$

6.4.4 Reserve Sharing

Reserve sharing is a practice of estimating how much reserve can be transferred between reserve zones. Reserve sharing can improve system economic efficiency by lowering the total reserve quantity required across the system. One way of modeling reserve sharing relies only on off-line studies to estimate available transfer capability (ATC) between zones, for example, MISO determines ten-minute requirements two days ahead by simulating the reserve deliverability between zones [71]. However, ATC estimates, based on off-lines study, may not be accurate since the real operating condition may be different from the off-line study. The other approach is dynamically updating reserve sharing capability based on the interface flows in the current DAM or RTM solution with a pre-determined capacity margin. That is, additional reserves are required for zones that import more power than anticipated and vice versa. PJM and ISO-NE employ such dynamic reserve sharing models in DAM and RTM [18], [75]. For both these two approaches, intra-zonal congestion may prohibit the reserve sharing. Dynamic reserve zone is able to lower intra-zonal congestion such that improve the efficiency of reserve sharing model.

Equations (6—15)–(6—17) represent the basic structure of a dynamic reserve sharing model [69], which is a generalization of (1). This formulation allows reserve to be shared between adjacent zones and is similar to the nested zone formulation used in ISO-NE [18]. The variable $\tilde{r}_{z,j}^{t}$ represents how much reserve in zone z is classified as deliverable to zone j in period t. Equation (6—15) requires there to be enough portable reserve to cover any generator contingency, (6—16) models reserve held within the zones, and (6—17) limits how much reserve may be shared between zones.

$$\sum_{z \in Z} \tilde{r}_{zjt} \geq p_{ct} + r_{ct}, \forall j \in Z, c \in G(j), t \in T \quad (6—15)$$

$$\tilde{r}_{zjt} \leq \sum_{g \in G(h)} r_{gt}, \forall j \in Z, z \in Z, t \in T \quad (6—16)$$

$$\tilde{r}_{zjt} \leq S_{zjt}, \forall j \in Z, z \in Z, t \in T \quad (6—17)$$

The sharing bounds (S) may be based on off-line analysis and dynamically updated as flows change on zonal interfaces [18]. The above formulation is suitable for modeling reserve sharing between adjacent zones. Nested zones also exist in practice in ISO-NE [18]. Nested zones assume that reserve is only constrained in the direction of the central zone, which may be a load pocket. Reserve sharing models may mischaracterize congestion, making it necessary for operators to adjust the solution, which may be done by disqualifying reserves located behind transmission bottlenecks.

6.4.5 Modified IEEE RTS96 Test Case

A modified IEEE Reliability Test System (RTS) 96 is used to examine the market impact of the proposed dynamic reserve policies. The system has 73 nodes, 99 units, and 117 lines, and 51 loads [49], [79]. Modifications to the test case follow [68], [69]: line (11–13) is removed, 480 MW of load is shifted from nodes 14, 15, 19, and 20 to node 13, and the capacity of line (14–16) is decreased to 350 MW. These modifications affect each of the three identical areas within the system. A small amount of congestion is induced by removing hydro from all other areas and tripling the capacity of inexpensive hydro power in the area consisting of nodes 1–24.

Wind farms with 1000 MW of capacity are placed at nodes 23 and 47 respectively, which are both central locations containing 660 MW of coal generation each. The wind is placed at central parts of the system because isolated areas may require additional transmission investments that are beyond the scope of this thesis. These two wind farms

comprise about 16% of the installed capacity. Wind energy has a production bid of zero and can be accepted up to the forecasted amount.

The area consisting of nodes 49–73 is usually import constrained because there are no local wind or hydro plants. Statistical clustering is used to partition zones based on WPTDFDs (8). The line weights π_l are calculated by simulating the system dispatch using a single zone model. Seasonal zones are calculated as in Chapter 5, where line weights are based on average line utilizations over a season. The seasonal zones are shown in Figure 6.3. The dynamic zone line weights are based on post-contingency flows. For the dynamic reserve zone process, the number of zones is one if there are no post-contingency violations and the number of zones is three otherwise.

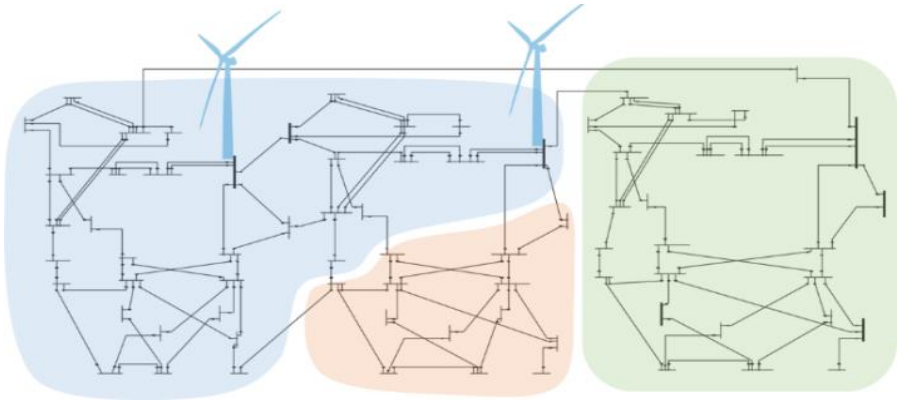

Figure 6.3 RTS96 Two Wind Locations and Three Seasonal Reserve Zones.

Only spinning reserves are considered in this analysis. Each generator's reserve bid is 25% of the energy bid, as is done by [80]. Constraint (7) limits reserve sharing by the import capability S between zones. Similar as [75], the sharing limit is defined to equal the pre-determined interface capacity minus the power flows. The interface capacity is taken as the aggregate capacity across the individual lines less 5% because it may not be able to

fully utilize every line during a coordinated contingency response. This is a simplified representation of the more sophisticated reserve sharing assumptions used in practice.

6.4.6 Wind Modeling

Autoregressive integrated moving average (ARIMA) models are popular for describing how wind speed changes over time [81]. They are particularly convenient for simulation because movement is completely dictated by Gaussian error terms that can be produced using a random number generator. ARIMA generalizes autoregressive (AR) and moving average (MA) models, which capture temporal correlation present in the data. Reference [82] proposes an efficient way to also account for spatial correlation between wind sites by generating statistically dependent error terms across locations. Wind modeling in this section adopts the methodology of [82] to generate wind scenarios that have both spatial and temporal correlations.

The wind data for the first two weeks of August 2005 are taken from NREL's Western Wind dataset [83]. Figure 6.4 (a) maps 510 individual turbines that are distributed across two clusters; these clusters are aggregated to create two separate wind locations. Hourly ARIMA models are fit for each wind location and wind speeds are then converted to power using an estimate of the aggregate power curve of each cluster. A seasonal ARIMA model is adopted that includes an AR term for the most recent hour and a 24-hour MA term with seasonal differencing to capture daily seasonality. Since the model is fit using only historical data, the deviation between samples tends to exceed typical forecast errors seen in practice [84]. This bias is corrected by normalizing the sampled wind speeds so that the power stays within 20% of the mean approximately 80% of the time. Figure 6.4 (b) shows an example of 15 wind scenarios sampled from this model.

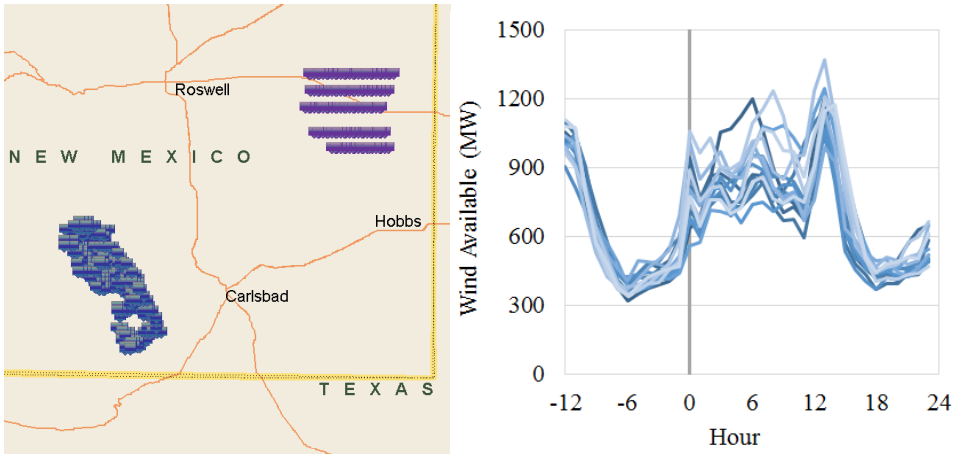

Figure 6.4 (a) Wind Data locations. (b) Fifteen Scenario Simulation Samples

6.4.7 Numerical Results

The seasonal and dynamic zones are analyzed across all seven days of the peak week (from Day 351 to Day 357). Each day is tested against 100 wind scenarios (different from 100 wind scenarios used to generate dynamic zones). The same wind forecast and scenarios are used for each day; thus, uncertainty is highest on the weekend day 356 and day 357. The peak day has 10.8% energy from forecasted wind and the lowest load day has 14.5% energy from forecasted wind.

Figure 6.5 (a) shows the number of reserve disqualifications for the seasonal and dynamic zones; each marker represents a single wind scenario for a day. Based on Figure 6.5 (a), the number of reserve disqualifications required by dynamic zone is much fewer than that of seasonal zone: note that only one dynamic zone scenario exceeds 25 disqualifications whereas half of the seasonal zone simulations exceed this amount. More reserve disqualifications are required as wind increases relative to load, which suggests that dynamic zones could offer even more improvement as wind penetration increases.

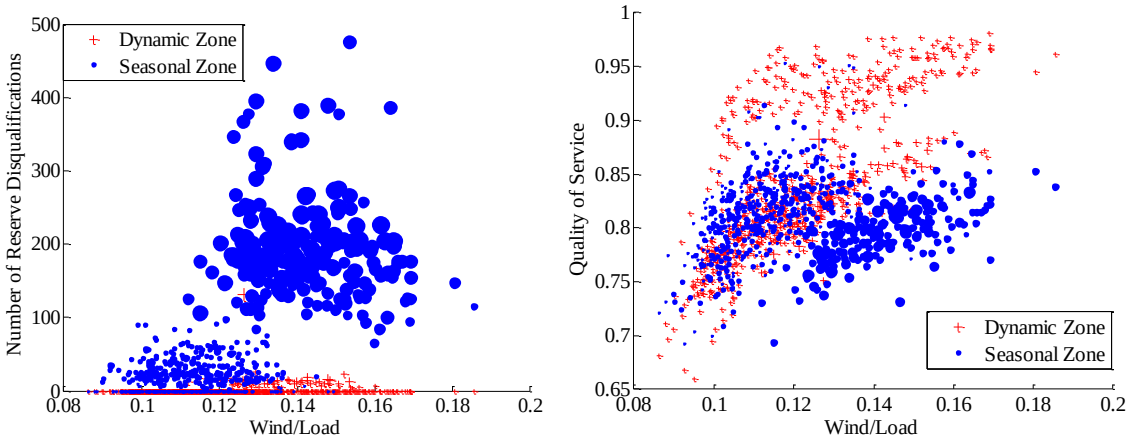

Figure 6.5 Reliability and Quality of Service Statistics. (a) The Number of Reserve Disqualifications for Different Wind scenarios, Where Marker Size Represents the Sum of Contingency Violations Prior to Reserve Disqualification. (b) Quality of Service, $\overline{QOS}$, Where Marker Size Represents the Number of Reserve Disqualifications

Table 6.1 Average System Reliability Results over One Hundred Wind Scenarios

Day	Initial Violations (MW)		#DQs		QOS	
	Seasonal	Dynamic	Seasonal	Dynamic	Seasonal	Dynamic
351	15.13	0.00	9.6	0.0	79.8%	79.3%
352	0.00	0.00	0.0	0.0	81.5%	78.9%
353	30.85	0.03	16.5	0.0	81.2%	80.2%
354	127.20	0.01	44.7	0.0	80.7%	79.7%
355	31.16	0.00	21.6	0.0	84.2%	90.5%
356	1149.02	12.79	216.8	7.3	79.4%	89.3%
357	781.56	0.76	167.0	1.0	80.0%	90.8%
Average	304.99	1.94	68.0	1.2	81.0%	84.1%

Table 6.2 Average System Market Results over One Hundred Wind Scenarios for Operating Cost and Load Payment

Day	Forecasted Wind/Load	Operating Cost		Load Payment	
		Seasonal	Dynamic	Seasonal	Dynamic
351	11.64%	$1,968,844	$1,965,208	$ 8,924,080	$9,127,960
352	10.83%	$2,629,842	$2,623,638	$13,002,000	$14,009,800
353	11.05%	$2,426,831	$2,424,256	$10,897,400	$10,754,000
354	11.28%	$2,236,601	$2,236,087	$ 9,088,700	$9,651,320
355	11.52%	$2,058,041	$2,054,286	$ 8,341,460	$8,397,860
356	14.07%	$1,032,966	$1,026,275	$ 2,268,850	$2,300,890
357	14.45%	$970,591	$966,097	$ 2,463,550	$2,147,260
Average	12.12%	$1,903,388	$1,899,407	$ 7,855,149	$8,055,584

Note that the size of the marker in Figure 6.5 (a) represents the sum of contingency violations of the SCUC solution prior to any reserve disqualification. For example, the sum of contingency violations (across all periods, wind scenarios, and contingencies) per day for the seasonal zonal approach is over 300 MW on average, whereas the dynamic zones have a sum of 2 MW on average. Table 6.1 presents the average system reliability results over 100 wind scenarios. From Table 6.1, the initial violation of DAM of dynamic zone is much lower than that of seasonal zone, and solutions with higher initial violations require more number of reserve disqualifications to obtain an reliable solution in the RTM. These results indicate that dynamic zones can significantly improve reliability and thereby significantly reduce the number of reserve disqualifications.

Figure 6.5 (b) presents the results of the quality of service $\overline{QOS}$ between seasonal and dynamic zones. Values of $\overline{QOS}$ indicate that the percentage of reserve procured from the DAM is deliverable in real-time. The upward slope in Figure 6.5 (b) indicates that more reserve can be delivered on low load days and during individual scenarios that have high wind availability. Conventional generators generally provide more reserve when wind generation is high. The wind scenarios that exceed the forecast can be interpreted as additional unanticipated capacity, which helps the entire system achieve a higher $\overline{QOS}$ during the contingency analysis screening. The marker size in Figure 6.5 (b) represents the number of reserves disqualified. From Table 6.1 and Figure 6.5 (b), the average quality of service is higher using dynamic zones, especially when the number of reserve disqualifications performed from the seasonal model is large. These results indicate that overall dynamic zones tend to result in higher $\overline{QOS}$ and that $\overline{QOS}$ is lower when more reserve disqualifications are necessary.

Table 6.3 Average System Market Results over One Hundred Wind Scenarios for Energy Revenue and Reserve Revenue

Day	Forecasted Wind/Load	Energy Revenue		Reserve Revenue	
		Seasonal	Seasonal	Seasonal	Dynamic
351	11.64%	$8,165,179	$8,347,676	$137,979	$176,800
352	10.83%	$11,935,186	$12,889,251	$156,216	$157,277
353	11.05%	$9,986,626	$9,837,727	$115,685	$173,466
354	11.28%	$8,302,965	$8,810,239	$124,464	$190,266
355	11.52%	$7,616,376	$ 7,666,923	$97,907	$112,877
356	14.07%	$1,974,204	$ 2,013,131	$93,643	$99,017
357	14.45%	$2,150,320	$1,873,475	$99,679	$101,562
Average	12.12%	$7,161,551	$7,348,346	$117,939	$144,466

Table 6.2 and Table 6.3 summarize the average market results between seasonal and dynamic zones over the 100 wind scenarios. Production cost of dynamic zone is slightly, but consistently, lower. What makes the results interesting is that the higher relative improvement is on days where wind provides a larger proportion of the energy. This observation is further validated by testing day 352 with twice as much wind penetration level: using the dynamic zones, the production cost decreases by 2% compared with the seasonal zone and, furthermore, fewer reserve disqualifications are required using dynamic zone.

The load payments in Table 6.1 and energy and reserve revenues Table 6.2 are calculated based on the multi-settlement policy described by [85]. The reserve revenue for each resource is given by (6—8). Transactions occur in the DAM based on the locational marginal prices and spinning reserve prices. Transactions occur in the RTM in a similar manner but are settled relative to the quantities cleared in the DAM. For example, a generator cleared at 100 MW in the DAM and 101 MW in the RTM receives the day-ahead price for the first 100 MW and the real-time price for the last MW. Individual generators receive a make-whole uplift payment if their cleared bid costs exceed revenue from energy

and ancillary services combined. Figure 6.6 demonstrates the LMP percentile for both dynamic zone and seasonal zone, and the average LMPs across tested week of dynamic zone and seasonal zone are very similar.

The market-wide reserve revenues are consistently higher using the dynamic zones. These higher payments correspond to a higher quality of service $\overline{QOS}$ when a high proportion of energy comes from wind. Load payments and energy revenues tend to be higher using dynamic zones, and uplifts lower, but the results are not consistent enough to make general predictions, especially considering that market results are known to vary around near-optimal SCUC solutions [86]. While the results in Table 6.1 are relatively similar, the results in Table 6.3 demonstrate that the dynamic reserve zones have much fewer number of reserve disqualifications and require substantially fewer reserve disqualification, which generally means that the $\overline{QOS}$ will be better. Fewer disqualifications tend to result in a better $\overline{QOS}$.

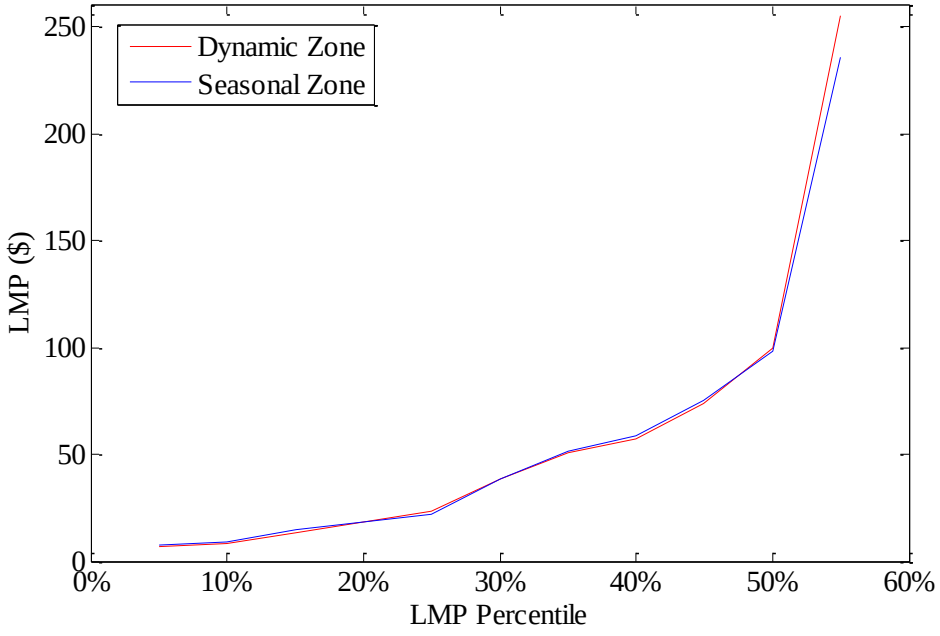

Figure 6.6 Average LMP Percentile

Market complexity is something that is important to consider [87]. Should the markets be simple and transparent or should they be complex and better reflect operational realities? Inaccurate DAM policies may need to overcommit units in order to obtain a reliable solution. This excess capacity can suppress market prices because prices do not capture the effects of binary commitments decisions [78], only to be stripped away by reserve disqualification procedures (if the reserve is not deliverable) outside of the market environment. The advanced reserve policies investigated in this chapter are anticipated to produce price signals that better reflect the true value of ancillary services as compared to existing imprecise reserve policies. Also note that the reserve disqualification procedure used in this chapter is more efficient that what operators use today and operators may benefit more comparing with the numerical results presented by using proposed dynamic zone model.

6.5 Case Study II

6.5.1 Proposed Clearing Process

Two different reserve zone models are compared, dynamic reserve zone and seasonal reserve zone. The process of determining dynamic reserve zone follows the algorithm Chapter 6 Section 6.2. The seasonal reserve zone is determined based on historical power flow data. The historical data is generated by running optimal power flow through the winter. The flowchart in Figure 6.7 shows the proposed market clearing process for case study II. The zonal models will be input to the day-ahead SCUC model. The market solution of the SCUC will be adjusted by the type II reserve disqualification presented in Chapter 6 Section 6.3 until the market solution is N-1 reliable. Once the market solution of

SCUC gets N-1 reliability approved, the commitments of generators, which has minimum-down time larger than three hours, will be fixed for look ahead unit commitment (LAC). It is assumed that all the net load scenarios (wind uncertainties and load uncertainties) are revealed in the LAC process and the only uncertainties in the real-time market are contingencies. Figure 6.8 presents the details of LAC clearing process. In Figure 6.8, to ensure the LAC solution is N-1 reliable, reserve disqualification will be repeated until it is N-1 reliable for each net load scenario *s*.

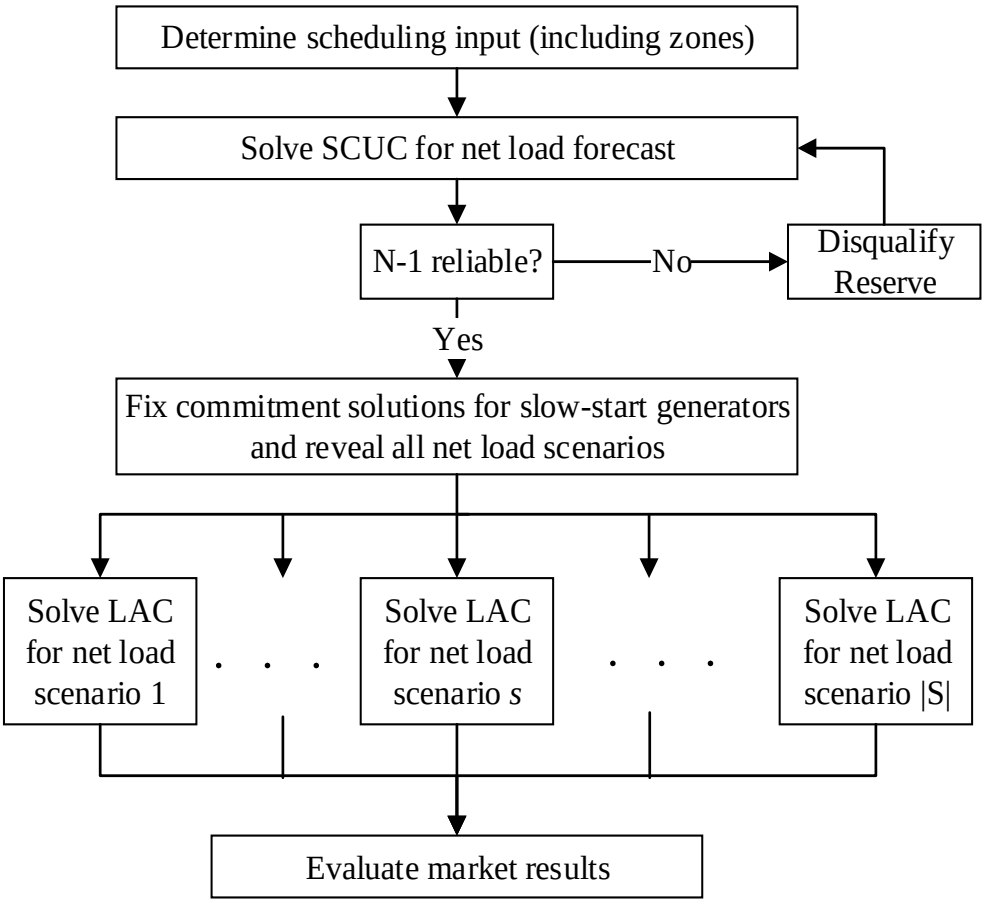

Figure 6.7 Proposed Market Clearing Process for Case Study II

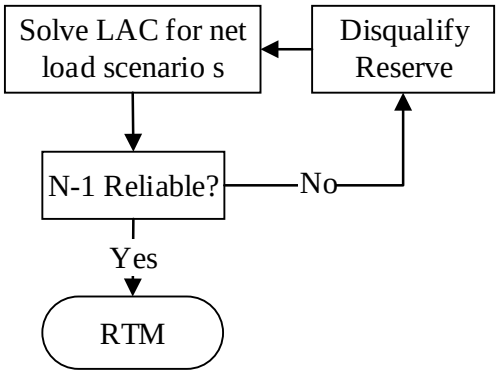

Figure 6.8 Detailed LAC Clearing Process

6.5.2 Wind and Load Scenarios Generation

To mimic the uncertainty and variability of wind output and load, one hundred wind scenarios and load scenarios are generated. Various methods can be used to generate uncertainty scenarios [15], [19], [39], [40], [43].

To generate wind scenarios, the same ARIMA model is presented in Chapter 6 Section 6.4.6 is used. The historical wind data is taken from NREL's Western Wind dataset for the first three weeks of August 2005 [83] is used to tune the parameters of ARIMA model. The error (residuals) of the ARIMA model follows normal distribution.

Monte Carlo simulation [1] is used to produce the wind scenarios, and for each period *t*, it is assumed that the mean of the probability distribution is the forecasted load, and the folded Gaussian distribution is employed to accurately tune the forecasting error, which is designed as 3%. The load scenarios generation process is similar as Chapter 5 Section 5.6.

Note that it is assumed that wind scenarios and load scenarios are independent, and the wind scenario *s* will be combined with load scenario s to produce the net load scenario *s* for each node.

6.5.3 MISO's SCUC Formulation

MISO co-optimizes energy and ancillary service the day-ahead market with energy bids and reserve bids to ensure adequate generation capacity to serve next day's demand [93]. The security constrained unit commitment (SCUC) at MISO accounts for the transmission constraints. Before the day-ahead market solution gets approved, none of transmission constraints should be violation during contingency analysis, otherwise an adjustment will be made to SCUC formulation [89]. To lower expected transmission violation after reserve deployment, in [75], security constrained economic dispatch (SCED) is enhanced by incorporating post zonal reserve deployment and modelling the largest contingency in each reserve zone. The SCED formulation with post zonal reserve deployment transmission constraints is also extended to MISO's SCUC model. The proposed SCUC formulation with consideration of post regulation and contingency reserve deployment is shown as below,

$$\underset{p_{gt}, r^{x}_{gt}, su_{gt}, sd_{gt}}{\text{Min}} \sum_{t\in T}\sum_{g\in G}[C_g p_{gt} + C_g^{SU} su_{gt} + C_g^{SD} sd_{gt} + C_g^{NL} u_{gt} + C_g^{REG} r_{gt}^{REG} + c_g^{SPIN} r_{gt}^{SPIN} + c_g^{NL} r_{gt}^{SUPP}] \quad (6—18)$$

Subject to:

Power balance equation (λ_t)

$$\sum_{n\in N}(i_{nt}) = 0 \quad (6—19)$$

Power injection

$$i_{nt} = \sum_{n_g=n}(p_{gt}) + \sum_{n_w=n}(sp_{wt}) - D_{nt}\,,\ \forall n \in N \quad (6—20)$$

Transmission constraints ($\mu_{i,t}$)

$$f_{kt} \le F_k^{max} \quad \forall k \in K \quad (6—21)$$

$$f_{kt} = \sum_{g\in G}\left\{p_{gt} PTDF^R_{n_j,k}\right\} + \sum_{n\in N}\left\{i_{nt} PTDF^R_{n,k}\right\} \quad \forall k \in K \quad (6—22)$$

Market-wide regulation reserve requirement (γ_t^{MRR})

$$\sum_{z\in Z} r_{zt}^{REG} \geq R_{MKT,t}^{REG} \quad (6—23)$$

Market-wide regulation plus spinning reserve requirement (γ_t^{MRS})

$$\sum_{z\in Z}\{r_{zt}^{REG} + r_{zt}^{SPIN}\} \geq R_{MKT,t}^{REG} + R_{MKT,t}^{SPIN} \quad (6—24)$$

Market-wide operating reserve requirement (γ_t^{MOR})

$$\sum_{z\in Z}\{r_{zt}^{REG} + r_{zt}^{SPIN} + r_{zt}^{SUPP}\} \geq R_{MKT,t}^{REG} + R_{MKT,t}^{SPIN} + R_{MKT,t}^{SUPP} \quad (6—25)$$

Zonal regulation reserve requirement (γ_{zt}^{ZRR})

$$\sum_{g\in G^z} r_{gt}^{REG} \geq r_{zt}^{REG},\ z \in Z \quad (6—26)$$

Zonal regulation plus spinning reserve requirement (γ_{zt}^{ZRS})

$$\sum_{g\in G^z}\{r_{gt}^{REG} + r_{gt}^{SPIN}\} \geq r_{zt}^{REG} + r_{zt}^{SPIN},\ z \in Z \quad (6—27)$$

Zonal operating reserve requirement (γ_t^{MRS})

$$\sum_{g\in G(z)}\{r_{gt}^{REG} + r_{gt}^{SPIN} + r_{gt}^{SUPP}\} \geq r_{zt}^{REG} + r_{zt}^{SPIN} + r_{zt}^{SUPP},\ z \in Z \quad (6—28)$$

Post regulation reserve up deployment (μ_{kt}^{REGUP})

$$f_{kt} + \sum_{z\in Z}\left\{r_{zt}^{REG} PTDF_{\mathrm{z},k}^{R}\right\} - PTDF_{LC,k}^{R} R_{MKT,t}^{REG} \leq F_k^{max} \quad (6—29)$$

Post regulating reserve down deployment (μ_{kt}^{REGDN})

$$f_{kt} - \sum_{z\in Z}\left\{r_{zt}^{REG} PTDF_{\mathrm{z},k}^{R}\right\} + PTDF_{LC,k}^{R} R_{MKT,t}^{REG} \leq F_k^{max} \quad (6—30)$$

Post zonal contingency event ($\mu_{i,z,t}^{CR}$)

$$f_{kt} - E_{z,t} PTDF_{\mathrm{z},k}^{R} + DF_{z,t}^{SPIN} \sum_{z'\in Z}\left\{r_{z',t}^{SPIN} PTDF_{z',k}^{R}\right\} + DF_{z,t}^{SUPP} \sum_{z'\in Z}\left\{r_{z't}^{SUPP} PTDF_{z',k}^{R}\right\} \leq \bar{F}_k^{max},\ z \in Z \quad (6—31)$$

Resource limit constraints

$$p_{gt} + r_{gt}^{REG} + r_{gt}^{SPIN} + r_{gt}^{SUPP} \leq u_{gt} P_g^{max}, t \in T, g \in G \quad (6—32)$$

$$p_{gt} - r_{gt}^{REG} \geq u_{gt} P_g^{min}, t \in T, g \in G \quad (6—33)$$

Minimum-up and -down constraints

$$\sum_{t'=t-UT_g+1}^{t} su_{gt'} \leq u_{gt},\ t \in \left(UT_g, \ldots, T\right) \quad (6—34)$$

$$\sum_{t'=t-DT_g+1}^{t} sd_{gt'} \leq 1 - u_{gt}\,, t \in \left(DT_g\,, .., T\right) \quad (6—35)$$

Ramp constraints

$$p_{gt} - p_{g,t-1} \leq R_g^{HR}, t \in T, g \in G \quad (6—36)$$

$$p_{g,t-1} - p_{gt} \leq R_g^{HR}, t \in T, g \in G \quad (6—37)$$

$$0 \leq r_{gt}^{REG} \leq \overline{R}_{gt}^{REG}, t \in T, g \in G \quad (6—38)$$

$$0 \leq r_{gt}^{SPIN} \leq \overline{R}_{gt}^{SPIN}, t \in T, g \in G \quad (6—39)$$

$$0 \leq r_{gt}^{SUPP} \leq \overline{R}_{gt}^{SUPP}, t \in T, g \in G \quad (6—40)$$

Additional constraints

$$u_{gt} \in \{0,1\}, 0 \leq su_{gt}, sd_{gt} \leq 1 \quad (6—41)$$

$$0 \leq sp_{wt} \leq P_{wt} \quad (6—42)$$

Where

$$D_{z,t}^{SPIN} = \min\{1, \frac{E_{z,t}}{R_{MKT,t}^{SPIN}}\} \quad (6—43)$$

$$D_{z,t}^{SUPP} = \max\{0, \frac{E_{z,t} - R_{MKT,t}^{SPIN}}{R_{MKT,t}^{SUPP}}\}. \quad (6—44)$$

Note that $PTDF_{z,k}^{R}$ represents the zonal PTDF on transmission line *k* and it is calculated based on the average PTDF of the nodes in the same zone. Therefore, it is assumed that the reserves cleared in the same zone have the same impact on the system. Constraints (6—29), (6—30), and (6—31) balance the reserves on a zonal basis by using the zonal PTDFs. Improving the zonal PTDF can improve the accuracy of MISO's SCUC reserve requirements.

Involving (6—43) and (6—44) will cause the formulation nonlinear, which may be very difficult to solve. To avoid the nonlinearity of proposed formulation, for the first round to solve this proposed SCUC formulation, constraints (6—31) are not considered. After the

first round, $E_{k,t}$ can be determined. The SCUC will be solved repeatedly, until the value of $E_{k,t}$ is stable.

Based on the concept of marginal pricing [90], the reserve market clearing price and energy price can be calculated as below,

$$MCP_{z,t}^{REG} = \gamma_{zt}^{ZRR} + \gamma_{zt}^{ZRS} + \gamma_{zt}^{ZOR} \quad (6—45)$$

$$MCP_{z,t}^{SPIN} = \gamma_{zt}^{ZRS} + \gamma_{zt}^{ZOR} \quad (6—46)$$

$$MCP_{z,t}^{SUPP} = \gamma_{zt}^{ZOR} \quad (6—47)$$

$$LMP_{n,t} = \lambda_t + \sum_{k\in K}\{(\mu_{k,t} + \mu_{k,t}^{REGUP} + \mu_{k,t}^{REGDN})PTDF_{n,k}^{R}\} + \sum_{z\in Z}\sum_{k\in K}\{\mu_{k,z,t}^{CR} PTDF_{z,k}^{R}\} \quad (6—48)$$

6.5.4 Look Ahead Unit Commitment

ISOs now prefer to have multiple scheduling horizons as compared to a one shot day-ahead scheduling; with more uncertainties, a preferred approach is to use a multi-stage approach to adjust decisions based on the change in the uncertainties [91]. During the transition process from the day-ahead market to the real time market, a look-ahead unit commitment (LAC) is allowed to commit additional generators. PJM implements a two hour LAC model, which focuses on fast-start units [92].

In MISO's scheduling process, units with long lead times will be studied by multi-day forward reliability assessment commitment (FRAC). The majority of commitments decisions are made in the DAM and day-ahead FRAC. LAC is used to create a bridge between the DAM as well as the reliability assessment commitment (RAC) and the RT-SCED. MISO uses a three hours LAC to ensure sufficient generation and ramp capacity with the most recent uncertainty forecasts and outage scheduler [93]. Intra-day reliability

assessment commitment (IRAC) has a similar formulation as RAC, but the time window of IRAC is from the current operating point to the end of the operating day. IRAC and LAC are better equipped with the most recent system operating information to improve commitment decisions.

In this Section, to approximate the market clearing process at MISO, LAC is also employed to adjust the DAM commitment decisions of resources whose minimum down time is less than or equal to three hours with consideration of the revealed net load scenarios. The LAC formulation is similar as the SCUC, except that many slow units are fixed.

6.5.5 Numerical Results

Table 6.4 Average Number of Reserve Disqualifications for Each Day

Model	Day 1	Day 2	Day 3	Day 4	Day 5	Day 6	Day 7
Dynamic	0.34	2.11	1.72	15.95	0.65	10.63	8.74
Seasonal	0.88	3.69	3.95	20.58	0.72	15.75	10.65

In statistics, a confidence interval (CI) is an indicator of estimating the range of the results and it provides the probability of the true population mean falling within the calculated interval [94]. CI is a tool that can be used to analyze the simulation results as well as validate the credibility of the results.

Reserve disqualification will be applied if the LAC solution is not N-1 reliable. Table 6.4 presents the average number of reserve disqualifications for one hundred net load scenarios each day. The dynamic reserve zone dramatically reduces the number of reserve disqualifications. By improving the reserve zone, the accuracy of zonal sensitivities are increased. Post regulation reserve up/down deployment constraints and post contingency event constraints better reflect the system stage with regulation reserve or contingency reserve deployed. Therefore, the location of the procured reserve is preferred.

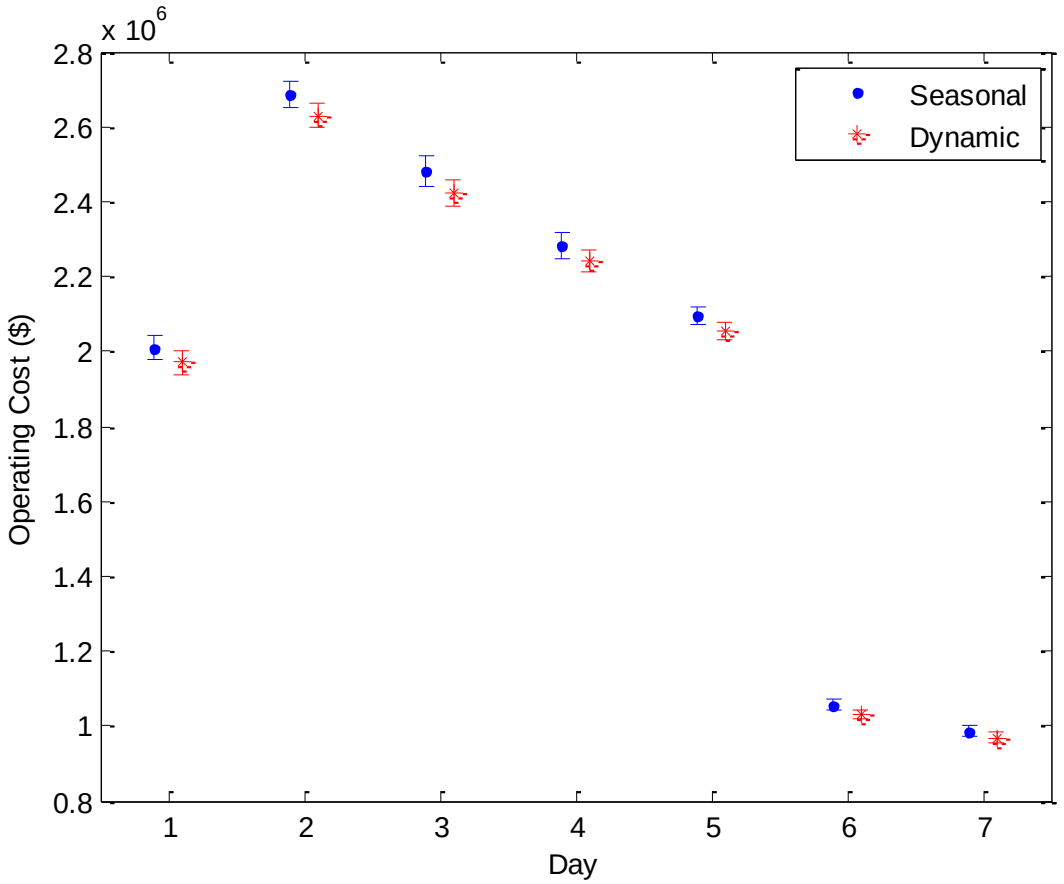

Figure 6.9 95% Confidence Interval of Operating Cost of Each Day for Dynamic and Seasonal Model

In Figure 6.9, the blue dot represents average operating costs after reserve disqualification (N-1 reliability approval) of the seasonal model and the red asterisk represents the results for the dynamic zone model. For results of each model, the top of each bar represents the upper bound of the 95% confidence interval and the bottom of each bar represents the lower bound of the 95% confidence interval. Obviously, the operating cost of the dynamic zone model is expected to be lower than the seasonal model. The average operating cost of the dynamic model for seven days is $1.90 million and the seasonal model is $1.95 million. The dynamic model updates the reserve zone on an hourly basis and the accuracy of zonal PTDFs ($PTDF_{k,z}$) will be improved with the consideration of system operating conditions and, thus, the SCUC model will be more accurate. As a

result, the market solution for the dynamic zone provides a better starting point for LAC and RTM, which results in the lower operating cost. Therefore, the proposed dynamic model has effectively improved the market efficiency and has provided more accurate price signals while also lowering the number of undesirable manual reserve disqualifications, which ensures that the market solution produces a more reliable solution.

The average load payment for seven days of the dynamic model is $7.11 million and that of the seasonal model is $7.56 million. Therefore, the load payment has been reduced by using the dynamic model since the average LMP of dynamic model is lower. The regulation reserve payment from the dynamic model has 1.2% higher average reserve payments than that of the seasonal model. The contingency reserve payment is the sum of the spinning reserve payment and the supplemental reserve payment. The average of the contingency reserve payment for the dynamic model is $0.17 million and the seasonal model is $0.13 million.

7. A NODAL REGULATION RESERVE PRICING MODEL

7.1 Introduction

Based on the response time and functionality, reserves can be categorized into three types [95]: regulation, spinning, and supplemental. The response time of each reserve product is longer than the preceding reserve product. Regulation (load following) reserve automatically adjusts its generation based on the feedback of area control error through central automatic control, which is also referred as automatic generation control (AGC). Regulation reserve can also be used to follow small system perturbations such as slow and small renewable or load deviations within several seconds. At MISO, regulation reserve is cleared as a 5-min product. Spinning reserve and supplemental reserve, which are 10 min products, are acquired to protect against large system perturbations such as contingencies [71]. However, each market may define reserve products differently based on the needs of its system.

From the previous chapters, spinning and non-spinning reserve requirements have been studied and the proposed dynamic reserve zone determination method can be extended to regulation reserve. However, in this chapter, different from contingency reserve, regulation reserve will be studied on a nodal basis to further improve the models' accuracy.

Similar as SCUC discussed in Chapter 5 and 6, deterministic SCED allocates reserve with pre-defined reserve requirements at minimum cost. As discussed in the previous chapters of this thesis, allocated reserve may not be deliverable in real-time due to network congestion. In Chapter 5 and Chapter 6, updating reserve zones on a more frequent basis enables a more accurate representation of operating conditions, identification of key transmission bottlenecks, the preferred locations for reserves, and better reserve sharing

rules across zones. However, zonal reserve requirements cannot fully solve the issue of undeliverable reserve due to the inaccuracy of zonal approximations that cannot ensure reserve deliverable on a nodal basis. Intra-zonal congestion causes significant cost to alleviate it for most ISOs using manual corrections.

The improvement of the SCED formulation described in this chapter is needed to lower ISOs' manual corrections. The contributions of this chapter are as follows,

1) Post regulation reserve deployment constraints are modeled in security constrained economic dispatch (SCED) on a nodal basis. Nodal formulation will improve the accuracy of calculating the post deployment power flow, improve the locations of the reserve, and result in more accurate price signals. The same model can also be applied to unit commitment models.
2) A nodal regulation reserve pricing scheme is developed to better reflect the quality of service offered by generators on a nodal basis. The impact of modeling nodal basis post reserve deployment on electricity market, such as locational marginal prices (LMP) and reserve market clearing prices, are studied.

7.2 Existing MISO Practice

MISO co-optimizes energy and ancillary service every 5 min in the real–time SCED (RT-SCED) with energy bids and reserve bids [71]. The RT-SCED at MISO accounts for the transmission constrains that are determined by state estimation (SE) and real-time contingency analysis (RTCA) [98]. Transmission constraints, which cause transmission violations, will be added to the set of transmission constraints considered. To lower expected transmission violations after reserve deployment, in [67], RT-SCED is enhanced

by incorporating post zonal reserve deployment and modeling the largest contingency in each reserve zone. The resulting RT-SCED formulation is as follows,

$$\underset{p_{g,t},r_{g,t}^{REG},r_{g,t}^{SPIN},r_{g,t}^{SUPP}}{\text{Min}} \sum_{j\in J}\left\{C_g p_{gt} + C_g^{REG} r_{gt}^{REG} + C_g^{SPIN} r_{gt}^{SPIN} + C_g^{NL} r_{gt}^{SUPP}\right\} \quad (7—1)$$

s.t.:

Power balance equation (λ_t)

$$\sum_{n\in N}(i_{nt}) = 0 \quad (7—2)$$

Power injection

$$i_{nt} = \sum_{n_g=n}\left(p_{gt}\right) - D_{nt}\,,\ \forall n \in N \quad (7—3)$$

Transmission constraints ($\mu_{i,t}$)

$$f_{kt} \le F_k^{max} \quad \forall k \in K \quad (7—4)$$

$$f_{kt} = \sum_{g\in G}\left\{p_{gt} PTDF_{n_j,k}^{R}\right\} + \sum_{n\in N}\left\{i_{nt} PTDF_{n,k}^{R}\right\} \quad \forall k \in K \quad (7—5)$$

Market-wide regulation reserve requirement (γ_t^{MRR})

$$\sum_{z\in Z} r_{z,t}^{REG} \ge R_{MKT,t}^{REG} \quad (7—6)$$

Market-wide regulation plus spinning reserve requirement (γ_t^{MRS})

$$\sum_{z\in Z}\{r_{z,t}^{REG} + r_{z,t}^{SPIN}\} \ge R_{MKT,t}^{REG} + R_{MKT,t}^{SPIN} \quad (7—7)$$

Market-wide operating reserve requirement (γ_t^{MOR})

$$\sum_{z\in Z}\{r_{z,t}^{REG} + r_{z,t}^{SPIN} + r_{z,t}^{SUPP}\} \ge R_{MKT,t}^{REG} + R_{MKT,t}^{SPIN} + R_{MKT,t}^{SUPP} \quad (7—8)$$

Base zonal regulation reserve requirement ($\gamma 0_{z,t}^{ZRR}$)

$$\sum_{g\in G(z)} r_{gt}^{REG} \ge R_{z,t}^{REG} \quad (7—9)$$

Base zonal regulation plus spinning reserve requirement ($\gamma 0_{z,t}^{ZRS}$)

$$\sum_{g\in G(z)}\{r_{gt}^{REG} + r_{gt}^{SPIN}\} \ge R_{z,t}^{REG} + R_{z,t}^{SPIN} \quad (7—10)$$

Base zonal operating reserve requirement ($\gamma 0_{z,t}^{ZOR}$)

$$\sum_{g\in G(z)}\{r_{gt}^{REG}+r_{gt}^{SPIN}+r_{gt}^{SUPP}\}\geq R_{z,t}^{REG}+R_{z,t}^{SPIN}+R_{z,t}^{SUPP} \quad (7—11)$$

Zonal regulation reserve requirement ($\gamma_{z,t}^{ZRR}$)

$$\sum_{g\in G(z)} r_{g,t}^{REG}\geq r_{z,t}^{REG} \quad (7—12)$$

Zonal regulation plus spinning reserve requirement ($\gamma_{z,t}^{ZRS}$)

$$\sum_{g\in G(z)}\{r_{gt}^{REG}+r_{gt}^{SPIN}\}\geq r_{z,t}^{REG}+r_{z,t}^{SPIN} \quad (7—13)$$

Zonal operating reserve requirement ($\gamma_{z,t}^{ZOR}$)

$$\sum_{g\in G(z)}\{r_{gt}^{REG}+r_{gt}^{SPIN}+r_{gt}^{SUPP}\}\geq r_{z,t}^{REG}+r_{z,t}^{SPIN}+r_{z,t}^{SUPP} \quad (7—14)$$

Post regulation reserve up deployment ($\mu_{k,t}^{REGUP}$)

$$f_{kt}+\sum_{z\in Z}\left\{r_{zt}^{REG}PTDF_{z,k}^{R}\right\}-PTDF_{LC,k}^{R}R_{MKT,t}^{REG}\leq F_{k}^{max} \quad (7—15)$$

Post regulation reserve down deployment ($\mu_{k,t}^{REGDN}$)

$$f_{kt}-\sum_{z\in Z}\left\{r_{zt}^{REG}PTDF_{z,k}^{R}\right\}+PTDF_{LC,k}^{R}R_{MKT,t}^{REG}\leq F_{k}^{max} \quad (7—16)$$

Post zonal contingency event ($\mu_{i,k,t}^{CR}$)

$$f_{kt}-E_{z,t}PTDF_{z,k}^{R}+DF_{z,t}^{SPIN}\sum_{z'\in Z}\left\{r_{z',t}^{SPIN}PTDF_{z',k}^{R}\right\}+DF_{z,t}^{SUPP}\sum_{z'\in Z}\left\{r_{z't}^{SUPP}PTDF_{z',k}^{R}\right\}\leq \bar{F}_{k}^{max},\ t\in T,k\in K,g\in G \quad (7—17)$$

Resource limit constraints

$$p_{gt}+r_{gt}^{REG}+r_{gt}^{SPIN}+r_{gt}^{SUPP}\leq \bar{U}_{gt}p_{g}^{max},t\in T,g\in G \quad (7—18)$$

$$p_{gt}-r_{gt}^{REG}\geq \bar{U}_{gt}p_{g}^{min},t\in T,g\in G \quad (7—19)$$

Ramp constraints

$$p_{gt}-p_{g,t-1}\leq R_{g}^{HR},t\in T,g\in G \quad (7—20)$$

$$p_{g,t-1}-p_{gt}\leq R_{g}^{HR},t\in T,g\in G \quad (7—21)$$

$$0\leq r_{gt}^{REG}\leq \overline{R}_{gt}^{REG},t\in T,g\in G \quad (7—22)$$

$$0\leq r_{gt}^{SPIN}\leq \overline{R}_{gt}^{SPIN},t\in T,g\in G \quad (7—23)$$

$$0\leq r_{gt}^{SUPP}\leq \overline{R}_{gt}^{SUPP},t\in T,g\in G \quad (7—24)$$

Where

$$DF_{z,t}^{SPIN} = \min\{1, \frac{E_{z,t}}{R_{MKT,t}^{SPIN}}\} \quad (7—25)$$

$$DF_{z,t}^{SUPP} = \max\{0, \frac{E_{z,t}-R_{MKT,t}^{SPIN}}{R_{MKT,t}^{SUPP}}\}. \quad (7—26)$$

The determination process of $DF_{k,t}^{SPIN}$ and $DF_{k,t}^{SUPP}$ follows the procedures in [75]. Based on the concept of marginal pricing [95], the reserve market clearing price and energy price can be calculated as below,

$$MCP_{z,t}^{REG} = \gamma_{zt}^{ZRR} + \gamma_{zt}^{ZRS} + \gamma_{zt}^{ZOR} + \gamma 0_{zt}^{ZRR} + \gamma 0_{zt}^{ZRS} + \gamma 0_{zt}^{ZOR} \quad (7—27)$$

$$MCP_{z,t}^{SPIN} = \gamma_{zt}^{ZRS} + \gamma_{zt}^{ZOR} + \gamma 0_{zt}^{ZRS} + \gamma 0_{zt}^{ZOR} \quad (7—28)$$

$$MCP_{z,t}^{SUPP} = \gamma_{zt}^{ZOR} + \gamma 0_{zt}^{ZOR} \quad (7—29)$$

$$LMP_{n,t} = \lambda_t + \sum_{k\in K}\{(\mu_{k,t} + \mu_{k,t}^{REGUP} + \mu_{k,t}^{REGDN})PTDF_{n,k}^{R}\} + \sum_{k\in K}\sum_{z\in Z}\{\mu_{k,z,t}^{CR}PTDF_{z,k}^{R}\} \quad (7—30)$$

Different reserve products have different response times and reserves with shorter response times are supposed to provide a higher quality service, and they can be substituted for lower quality service products. To be more specific, regulation reserve can be used to replace both spinning reserve and supplemental reserve; similarly, spinning reserve can be used to substitute supplemental reserve. In the proposed formulation, based on duality theory, the shadow prices ($\gamma_{zt}^{ZRR}, \gamma_{zt}^{ZRS}, \gamma_{zt}^{ZOR}, \gamma 0_{zt}^{ZRR}, \gamma 0_{zt}^{ZRS}, \gamma 0_{zt}^{ZOR}$) are nonnegative, which creates the relationship between different reserve products as shown below,

$$MCP_{z,t}^{REG} \geq MCP_{z,t}^{SPIN} \geq MCP_{z,t}^{SUPP} \quad (7—31)$$

In this model, post reserve deployment constraints implicitly balance the reserve quantity in each zone while meeting the market-wide reserve requirements. However, this

formulation models the post regulation reserve deployment constraints on a zonal basis, which assumes that nodes in the same zone have the same zonal sensitivities. However, nodes in the same zone may have quite different nodal sensitivities on some transmission lines, some of which may be prone to transmission bottlenecks.

7.3 Post Nodal Regulation Reserve Deployment Formulation

The transition from zonal energy clearing process to nodal energy clearing process is widely recognized as a success. This inspires the transition of zonal reserve requirements to nodal reserve requirements in this chapter. The regulation reserve is deployed more frequently compared to the spinning and supplemental reserve due to the low probability of contingencies. Thus, in this chapter, only regulation reserve will be modeled on a nodal basis. For the post nodal regulation reserve deployment formulation, it is assumed that the load increase happens in the load center and the assumption is the same as MISO's current formulation, and the maximum load increase for period t is assumed to be $R_{MKT,t}^{REG}$. The proposed formulation with consideration of post nodal regulation reserve constraints is listed as follows,

Objective: (7—1)

s.t.:

Equations (7—2) — (7—14) and (7—17) — (7—24)

Nodal post regulation reserve up deployment (δ_{kt}^{REGUP})

$$f_{kt} + \sum_{g \in G} r_{g,t}^{REG} PTDF_{n_j,k}^{R} - PTDF_{LC,k}^{R} R_{MKT,t}^{REG} \leq \overline{F}_k^{max} \qquad (7—32)$$

Nodal post regulation reserve down deployment (δ_{kt}^{REGDN})

$$f_{kt} - \sum_{g \in G} r_{g,t}^{REG} PTDF_{n_j,k}^{R} + PTDF_{LC,k}^{R} R_{MKT,t}^{REG} \leq \overline{F}_k^{max} \qquad (7—33)$$

Equations (7−32) and (7−33) capture the regulation reserve deployment impacts on transmission lines more accurately by utilizing nodal sensitivities. Hence, the reserve quantity will be balanced at a higher resolution, i.e., on a nodal basis. Note that, in comparison to stochastic programming where each post nodal balance constraint is explicitly modeled [10], the proposed nodal regulation reserve deployment formulation is an improved deterministic reserve requirement model. The proposed formulation examines the post regulation reserve deployment for the case when the load increase is equal to the market-wide reserve requirement, $R_{MKT,t}^{REG}$, and all the cleared regulation reserves are deployed. The proposed formulation more accurately captures the impacts of deploying regulation reserve, as compared to the zonal method, while still maintaining a deterministic structure that is computationally tractable and does not have pricing issues in comparison to stochastic programming.

7.4 Nodal Regulation Reserve Price and Scarcity pricing

Nodal post regulation reserve deployment constraints will lead to nodal regulation reserve prices. The reserve market clearing prices (MCP) and the energy clearing prices can be calculated as shown below,

$$MCP_{n,t}^{REG} = \gamma_{zt}^{ZRR} + \gamma_{zt}^{ZRS} + \gamma_{z_n t}^{ZOR} + \gamma 0_{zt}^{ZRR} + \gamma 0_{zt}^{ZRS} + \gamma 0_{z_n t}^{ZOR} + \sum_{k\in K} PTDF_{n,k}^{R}\left(\delta_{k,t}^{REGUP} - \delta_{k,t}^{REGDN}\right) \quad (7—34)$$

$$MCP_{\mathrm{n},t}^{SPIN} = \gamma_{z_n \mathrm{t}}^{ZRS} + \gamma_{z_n \mathrm{t}}^{ZOR} + \gamma 0_{z_n \mathrm{t}}^{ZRS} + \gamma 0_{z_n \mathrm{t}}^{ZOR} \quad (7—35)$$

$$MCP_{n,t}^{SUPP} = \gamma_{z_n \mathrm{t}}^{ZOR} + \gamma 0_{z_n \mathrm{t}}^{ZOR} \quad (7—36)$$

$$LMP_{n,t} = \lambda_t + \sum_{k\in K}\left\{(\mu_{k,t} + \delta_{k,t}^{REGUP} + \delta_{k,t}^{REGDN})PTDF_{n,k}^{R}\right\} + \sum_{k\in K}\sum_{z\in Z}\left\{\mu_{k,z,t}^{CR} PTDF_{n,k}^{R}\right\}. \quad (7—37)$$

Note that $\sum_{k \in K} PTDF_{n,k}^{R}\left(\delta_{k,t}^{REGUP} - \delta_{k,t}^{REGDN}\right)$ is part of the congestion component of the regulation reserve price. The congestion component may lead to $MCP_{n,t}^{REG} < MCP_{\mathrm{n},t}^{SPIN}$ for some nodes; this is known as a price reversal and was a problem that existed in early ancillary service market designs that led to market manipulation and the exercise of market power. Under the zonal reserve formulation, such situations may lead to a reverse clearing priority of regulation reserve, spinning reserve, and supplemental reserve. For example, a regulation reserve shortage may happen ahead of spinning reserve as a result of market manipulation. This may happen even without any market manipulation if the constraints are not formulated carefully. The shortage of high priority regulation reserve ahead of spinning or supplemental reserve will impose operational issues. With the implementation of this new approach, improvements in the market design and settlement schemes should be implemented in order to avoid such price reversals. Similar adjustments that were considered for earlier ancillary services market designs, which fell prey to market manipulation and price reversals, can be considered here to ensure price reversals do not occur.

If price reversals occur, note that the negative congestion component is a sign that the reserve is not desired at that corresponding location. Therefore, cleared regulation reserve capacity on these nodes is expected to be minimal. However, regulation reserve on these nodes may be cleared to substitute for spinning reserve. Empirical evidence from this study supports these conjectures. As is discussed in Chapter 7 Section 7.3, the regulation price falls below the spinning reserve price only at nodes where no regulation reserve was procured; the proposed nodal model identifies nodes where regulation reserve is not beneficial whereas the zonal model is not able to make this preferred determination.

Furthermore, such improperly procured reserves from the zonal model, which are at nodes that have a poor deliverability (cause additional congestion problems), are likely to be disqualified anyways through the reserve disqualification procedures employed by MISO (similar procedures occur at other ISOs, e.g., ISONE refers to this as a reserve downflag). By enhancing the market model to procure deliverable reserves, the market surplus overall will be improved and the pricing signals are more accurate; the proposed model also reduces costly out of market corrections that distort market signals and are determined by operators based on ad-hoc policies.

7.5 IEEE RTS-96 Test Case

To validate the effectiveness and performance of proposed nodal post regulation reserve formulation, a modified IEEE Reliability Test System (RTS)-96 with 73 nodes, 99 units, 117 lines, and 51 loads, is used.

A twenty-four hours SCUC model is solved first to determine unit output and commitments for twenty-four periods, and each period can be viewed as a starting point for the RT-SCED. For each period, the RT-SCED will be solved for both nodal and zonal models, where zonal model refers to the MISO's current formulation in Section 7.2, and nodal model refers to the proposed formulation in Section 7.3.

Regulation, spinning, and supplemental reserves are considered in this analysis. Each generator's regulation reserve bid is 25% of its energy bid, and spinning reserve bid is 10% of its energy bid, and supplemental reserve bid is 5% of its energy bid. The market-wide regulation reserve requirements, regulation reserve plus spinning reserve requirements, and operating reserve requirements are set as 60MW, 150MW, and 300MW respectively. All testing is performed using CPLEX v12.6 on a 2-core 2.8 GHz computer with 12 GB RAM.

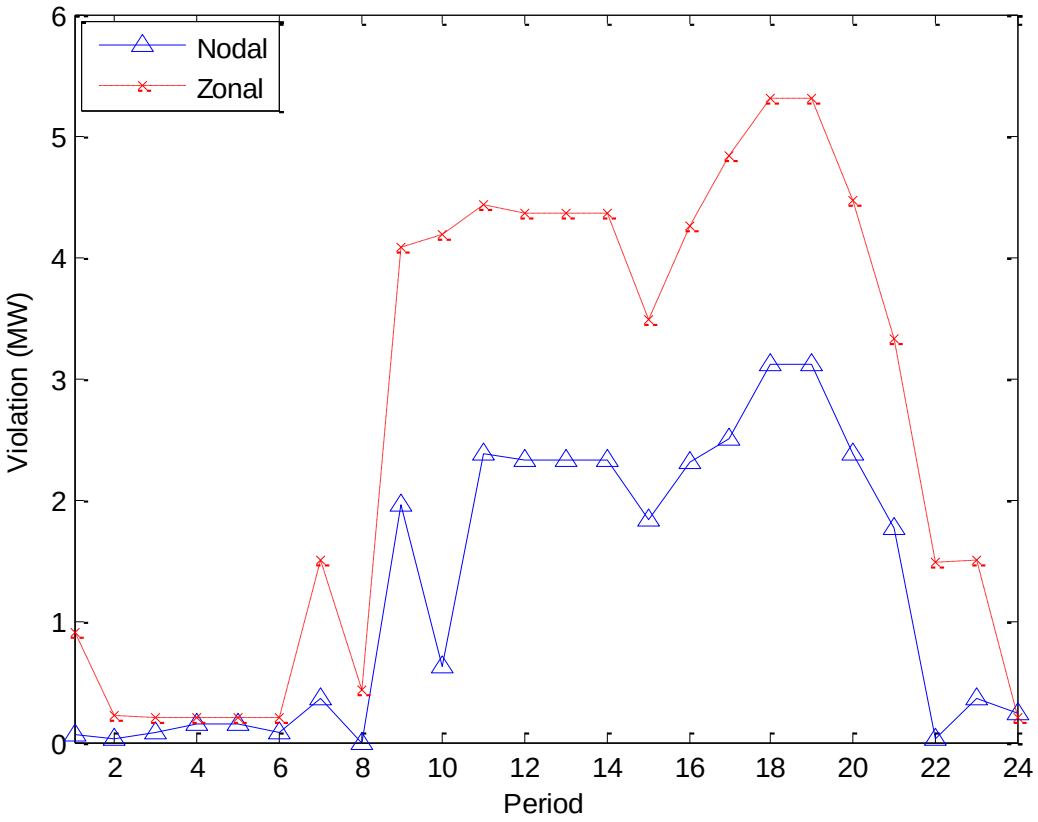

Figure 7.1 Average Post Regulation Reserve Deployment Transmission Violation (MW)

An evaluation problem is established to evaluate the transmission violation considering one thousand load scenarios based on the RT-SCED solution from each model. One thousand load scenarios with equal probability are generated by Monte Carlo simulation, and they are used to mimic the real-time load variation [1]. From Figure 7.1, the average transmission violations are presented for each period based on the one thousand load scenarios. For most of the periods, nodal model has much less average transmission violations comparing with the zonal model. To further confirm the improvement of the proposed regulation reserve pricing scheme on system reliability, the maximum transmission violation for each period is presented in Figure 7.2. From Figure 7.2, the worst case of the transmission violations (i.e., maximum transmission violation) of nodal model is much better than that of zonal model. The average maximum transmission violation of

nodal model is 10.7MW and that of zonal model is 26.9MW. The higher value of maximum transmission violation tends to incur more reserve disqualifications and additional operating cost. The improvement on average transmission violation and the maximum transmission violation indicates that the nodal model improves the modeling accuracy and better formulates the post regulation reserve deployment. Therefore, the proposed nodal model improves the solution reliability.

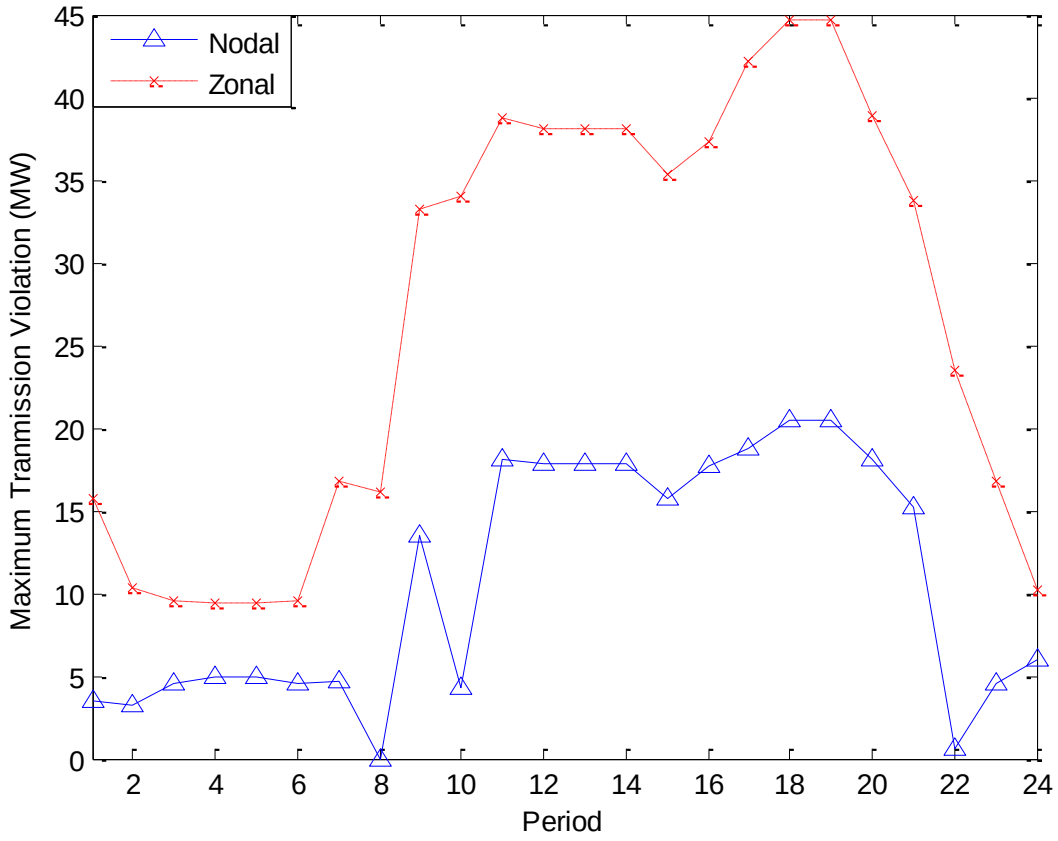

Figure 7.2 Maximum Transmission Violation (MW)

Figure 7.3 shows the objective, i.e. operating cost of the RT-SCED, before the reserve disqualifications, for both nodal and zonal model. It can be easily observed that the operating costs of these two models are very close except period 10. The operating cost of nodal model at period 10 is higher than that of zonal model. What makes this result

noteworthy is that the improvement on transmission violation is improved most in period 10 by using the nodal model and the violations drop from 4.19MW to 0.63MW. Binding post nodal regulation deployment constraints drive up the operating cost. However, these constraints help improve the solution reliability dramatically as well as reduce the need for costly out of market corrections that distort market signals.

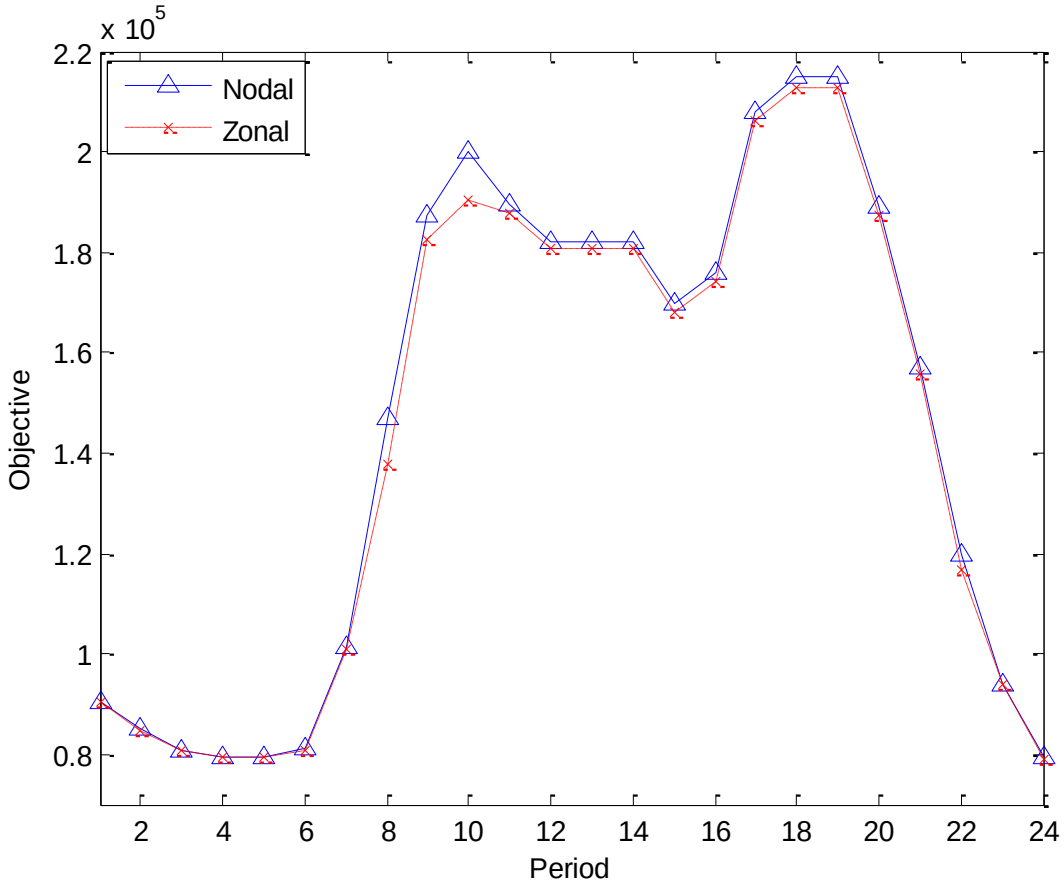

Figure 7.3 Average RT-SCED Objective ($)

Based on the discussion of nodal reserve pricing in Chapter 7 Section 7.5, post regulation reserve deployment constraints include a congestion component on the regulation reserve price. In Figure 7.6, the average regulation reserve price for twenty-four periods is calculated on a nodal basis by (7—34). For the zonal model, the nodes in the

same zone will have the same zonal price as calculated in (7—27) and the zonal regulation prices for the zonal model are $7.16/MW, $13.28/MW, and $12.74/MW respectively. Obviously, the regulation reserve price for the nodal model varies by nodes and sends better price signals. Similar to LMPs, the congestion component contributes to the difference of regulation reserve prices between different nodes. Resources that alleviate the congestion will receive a positive congestion component and resources that aggravate the congestion will receive a negative congestion component. Nodal model will encourage resources with higher regulation reserve prices to provide regulation reserve and vice versa.

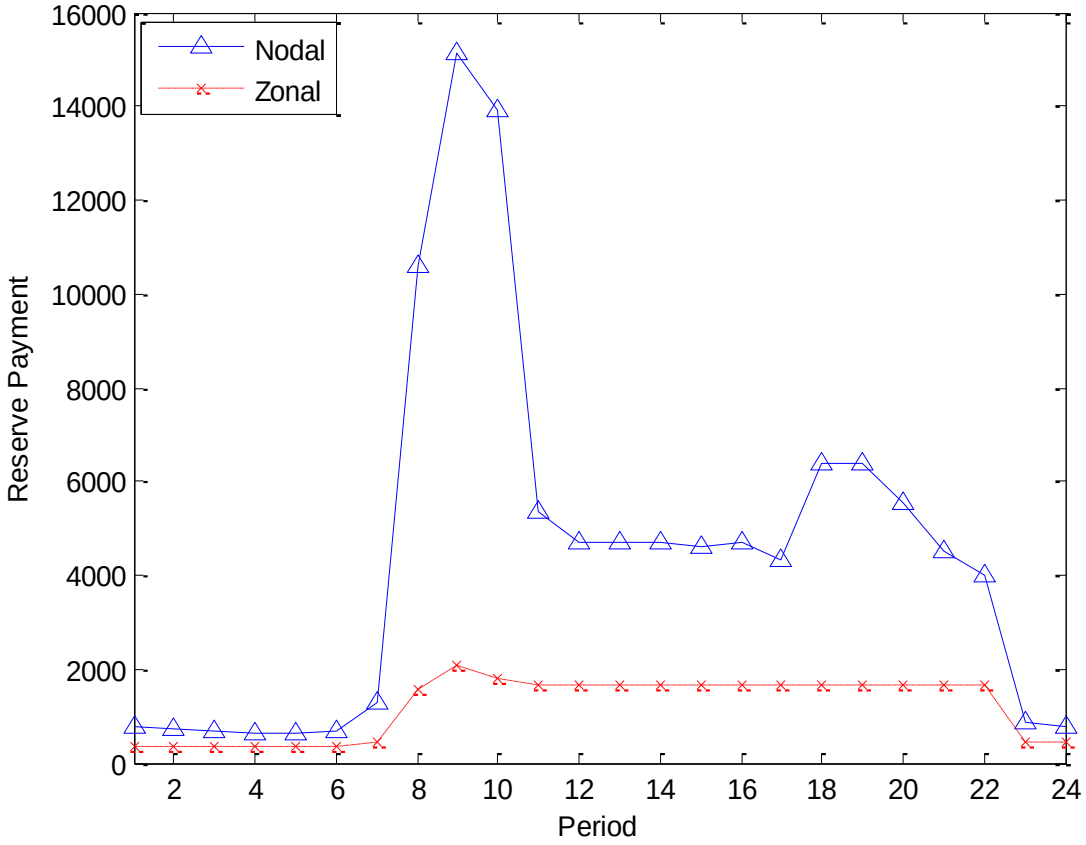

Figure 7.4 Reserve Payment for Each Period ($)

From Figure 7.6 nodes 34-38 and 40-41 have negative nodal regulation reserve prices; as a result, the regulation reserves, at those nodes, are not preferred. For instance, the

average regulation reserve prices at node 14 and 15 are $192.70/MWh and $-16.63/MWh, respectively, and they receive average congestion components of $119.91/MWh and $-89.4/MWh. Furthermore, nodal regulation reserve prices on nodes 15-19, 21-22, 60-61, 68, 71, and 73 are less than the spinning reserve prices for all nodes within that same zone. Based on utilizing MISO data involving 24 different RT-SCED runs combined with 1,000 different potential load scenarios for each of the 24 periods (a total of 24,000 ex-post simulations were conducted to analyze the performance of this technique), no regulation reserve is cleared on these nodes. However, the zonal model, on average, clears 24.4MW of regulation reserve from resources at these nodes. This is a very important result as it clearly demonstrates the value of the nodal approach. Note also that the procured reserve at these nodes by the zonal model would likely be disqualified by MISO's reserve disqualification procedure since the actual regulation reserve is not deliverable (i.e., the reserve is undesirable at these nodes).

In Figure 7.4, the total reserve payment of nodal model is much higher than that of zonal model for some periods. The reason is that nodal model may drive the regulation reserve prices at "good" locations, and regulation reserve at these locations are preferred because they can counter the network congestion. Thus, the reserve payment of nodal model is expected to be higher. The objectives, i.e. operating cost, of these two models are very similar and the increase of reserve payment can be viewed as welfare transfer from load to supply. Such welfare transfer may lower the uplift payment.

Figure 7.5 and Figure 7.7 present the impacts on LMPs for the nodal model. Figure 7.7 shows that some of the LMPs of the nodal model are slightly higher than those of the zonal

model. This indicates that the congestion components of these LMPs are larger. Acquiring the regulation reserve on a nodal basis may increase the congestion component of LMPs.

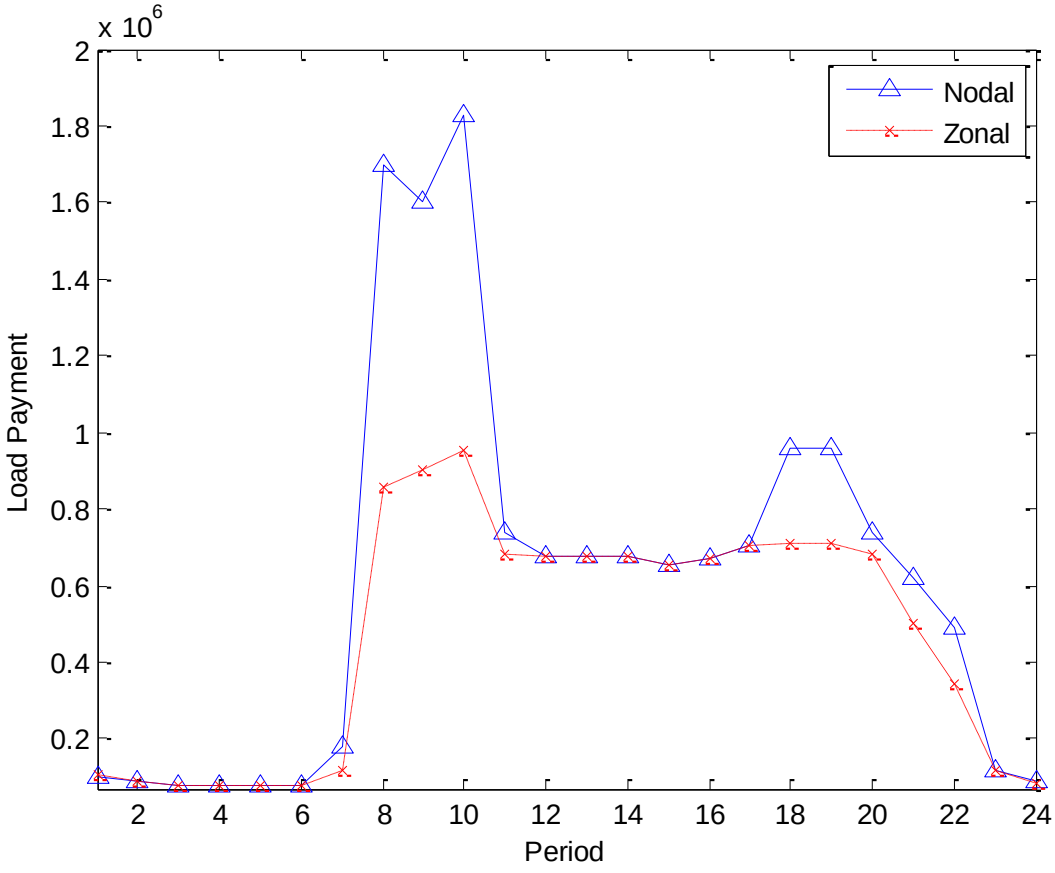

Figure 7.5 Load Payment for Each Period ($)

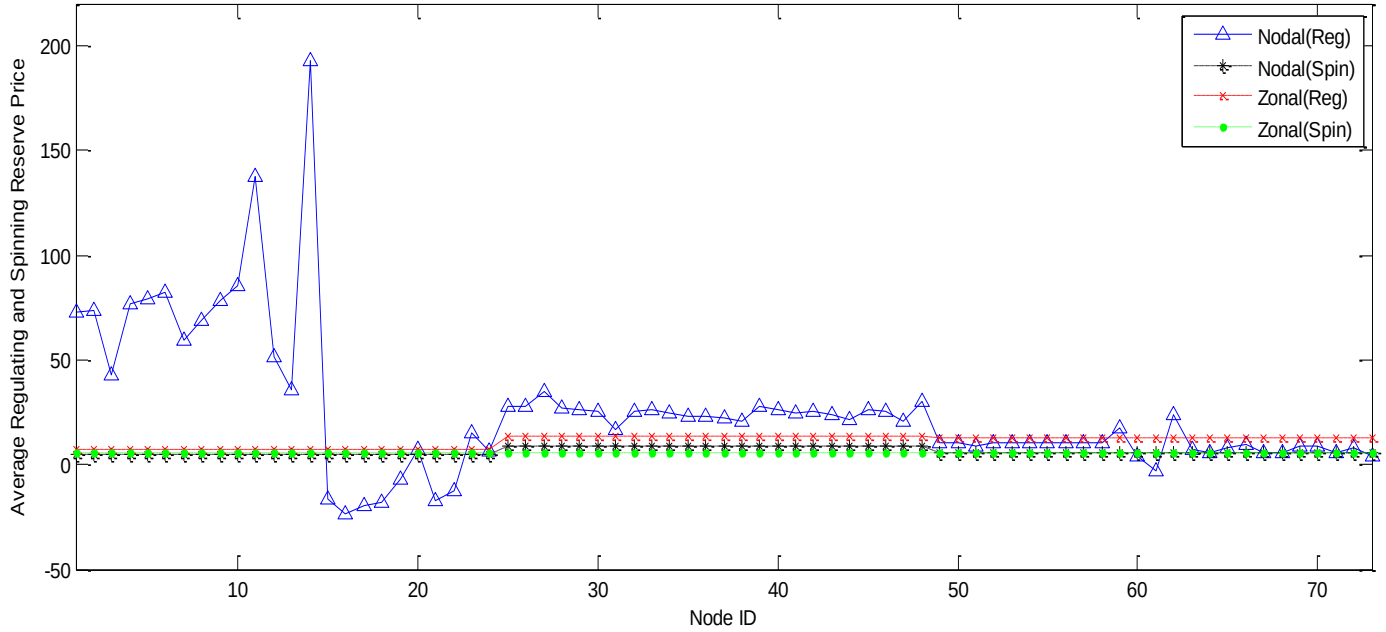

Figure 7.6 Average Regulation Reserve Price ($/MWh)

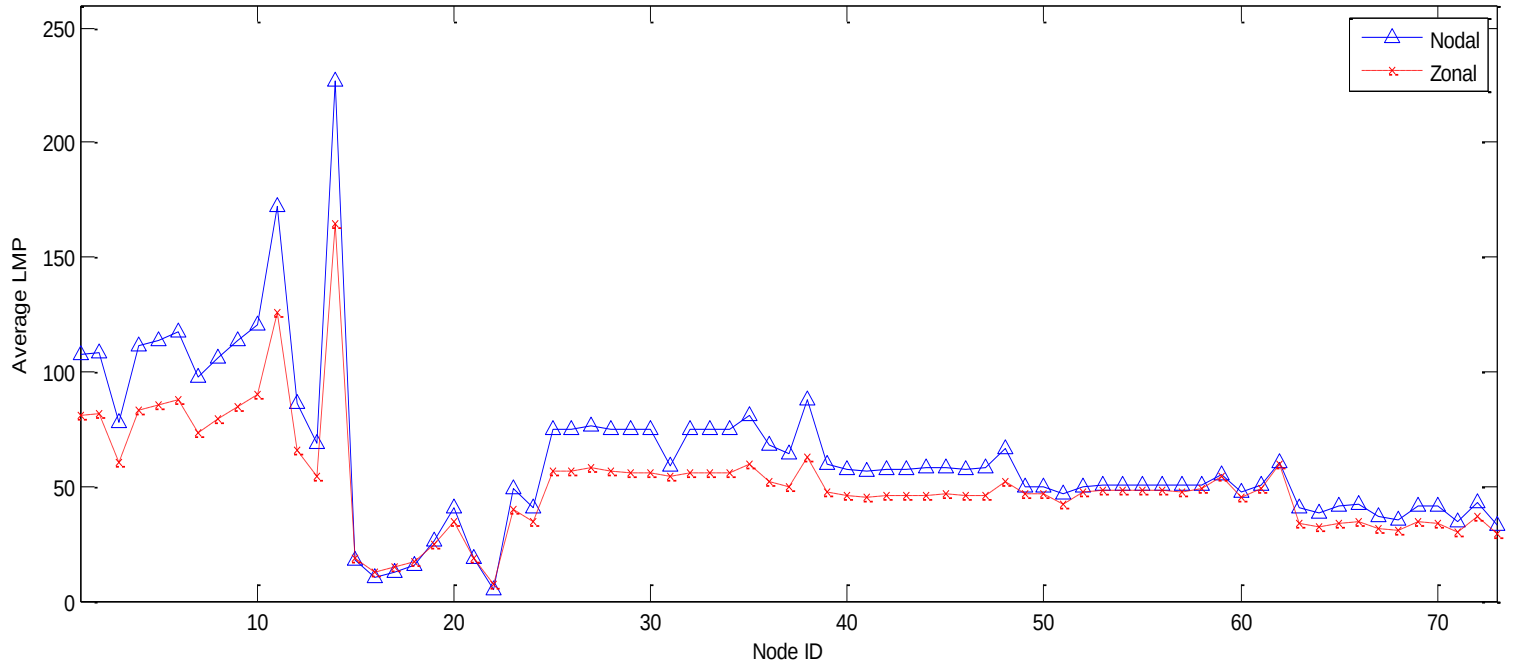

Figure 7.7 Average LMP for Each Bus ($/MWh)

7.6 MISO Test Case

In this section, a prototype of the proposed post nodal regulation reserve deployment formulation was implemented on the MISO's system with the assumption that the load increase happens in the load center. The tested RT-SCED case has 27 transmission constraints and about 1400 resources.

Table 7.1 Comparison of Zonal and Nodal Results

Model	Penalty Cost	Transmission Violation
Zonal	$120/MWh	15.34MW
Nodal	$120/MWh	0.64MW
Nodal	$300/MWh	0MW

For the MISO test case, the post zonal regulation reserve deployment and post nodal regulation reserve deployment are relaxed with a pre-defined penalty factor with the assumption that the load increase happens in the load center. Table 7.1 shows the post reserve deployment transmission violations for the zonal model, with a penalty factor set at $120/MWh, and the violations for the nodal model, with penalty factors set at $120/MWh and $300/MWh; these results correspond to time interval 19:35. The RT-SCED clearing process in MISO is replicated using both zonal and nodal models. In this case, the zonal model may require more reserve disqualifications to avoid the transmission violations. For the nodal model, as the penalty factor increases, violating the post nodal regulation reserve deployment constraints will be more expensive and the transmission violation decreases. With the assumption that the transmission violation cost is $2,000/MWh, the social welfare is improved by roughly 2% by using the nodal model (with penalty costs at $120/MWh and $300/MWh).

8. CONCLUSION

Current reserve zones are based on ad-hoc or rule of thumb approaches, such as utilities ownership and geographical boundaries, and are usually treated as static. With the growing concern to improve reserve requirements, there is a need to develop systematic approaches to determine reserve zones and reserve levels. A novel reserve zone partition method based on PTDFDs is proposed in this thesis. The PTDFD zone partitioning method is a heuristic method that does not guarantee optimality; however, one primary benefit of this method is that it is computationally tractable. Buses that have similar PTDFs on a group of transmission lines have similar impact on the grid, which is the basis for the choice to use PTDFDs to determine reserve zones. From the numerical results in Chapter 4 Section 4.3, improving reserve zones can improve deliverability of reserve, market efficiency, and reliability. Although optimality cannot be guaranteed, this reserve zones partition method provides more operational flexibility and validates the potential uses of reserve zones.

With high penetration of renewables in the system, there are more uncertainties in the grid, which create new challenges to power engineers. The proposed dynamic (daily-probabilistic) reserve zones in Chapter 5 Section 5.2 is used to generate reserve zone while the system has a high penetration of renewables. This proposed reserve zone determination method (daily-probabilistic) has been extensively studied with two approaches: a deterministic unit commitment framework and a stochastic unit commitment framework. These two approaches have been compared against three different models and across twelve days within the winter season. Sixty day-ahead 24-hour unit commitment models have been solved (5 for each of the 12 days) with 24 of those day-ahead unit commitment models being an extensive form stochastic unit commitment formulation (the remaining

models are deterministic unit commitment models). Contingency analysis and wind scenario analysis have been conducted on those 60 day-ahead unit commitment dispatch solutions, which required roughly 4.5 million simulations. The extensive numerical results demonstrate that a dynamic (daily-probabilistic) zonal partitioning method is preferred over seasonal methods as dynamic reserve zones are better equipped to reflect operational conditions of the network. The proposed dynamic reserve zone method, which relies on probabilistic power flow information, is more reliable. The proposed method improves reserve deliverability, leading to improvements in operating efficiency and reliability.

Stochastic programming has been suggested as a solution to manage future resource uncertainties in grid operations. However, even with advanced algorithms and hardware, implementation of stochastic programming is still a huge challenge for large-scale unit commitment problems today. Even deterministic unit commitment problems are a challenge as there are vast assumptions and approximations that are built in these optimization problems. Improving reserve requirements will be useful no matter if the formulation is a deterministic or a stochastic programming framework. A balanced approach between dynamic reserves and stochastic programming techniques will be the preferred short-term and long-term answer to this challenge. The proposed dynamic reserve zone partitioning method provides a computationally tractable way to manage the issue of reserve deliverability, which leads to an improvement in reliability and economic efficiency.

With the consideration of electricity market, the proposed dynamic policies can also improve the ancillary service market performance. Ancillary service markets are used to procure standby reserves that provide operators with additional flexibility to respond to

random disturbances. However, this flexibility is wasted when reserves are not deliverable due to transmission limitations. It is important to anticipate how uncertainty from intermittent renewable resources will affect congestion. It is desirable for the market model to anticipate what reserves will be deliverable in order to make efficient decisions and set prices that reflect the true locational scarcity of reserves.

Zonal reserve requirements ensure reserve is held within import-constrained areas. However, congestion may still prohibit the deliverability of reserve. In such cases, operators will adjust the solution by disqualifying reserves that are inhibited by transmission limitations. These adjustments occur outside of the DAM model and, therefore, are not reflected in day-ahead prices. Analysis on the IEEE RTS96 test case in Chapter 6 Section 6.7 demonstrates how updating zones on a more frequent basis can reduce the need for reserve disqualification and improve the real-time value of reserves procured in the DAM. The benefit of dynamic zones is magnified as the percentage of energy provided by uncertain resources (e.g., wind) increases. To enhance the credibility of numerical results, confidence interval of the market solutions are presented. The numerical results has shown that the proposed dynamic model can lower the operators' manual adjustments, i.e. reserve disqualification. Furthermore, the operating cost is lowered by using the proposed dynamic model. Therefore, the proposed hourly reserve zone improves the market solution of SCUC and LAC stages while also ensuring the market model more accurately captures system reliability.

Chapter 7 proposed a novel reserve requirements formulation, which incorporates the post regulation reserve deployment constraints on a nodal basis. Reserve acquired based on zonal approach may not be deliverable, and the proposed nodal model can improve the

reserve deliverability such that reduce or avoid the need of out of market corrections, i.e., regulation reserve disqualification. The market impact of nodal reserve is also studied in this Chapter. Regulation reserve price becomes more volatile due to added congestion component, and this change will encourage regulation reserve at "preferred" location to provide reserve. Another observation is that the reserve payment and load payment of nodal model are higher than those of zonal model, and it can be viewed welfare transfer.

In summary, this thesis aims to improve existing deterministic reserve requirements without incurring additional computational cost. The existing deterministic reserve requirements have very limited ability to acquire the reserves while considering the deliverability of the reserves, and there is no existing systematic way of determining reserve zones. In this thesis, a systematic way of determining dynamic reserve zone for contingency reserve is proposed to better locate the reserve. Also a nodal regulation reserve pricing scheme is also demonstrated to balance the reserve on a nodal basis. As more renewables are integrated in the power grid, network congestion becomes more unpredictable. Updating reserve zone on a more frequent basis or implementing nodal reserve requirements will be more beneficial. The results in this thesis confirms the importance and benefits of proposed dynamic reserve policies.

9. SUGGESTED FUTURE WORK

In this Chapter, additional future tasks are proposed to supplement the current work.

1. K-means will cluster the nodes with smallest PTDFD to the center of each cluster (zone). The average PTDFD between each node to the center of each cluster. The number of reserve zones can be determined by set a threshold to average PTDFD to the center of each cluster. If the average PTDFD to the center of each cluster exceed the threshold, it indicates that the number of reserve zone is not sufficient to guarantee the required similarity for each cluster (zone), and the number of reserve zones should be increased. The number of reserve zones can be fixed and input to the SCUC and/or SCED if all the average PTDFD to each cluster (zone) is below the threshold. The threshold value should be investigated with the consideration of market efficiency and reliability.
2. Nodal contingency reserve pricing can also be studied. The post contingency reserve deployment constraints can be reformulated on a nodal basis, and this change will also have impacts on electricity market. A study of nodal contingency reserve pricing should be performed to validate the feasibility and effectiveness of a nodal contingency reserve pricing scheme.

   Below is a potential formulation of a nodal reserve requirements, which include regulation, spinning, and supplemental reserves.

   Market wide regulation reserve requirements

$$\sum_{g \in G} r_{g,t}^{REG} \geq R_{MKT,t}^{REG} \quad (9—1)$$

   Market wide regulation and spinning reserve requirements

$$\sum_{g \in G} \{r_{g,t}^{REG} + r_{g,t}^{SPIN}\} \geq R_{MKT,t}^{REG} + R_{MKT,t}^{SPIN} \quad (9—2)$$

Market wide operating reserve requirements

$$\sum_{g\in G}\{r_{g,t}^{REG+} + r_{g,t}^{SPIN} + r_{g,t}^{SUPP}\} \geq R_{MKT,t}^{REG} + R_{MKT,t}^{SPIN} + R_{MKT,t}^{SUPP} \quad (9—3)$$

Post regulation-up deployment

$$f_{kt} + \sum_{g\in G} r_{g,t}^{REG} PTDF_{n_g,k}^{R} - PTDF_{LC,k}^{R}\left(R_{MKT,t}^{REG}\right) \leq F_k^{max} \quad (9—4)$$

Post regulation-down deployment

$$f_{kt} - \sum_{j\in J} r_{j,t}^{REG} PTDF_{n_g,k}^{R} + PTDF_{LC,k}^{R}\left(R_{MKT,t}^{REG}\right) \leq F_k^{max} \quad (9—5)$$

Post contingency contingency event

$$f_{i,t} - E_{z,t} PTDF_{n_{gz},k}^{R} + DF_{z,t}^{SPIN} \sum_{g\in G}\left\{r_{g,t}^{SPIN} PTDF_{n_g,k}^{R}\right\} + DF_{k,t}^{SUPP} \sum_{g\in G}\left\{r_{g,t}^{SUPP} PTDF_{n_g,k}^{R}\right\} \leq \overline{F}_k^{max} \quad (9—6)$$

Where $DF_{zt}^{SPIN} = \min\left\{1, \frac{E_{z,t}}{R_{MKT,t}^{SPIN}}\right\}, DF_{k,t}^{SUPP} = \max\{0, \frac{E_{z,t} - R_{MKT,t}^{SPIN}}{R_{MKT,t}^{SUPP}}\}$.

While there are still reserve zones modelled in the formulation, their purpose is no longer to capture reserve deployment but to help filter critical contingencies modelled in the post contingency event.

3. Stochastic programming has limitations such as market pricing, computation intensity, scenarios selection issues, but it can be used to determine the deterministic reserve requirements based on offline study. For instance, different scenarios can be generated ahead of day-ahead market SCUC, and the stochastic programming with modeled selected scenarios can be solved to output the deterministic reserve requirements for SCUC. The updated reserve requirements will carry the information of the scenarios generated each day. Such method is an alternative way of using stochastic programing in the power system operation problems while avoid its limitations.

4. Even though there are some limitations of stochastic programming's application on SCUC or SCED, developing a hybrid of stochastic and deterministic reserve policy is still beneficial. Stochastic programming can be used to model credible and dominant scenarios (contingencies) within allowable computational tolerance while deterministic reserve policy can be used to protect against the rest of the uncertainties.

REFERENCES

[1] R. Billinton and R. Allan, Reliability Evaluation of Power Systems, 2nd ed. New York: Plenum, 1996.

[2] CAISO, "Spinning and non-spinning reserve" [Online]. Available: http://www.caiso.com/docs/2003/09/08/2003090815135425649.pdf

[3] WECC, "WECC standard BAL-STD-002-0 – operating reserves," [Online]. Available: http://www.wecc.biz/Standards/Pending%20Standards/BAL-002-WECC-1.pdf

[4] A. Wood and B. Wollenberg, Power Generation, Operation and Control, 2nd edition. New York: Wiley, 1996.

[5] CAISO (2005), In Spinning Reserve Requirement. The California ISO, [Online]. Available : http://www.caiso.com/

[6] IESO (2004), the independent Electricity System Operator of Ontario Electrical System, 2004, [Online]. Available: http://www.ieso.ca

[7] UCTE (2005) Union for the Co-ordination of Transmission of Electricity Operation Handbook, [Online]. Available: http://www.ucte.org/pdf/ohb/Operation_Handbook_20.07.3004.pdf

[8] REE(1998) In Operacion del Sistema Electrico, Red Electrica de Espana, [Online]. Available: http://www.ree.es/cap03/pdf/po/PO_resol_30jul1998_b.pdf

[9] F. Bouffard, F. D. Galiana, and A. J. Conejo, "Market-clearing with stochastic security—Part I: formulation," *IEEE Trans. Power Syst*., vol. 20, no. 4, pp. 1818–1826, Nov. 2005.

[10] P. A. Ruiz,C. R. Philbrick, E. Zak, K. W. Cheung, and P. W. Sauer, "Uncertainty management in the unit commitment problem," *IEEE Trans. Power Syst.*, vol., 24, no. 2, pp. 642-651, May 2009.

[11] L. T. Anstine, R. E. Burke, J. E. Casey, R. Holgate, R. S. John, and H. G. Stewart, "Application of probability methods to the determination of spinning reserve requirements for the Pennsylvania-New Jersey-Maryland interconnection," *IEEE Trans. Power App. Syst.*, vol. PAS-82, no. 68, pp. 720–735, Oct. 1963.

[12] H. B. Gooi, D. P. Mendes, K. R. W. Bell, and D. S. Kirschen, "Optimal scheduling of spinning reserve," *IEEE Trans. Power Syst.*, vol. 14, no. 4, pp. 1485–1490, Nov. 1999.

[13] M. A. Ortega-Vazquez, and D. S. Kirschen, "Optimizing the Spinning Reserve Requirements Using A Cost/Benefit Analysis," *IEEE Trans. Power Syst.*, vol. 22, no. 1, pp. 24-33, Feb. 2007.

[14] L. Wu, M. Shahidehpour, and T. Li, "Cost of reliability analysis based on stochastic unit commitment," *IEEE Trans. Power Syst.*, vol. 23, no. 3, pp. 1364-1374, Aug. 2008.

[15] A. Papavasiliou, S. S. Oren, and R. P. O'Neill, "Reserve requirements for wind power integration: a scenario-based stochastic programming framework," *IEEE Trans. Power Syst.*, vol. 26, no. 4, pp. 2197-2206, Mar. 2011.

[16] L. Wu, M. Shahidehpour and T. Li, " Stochastic security-constrained unit commitment," *IEEE Trans. Power Syst.*, vol. 22, no. 2, pp. 800-811, May 2007.

[17] F. Galiana, F. Bouffard, J. M. Arroyo, and J. F. Restrepo, "Scheduling and pricing of coupled energy and primary, secondary, and tertiary reserves," *Proc. IEEE*, vol. 93, no. 11, pp. 1970-1983, Nov. 2005.

[18] T. Zheng, and E. Litvinov, "Contingency-based zonal reserve modeling and pricing in a co-optimized energy and reserve market," *IEEE Trans. Power Syst.*, vol. 23, no. 2, pp. 277-286, May 2008.

[19] A, Papavasiliou and S. S. Oren, "Multi-area stochastic UC for high wind penetration in a transmission constrained network," in the *FERC Software Conference 2011*, Washington DC, Jun. 28 2011.

[20] A. Kumar, S. C. Srivastava and S. N. Singh, "A zonal congestion management approach using real and reactive power rescheduling," *IEEE Trans. Power Syst.*, vol. 19, no. 1, pp. 554-562, Feb. 2004.

[21] ERCOT, "ERCOT Protocols, Section 7: Congestion Management" July, 2010 [Online]. Available at: www.ercot.com/content/mktrules/protocols/current/07-070110.doc

[22] Lagonotte, P., J. C. Sabonnadiere, J.-Y. Leost, J.-P. Paul, "Structural analysis of the electric system application to secondary voltage control in France," *IEEE Trans. Power Syst.*, vol. 4, no. 2, pp. 479-486, May. 1989.

[23] S. Blumsack, P. Hines, E. C. Sanchez, and C. Barrows, "The topological and electrical structure of power grids," in the *43rd Hawaii International Conference on System Sciences*, Kauai, Hawaii, Jan. 7-10 2010.

[24] Z. Wang, A. Scaglione and R. J. Thomas, "Electrical centrality measures for electric power grid vulnerability analysis," in *49th IEEE Conference on Decision and Control* , Atlanta, GA, Dec. 15-17, 2010.

[25] G. Chicco, R. Napoli, and F. Piglione, "Comparisons among clustering techniques for electricity customer classification," *IEEE Trans. Power Syst.*, vol. 21, no. 2, May 2006.

[26] Alexander Rakhlin, Andrea Caponnetto, Stablity of K-means Clustering. 2006 [Online]. Available: http://cbcl.mit.edu/publications/ps/rakhlin-stability-clustering.pdf

[27] L. I. Kuncheva, and D. P. Vetrov, "Evaluation of Stability of K-Means Cluster Ensembles with Respect to Random Initialization," *IEEE Trans. Pattern Analysis and Machine Intelligence*, vol. 28, no. 11, Nov. 2006

[28] U. M. Fayyad, C. Reina, and P. S. Bradley, "Initialization of iterative refinement clustering algorithms," in *Proc. 14th Intl. Conf. on Machine Learning (ICML)*, pp 194-198, 1998.

[29] J. Z. Huang, M. K. Ng, H. Rong, and Z. Li, "Automated Variable Weighting in K-Means Type Clustering," *IEEE Trans. Pattern Analysis and Machine Intelligence*, vol. 27, no. 5, Dec. 2005

[30] J. C. Bezdek, Pattern Recognition with Fuzzy Objective Function Algorithms, Plenum Press, New York 1981

[31] Uri Kroszynski and Jianjun Zhou, Fuzzy Clustering Principles, Methods and Examples, IKS, December 1998

[32] Teuvo Kohonen , "Intro to SOM by Teuvo Kohonen". SOM Toolbox, [Online]. Available: http://www.cis.hut.fi/projects/somtoolbox/theory/somalgorithm.shtml. Retrieved 2006-06-18

[33] G. Chicco, R. Napoli, F. Piglione, M. Scutariu, P. Postolache, and C.Toader, "Load pattern-based classification of electricity customers," *IEEE Trans. Power Syst.*, vol. 19, no. 2, pp. 1232–1239, May 2004.

[34] K. W. Hedman, R. P. O'Neill, and S. S. Oren, "Analyzing valid inequalities of the generation unit commitment problem," *in Proc. IEEE Power Systems Conference & Exposition*, 2009.

[35] C. Loutan and D. Hawkins, "Integration of renewable resources: transmission and operating issues and recommendations for integrating renewable resources on the California," CAISO Report November 2007.

[36] ISO-controlled grid," CAISO, Tech. Rep., Nov. 2007. [Online]. Available: http://www.caiso.com/1ca5/1ca5a7a026270.pdf

[37] GE Energy "The effects of integrating wind power on transmission system planning, reliability, and operations: report on phase 2," Prepared for The New York State

Energy Research and Development Authority, Mar. 2005. [Online]. Available: http://docs.wind-watch.org/NYSERDA-wind_integration_report.pdf

[38] Northern Arizona University, "Arizona Public Service wind integration cost impact study," Sept. 2007. [Online]. Available: http://www.uwig.org/aps_wind_integration_study_final9-07.pdf

[39] R. Doherty and M. O'Malley, "A new approach to quantify reserve demand in systems with significant installed wind capacity," *IEEE Trans. Power Syst.*, vol. 20, no. 2, pp. 587–595, May 2005.

[40] M. Ortega-Vazquez and D. Kirschen, "Estimating the spinning reserve requirements in systems with significant wind power generation penetration," *IEEE Trans. Power Syst.*, vol. 24, no. 1, pp. 114–123, Feb. 2009.

[41] M. A. Matos and R. J. Bessa, "Setting the operating reserve using probabilistic wind power forecasts," *IEEE Trans. Power Syst.*, vol. 26, no. 2, pp. 594-603, May 2011.

[42] J. Kiviluoma, P. Meibom, A. Tuohy, N. Troy, M. Milligan, B. Lange, M. Gibescu, and M. O'Malley, "Short-term energy balancing with increasing levels of wind energy," *IEEE Trans. Sustainable Energy*, vol. 3, no. 4, pp. 769-776 Oct 2012.

[43] H. Holttinen, M. Milligan, E. Ela, N. Menemenlis, J. Dobschinski, B. Rawn, R. J. Bessa, D. Flynn, and E. Gomez Lazaro, "Methodologies to determine operating reserves due to increased wind power," *IEEE Trans. Power Syst.*, vol. 3, no. 4, pp. 713–723, Oct. 2012.

[44] National Renewable Energy Laboratory, "Western wind and solar integration study," NREL, Tech. Rep., May 2010. [Online]. Available: http://www.nrel.gov/docs/fy10osti/47434.pdf

[45] K. W. Hedman, M. C. Ferris, R. P. O'Neill, E. B. Fisher, and S. S. Oren, "Co-optimization of generation unit commitment and transmission switching with N-1 reliability," *IEEE Trans. Power Syst.*, vol. 25, no. 2, pp. 1052-1063, May 2010.

[46] CAISO, "Intra-zonal congestion," CAISO Dept. of Market Monitoring, Tech. Report., Apr. 2007. [Online]. Available: http://www.caiso.com/1bb7/1bb77b241b920.pdf

[47] ERCOT, "Report on existing and potential electric system constraints and needs," ERCOT System Planning and Transmission Services, Tech. Report, Dec. 2007. [Online]. Available: http://www.ercot.com/content/news/presentations/2013/2012%20Constraints%20and%20Needs%20Report.pdf

[48] W. Yuan-Kang and H. Jing-Shan, "A literature review of wind forecasting technology in the world," in *Proc. IEEE Power Tech*, pp. 504 -509, Jul. 2007.

[49] University of Washington, "Power systems test case archive," Dept. Elect. Eng., 1999. [Online]. Available: http://www.ee.washington.edu/research/pstca/rts/pgtcarts.htm

[50] CAISO, "Price Inconsistency Market Enhancements – Revised Straw Proposal," 2012. [Online]. Available: http://www.caiso.com/Documents/RevisedStrawProposal-PriceInconsistencyMarketEnhancements.pdf

[51] CAISO, "Parameter Tuning for uneconomic adjustments in the MRTU Market Optimizations," Department of Market and Product Development, May 6, 2008. [Online]. Available: http://www.caiso.com/Documents/IssuePaper-ParameterTuning_UneconomicAdjustmentsinMRTUMarketOptimization06-May-2008.pdf

[52] SPP, "Market Protocols – SPP Integrated Market place Revision 12.0," Market Design, Nov. 5, 2012. [Online]. Available: http://www.spp.org/publications/Integrated%20Marketplace%20Protocols%2012%200.pdf

[53] ERCOT, "ERCOT Business Practice – Setting Shadow Price Caps and Power Balance Penalties in Security Constrained Economic Dispatch", Nov. 16, 2010. [Online]. Available: http://www.ercot.com/content/meetings/natf/keydocs/2010/0930/09_ercot_busPract_shadow_price_caps_power_balance_penal.doc

[54] S. S. Soman, H. Zareipour, O. Malik, and P. Mandal, "A review of wind power and wind speed forecasting methods with different time horizons," in *Proc. North American Power Symp.*, 2010.

[55] G. M. Masters, Renewable and Efficient Electric Power Systems, New York: Wiley Interscience, 2004.

[56] K. Dietrich, J. M. Latorre, L. Olmos, A. Ramos, and I. J. P ́erez-Arriaga, "Stochastic unit commitment considering uncertain wind production in an isolated system," in *4th Conf. energy economics and technology*," Dresden, Germany, 2009.

[57] H. Bludzuweit, J. A. Dom ́nguez-Navarro, and A. Llombart, "Statistical analysis of wind power forecast error," *IEEE Trans. Power Syst.*, vol. 23, pp. 983-991, Aug. 2008.

[58] F. Bouffard and F. D. Galiana, "Stochastic security for operations planning with significant power generation," *IEEE Trans. Power Syst.*, vol. 23, no. 2, pp. 306–316, May 2008.

[59] U. Focken, M. Lange, K. Monnich, H. P. Waldl, H. G. Beyer, and A. Luig, "Short-term prediction of the aggregated power of wind farms – a statistical analysis of the

reduction of the prediction error by spatial smoothing effects," *J. Wind Eng. Ind. Aerodynam.*, vol. 90, no. 3, pp. 231-246, Mar. 2002.

[60] CAISO, "Integration of renewable resources: technical appendices for California ISO renewable integration studies – version 1," Oct. 2010. [Online]. Available: http://www.caiso.com/282d/282d85c9391b0.pdf

[61] J. Dupacová, N. Gröwe-Kuska, and W. Römisch, "Scenario reduction in stochastic programming: An approach using probability metrics," *Math. Program, series A*, vol. 3, pp. 493–511, 2003.

[62] N. Gröwe-Kuska, H. Heitsch, and W. Römisch, "Scenario reduction and scenario tree construction for power management problems," in *Proc. IEEEE Power Tech Conf.*, Bologna, Italy, vol. 3, pp. 23-26, Jun. 2003.

[63] MISO, "2011-01-28 Docket No. ER11-2794-000," Jan., 2011. [Online]. Available: https://www.midwestiso.org/Library/Repository/Tariff/FERC%20Filings/2011-01-28%20Docket%20No.%20ER11-2794-000.pdf

[64] S. M. Ryan, R. J.-B. Wets, D. L. Woodruff, C. Silva-Monroy, and J.- P. Watson, "Toward scalable, parallel progressive hedging for stochastic unit commitment," *IEEE PES General Meeting*, pp. 1-5, Jul. 2013.

[65] J.-P. Watson, "Stochastic unit commitment: scalable computation and experimental results," Presentation at *FERC Increasing Efficiency through Improved Software Conference*, Jun. 2013. [Online]. Available: http://www.ferc.gov/CalendarFiles/20130710155720-M4_Watson.pdf

[66] J.-P. Watson and D. L. Woodruff, "Progressive hedging innovations for a class of stochastic mixed-integer resource allocation problems," *Comp. Manage. Sci.*, vol. 8, pp. 355-370, Nov. 2011.

[67] Y. Chen, P. Gribik, and J. Gardner, "Incorporating post zonal reserve deployment transmission constraints into energy and ancillary services co-optimization," *IEEE Trans. Power Syst.*, vol. 29, no. 2, pp. 537-549, Mar. 2014.

[68] J. D. Lyon, K. W. Hedman, and M. Zhang, "Reserve requirements to efficiently manage intra-zonal congestion," *IEEE Trans. Power Syst.*, vol. 29, no. 1, pp. 251–258, Jan. 2014.

[69] J. D. Lyon, M. Zhang, and K. W. Hedman, "Locational reserve disqualification for distinct scenarios," *IEEE Trans. Power Syst.*, vol. 30, no. 1, pp. 357-364, Jan. 2015.

[70] M. Shields, M. Boughner, R. Jones, and M. Tackett, "Market subcommittee minutes/asm market design," MISO, printed copy, Aug. 2007.

[71] MISO, "MISO energy and operating reserve markets, business practices manual," BPM-002-r11, Jan. 2012. [Online]. Available: https://www.misoenergy.org/Library/BusinessPracticesManuals/Pages/BusinessPracticesManuals.aspx

[72] Y. M. Al-Abdullah, M. Abdi-Khorsand, and K. W. Hedman, "The role of out-of-market corrections in day-ahead scheduling," *IEEE Trans. Power Syst.*, accepted for publication.

[73] FERC, "Docket no. ER11-2794-000 – order conditionally accepting tariff revisions – MISO," Jun. 2011. [Online]. Available: http://www.ferc.gov/EventCalendar/Files/20110628160939-ER11-2794-000.pdf

[74] ISO-NE, SOP-RTMKTS.0060.0020, "Monitor system security v57," Feb. 2013. [Online]. Available: http://www.iso-ne.com/rules_proceds/operating/sysop/rt_mkts/sop_rtmkts_0060_0020.pdf

[75] ISO-NE, SOP-RTMKTS.0120.0030, "Implement transmission remedial action v20," Jun. 2012. [Online]. Available: http://www.iso-ne.com/rules_proceds/operating/sysop/rt_mkts/sop_rtmkts_0120_0030.pdf

[76] J. D. Lyon, Fengyu Wang, K. W. Hedman, and M. Zhang, "Market implications and pricing of dynamic reserve policies for systems with renewables," *IEEE Trans. Power Syst.*, accepted for publication.

[77] PJM, "2013 PJM reserve requirement study," [Online]. Available: http://www.pjm.com/~/media/committees-groups/committees/mrc/20131024/20131024-item-04-irm-study.ashx

[78] R. P. O'Neill, P. M. Sotkiewicz, B. F. Hobbs, M. H. Rothkopf, and W. R. Stewart, "Efficient market-clearing prices in markets with nonconvexities," *Eur. Journal of Oper. Res.*, vol. 164, pp. 269–285, Dec. 2003.

[79] C. Grigg, P. Wong, P. Albrecht, R. Allan, M. Bhavaraju, R. Billinton, Q. Chen, C. Fong, S. Haddad, S. Kuruganty, W. Li, R. Mukerji, D. Patton, N. Rau, D. Reppen, A. Schneider, M. Shahidehpour, C. Singh, "The IEEE reliability test system – 1996," *IEEE Trans. Power Syst.*, vol. 14, no. 3, pp. 1010–1020, Aug. 1999.

[80] F. Bouffard, F. D. Galiana, and A. J. Conejo, "Market-clearing with stochastic security—Part II: Case studies," *IEEE Trans. Power Syst.*, vol. 20, no. 4, pp. 1818–1826, Nov. 2005.

[81] M. Lei, L. Shiyan, J. Chuanwen, L. Hongling, and Z. Yan, "A review of the forecasting of wind speed and generated power," *Renewable and Sustain. Energy Reviews*, vol. 13, pp. 915–920, Feb. 2009.

[82] J. M. Morales, R. Minguez, and A. J. Conejo, "A methodology to generate statistically dependent wind speed scenarios," *Applied Energy*, vol. 87, pp. 843–855, Sep. 2009.

[83] NREL, "Western wind resource dataset," Jan. 2014. [Online]. Available: wind.nrel.gov/Web_nrel/

[84] B.-M. Hodge, A. Florita, K. Orwig, D. Lew, and M. Milligan, "A comparison of wind power and load forecasting error distributions," in World Renewable Energy Forum, May 2012. [Online]. Available: http://www.nrel.gov/docs/fy12osti/54384.pdf

[85] R. E. Kurlinski, "Real-time revenue imbalance in CAISO markets," CAISO Dept. of Mkt. Mon., Tech. Rep., Apr. 2013. [Online]. Available: http://www.caiso.com/Documents/DiscussionPaper-Real-timeRevenueImbalance_CaliforniaISO_Markets.pdf

[86] R. Sioshansi, R. O'Neill, and S. S. Oren, "Economic consequences of alternative solution methods for centralized unit commitment in day-ahead electricity markets," *IEEE Trans. Power Syst.*, vol. 23, no. 2, pp. 344–352, May 2008.

[87] C. Vournas and T. Bakirtzis, "Oral discussions on session: markets – part II," *IREP Symposium – Bulk Power Syst. Dynamics and Control –IX (IREP)*, Rethymnon, Greece, Aug. 25-28, 2013.

[88] X. Ma , H. Song , M. Hong , J. Wan , Y. Chen and E. Zak "The security-constrained commitment and dispatch for midwest ISO day-ahead co-optimized energy and ancillary service market", in *Proc. IEEE PES General Meeting*, 2009

[89] MISO, "Overview of MISO day-ahead market," [Online]. Available: http://www.atcllc.com/oasis/Customer_Notices/NCM_MISO_DayAhead111507.pdf

[90] F. C. Schweppe, M. C. Caramanis, R. D. Tabors, and R. E. Bohn, *Spot Pricing of Electricity*. Norwell, MA, USA: Kluwer,1988.

[91] N. Navid, T. Ramey, D. Chatterjee, "Operational and Practical Considerations for Stochastic Unit Commitment Solutions", *Technical Conference On Increasing Real-Time And Day-Ahead Market Efficiency Through Improved Software*, June 23-25, 2014, Washington, DC.

[92] Q. Wang, X. Wang, K. Cheung, Y. Guan, F. Bresler, "A two-stage robust optimization for PJM look-ahead unit commitment," *PowerTech, 2013 IEEE Grenoble* , vol. 1, no. 6, pp.16-20 June 2013.

[93] Y. Chen, V. Ganugula, J. Williams, J. Wan, and Y. Xiao, "Resource transition model under MISO MIP based look ahead commitment," *IEEE Power and Energy Society General Meeting*, July 2012.

[94] M. Kutner, C. Nachtsheim, J. Neter, W. Li, Applied Linear Statistical Models. New York: McGraw-Hill, 2005.

[95] SANDIA Report, "Project report: a survey of operating reserve markets in U.S. ISO/RTO-managed electric energy regions", Sep. 2012. [Online]. Available: http://prod.sandia.gov/techlib/access-control.cgi/2012/121000.pdf

[96] J. Wang, M. Shahidehpour, and Z. Li, "Contingency-constrained reserve requirements in joint energy and ancillary services auction," *IEEE Trans. Power Syst.*, vol. 24, no. 3, pp. 1457-1468, Aug. 2009.

[97] MISO, "MISO Resources Not Qualified for Reserves in Real Time Market", Oct., 2013. [Online]. Available: www.misoenergy.org/Library/Repository/Meeting%20Material/Stakeholdr/MSC/2013/20131001/20131001%20MSC%20Item%2005c%20MISO%20Resources%20Not%20Qualified%20for%20Reserves%20in%20RT%20Market.pdf

[98] X. Ma, Y. Chen, and J. Wan, "The security-constrained economic dispatch for Midwest ISO's real-time co-optimized energy and ancillary service market," in Proc. *IEEE PES General Meeting*, 2009.

APPENDIX A

UNIT COMMITMENT FORMULATION WITH RESERVE ZONES

Minimize

$\sum_{t\in T}\sum_{g\in G}[C_g p_{gt} + C_g^{SU} su_{gt} + C_g^{SD} sd_{gt} + C_g^{NL} u_{gt}]$ (Objective)

Subject to:

$0 \le su_{gt} \le 1, t \in T, g \in G$ (Start-up Variable)

$0 \le sd_{gt} \le 1, t \in T, g \in G$ (Shut-down Variable)

$su_{gt} - sd_{gt} = u_{gt} - u_{g,t-1}, t \in T, g \in G$ (Start-up and Shut-down)

$\sum_{t'=t-UT_g+1}^{t} su_{g,t'} \le u_{gt}\ , t \in \left(UT_g\ , .., T\right), g \in G$ (Minimum-up Time)

$\sum_{t'=t-DT_g+1}^{t} sd_{g,t'} \le 1 - u_{gt}\ , t \in \left(DT_g\ , .., T\right), g \in G$ (Minimum-down Time)

$\sum_{k\in K^+(n)} f_{kt} - \sum_{k\in K^-(n)} f_{kt} + \sum_{g\in G(n)} p_{gt} = D_{nt}, t \in T, n \in N$ (Node Balance)

$f_{kt} = B_k(\theta_{nt} - \theta_{mt}), t \in T, k = (n,m) \in K$ (Power Angles)

$-F_k^{max} \le f_{kt} \le F_k^{max}, t \in T, k \in K$ (Thermal Limits)

$u_{gt}P_g^{min} \le p_{gt} \le u_{gt}P_g^{max}, t \in T, g \in G$ (Generation Output Limits)

$p_{gt} - p_{g,t-1} \le R_g^{HR}, t \in T, g \in G$ (Hourly Ramp-up Rate)

$p_{g,t-1} - p_{gt} \le R_g^{HR}, t \in T, g \in G$ (Hourly Ramp-down Rate)

$r_{gt}^{SPIN} \le R_g^{10} u_{gt}, t \in T, g \in G$ (Ten Minutes Reserve Ramp)

$0 \leq r_{gt}^{SPIN} \leq u_{gt} P_g^{max} - p_{gt}$ (Reserve Variable)

$\sum_{g \in G}(r_{gt}^{SPIN}) \geq R_{MKT,t}^{SPIN}$ (Reserve Requirements)

$u_{gt} \in \{0,1\}, t \in T, g \in G$ (Commitment Variable)

APPENDIX B

OFFLINE CONTINGENCY ANALYSIS

Objective:

Minimize

$\sum_{c=1}^{M}(\rho_c \times ls_{nct} \times VOLL)$ (Objective)

Subject to:

$\sum_{k(n,;)} f_{kct} - \sum_{k(;,n)} f_{kct} + \sum p_{g(n),c,t} = D_{nt} - LS_{nct}$ (Post-contingency Node balance)

$-(u_{gt}p_g^{min} - p_{gt}) \leq r_{gct} \leq u_{gt}p_g^{max} - p_{gt}$ (Generation Output Limits)

$-R_g^{10}u_{gt} \leq r_{gct} \leq R_g^{10}u_{gt}$ (Ten Minutes Ramp Rate)

$p_{gct} = N_{g,c}p_{gt} + N_{g,c}s_{gct}$ (Output of Generator g during Contingency c)

$P_{kct} = B_k(\theta_{nct} - \theta_{mct})$ (Bus Angles during Contingency c)

$-\bar{F}_k^{max} \leq f_{kct} \leq \bar{F}_k^{max}$ (Thermal Limits)

$ls_{nct} \geq 0$ (Involuntary Load Shedding at Bus n during Period t)

APPENDIX C

TEST CASES INFORMATION

(1) RTS-96 System

The RTS-96 system [80]-[81] is duplicating the Single RTS system three times.

The detailed system information are listed below.

Table C.1 Unit Type and Cost for RTS-96 System

Unit Type	Capacity	Num. of Units	Start-up Cost ($)	Fuel Cost ($/MWh)	No-load Cost($/hour)
Oil/Steam	12	15	571.2	94.74	72.68
Oil/CT	20	12	75.85	163.02	1138.68
Hydro	50	18	0	0	0
Coal/Steam	76	12	1060.88	19.64	130.63
Oil/Steam	100	9	4754.4	75.64	839.45
Coal/Steam	155	12	1696.34	15.46	252.67
Oil/Steam	197	9	6510	74.75	1159.93
Coal/Steam	350	3	7953.04	15.89	358.23
Nuclear	400	6	2400	5.46	215.08

Table C.2 Generation Reliability Parameter for RTS-96 System

Unit Type	FOR	MTTF	MTTR	λ
Oil/Steam	0.02	2940	60	0.00034
Oil/CT	0.1	450	50	0.002222
Hydro	0.01	1980	20	0.000505
Coal/Steam	0.02	1960	40	0.00051
Oil/Steam	0.04	1200	50	0.000833
Coal/Steam	0.04	960	40	0.001042
Oil/Steam	0.05	950	50	0.001053
Coal/Steam	0.08	1150	100	0.00087
Nuclear	0.12	1100	150	0.000909

Table C.3 Detailed System Information for RTS96 System

Id	Bus	Min-up Time	Min-dn Time	Maximum Output	Minimum Output
1	1	1	1	20	15.8
2	1	1	1	20	15.8
3	1	8	4	76	15.2
4	1	8	4	76	15.2
5	2	1	1	20	15.8
6	2	1	1	20	15.8
7	2	8	4	76	15.2
8	2	8	4	76	15.2

Id	Bus	Min-up Time	Min-dn Time	Maximum Output	Minimum Output
9	7	8	8	100	25
10	7	8	8	100	25
11	7	8	8	100	25
12	13	12	10	197	68.95
13	13	12	10	197	68.95
14	13	12	10	197	68.95
15	14	1	1	0	0
16	15	4	2	12	2.4
17	15	4	2	12	2.4
18	15	4	2	12	2.4
19	15	4	2	12	2.4
20	15	4	2	12	2.4
21	15	8	8	155	54.25
22	16	8	8	155	54.25
23	18	48	48	400	100
24	21	48	48	400	100
25	22	1	1	50	0
26	22	1	1	50	0
27	22	1	1	50	0
28	22	1	1	50	0
29	22	1	1	50	0
30	22	1	1	50	0
31	23	8	8	155	54.25
32	23	8	8	155	54.25
33	23	24	48	350	140
34	25	1	1	20	15.8
35	25	1	1	20	15.8
36	25	8	4	76	15.2
37	25	8	4	76	15.2
38	26	1	1	20	15.8
39	26	1	1	20	15.8
40	26	8	4	76	15.2
41	26	8	4	76	15.2
42	31	8	8	100	25
43	31	8	8	100	25
44	31	8	8	100	25
45	37	12	10	197	68.95
46	37	12	10	197	68.95
47	37	12	10	197	68.95
48	38	1	1	0	0
49	39	4	2	12	2.4
50	39	4	2	12	2.4
51	39	4	2	12	2.4

Id	Bus	Min-up Time	Min-dn Time	Maximum Output	Minimum Output
52	39	4	2	12	2.4
53	39	4	2	12	2.4
54	39	8	8	155	54.25
55	40	8	8	155	54.25
56	42	48	48	400	100
57	45	48	48	400	100
58	46	1	1	50	0
59	46	1	1	50	0
60	46	1	1	50	0
61	46	1	1	50	0
62	46	1	1	50	0
63	46	1	1	50	0
64	47	8	8	155	54.25
65	47	8	8	155	54.25
66	47	24	48	350	140
67	49	1	1	20	15.8
68	49	1	1	20	15.8
69	49	8	4	76	15.2
70	49	8	4	76	15.2
71	50	1	1	20	15.8
72	50	1	1	20	15.8
73	50	8	4	76	15.2
74	50	8	4	76	15.2
75	55	8	8	100	25
76	55	8	8	100	25
77	55	8	8	100	25
78	61	12	10	197	68.95
79	61	12	10	197	68.95
80	61	12	10	197	68.95
81	62	1	1	0	0
82	63	4	2	12	2.4
83	63	4	2	12	2.4
84	63	4	2	12	2.4
85	63	4	2	12	2.4
86	63	4	2	12	2.4
87	63	8	8	155	54.25
88	64	8	8	155	54.25
89	66	48	48	400	100
90	69	48	48	400	100
91	70	1	1	50	0
92	70	1	1	50	0
93	70	1	1	50	0
94	70	1	1	50	0

Id	Bus	Min-up Time	Min-dn Time	Maximum Output	Minimum Output
95	70	1	1	50	0
96	70	1	1	50	0
97	71	8	8	155	54.25
98	71	8	8	155	54.25
99	71	24	48	350	140

(2) Modified IEEE 118-bus System

Table C.4 Unit Type and Cost for Modified IEEE 118-bus System

Unit Type	Capacity	Num. of Units	Start-up Cost ($)	Fuel Cost ($/MWh)	No-load Cost($/hour)
Oil/Steam	12	10	571.2	94.74	72.68
Oil/CT	20	4	75.85	163.02	1138.68
Hydro	50	10	0	0	0
Coal/Steam	76	6	1060.88	19.64	130.63
Oil/Steam	100	5	4754.4	75.64	839.45
Coal/Steam	155	7	1696.34	15.46	252.67
Oil/Steam	197	5	6510	74.75	1159.93
Coal/Steam	350	2	7953.04	15.89	358.23
Nuclear	400	3	2400	5.46	215.08

Table C.5 Generation Reliability Parameter for Modified IEEE 118-bus System

Unit Type	FOR	MTTF	MTTR	λ
Oil/Steam	0.02	2940	60	0.00034
Oil/CT	0.1	450	50	0.002222
Hydro	0.01	1980	20	0.000505
Coal/Steam	0.02	1960	40	0.00051
Oil/Steam	0.04	1200	50	0.000833
Coal/Steam	0.04	960	40	0.001042
Oil/Steam	0.05	950	50	0.001053
Coal/Steam	0.08	1150	100	0.00087
Nuclear	0.12	1100	150	0.000909

Table C.6 Detailed System Information for Modified IEEE 118-bus System

Id	Bus	Min-up Time	Min-dn Time	Maximum Output	Minimum Output
1	10	12	10	197	68.95
2	10	24	48	350	140
3	12	12	10	197	68.95
4	25	8	8	155	54.25

Id	Bus	Min-up Time	Min-dn Time	Maximum Output	Minimum Output
5	25	8	8	155	54.25
6	26	4	2	12	2.4
7	26	24	1	400	100
8	31	8	8	100	25
9	46	4	2	12	2.4
10	46	8	8	100	25
11	49	8	8	155	54.25
12	49	8	8	155	54.25
13	40	1	1	0	0
14	54	8	8	155	54.25
15	55	1	1	0	0
16	59	1	1	0	0
17	59	8	8	100	25
18	59	8	8	155	54.25
19	61	4	2	12	2.4
20	61	4	2	12	2.4
21	61	1	1	50	0
22	61	1	1	50	0
23	65	1	1	50	0
24	65	1	1	50	0
25	65	1	1	50	0
26	65	1	1	50	0
27	65	1	1	50	0
28	65	1	1	50	0
29	65	1	1	50	0
30	65	1	1	50	0
31	65	1	1	50	0
32	65	1	1	50	0
33	66	4	2	12	2.4
34	66	8	4	76	15.2
35	66	24	1	400	100
36	69	12	10	197	68.95
37	69	12	10	197	68.95
38	69	24	1	400	100
39	80	8	4	76	15.2
40	80	8	4	76	15.2
41	80	8	4	76	15.2
42	80	8	4	76	15.2
43	80	8	4	76	15.2
44	80	12	10	197	68.95
45	87	4	2	12	2.4
46	87	4	2	12	2.4
47	87	4	2	12	2.4

Id	Bus	Min-up Time	Min-dn Time	Maximum Output	Minimum Output
48	87	4	2	12	2.4
49	87	1	1	20	15.8
50	87	1	1	20	15.8
51	87	1	1	20	15.8
52	92	8	8	100	25
53	100	24	48	350	140
54	103	8	8	155	54.25
55	111	4	2	12	2.4
56	111	1	1	20	15.8
57	111	8	8	100	25

APPENDIX D

OUTAGE RATE CACULATION

Table D.1 Outage Rates of Generators and Transmission Lines (For modified IEEE-118 System)

Authors	Title	Time period Basis	Generator Outage Rate	Transmission Line Outage Rate	Outage Dependence Considered
A Papavasiliou and S. S. Oren	Multi-Area Stochastic Unit Commitment for High Wind Penetration in a Transmission Constrained Network	Hourly	1%	0.1%	No
M. V. F. Pereira and N. J. Balu	Composite Generation/Transmission Reliability Evaluation	Hourly	On the order of 1%	On the order of 0.01%	Yes
F. Bouffard et al.	Market-Clearing With Stochastic security-Par 2:Case Studies	Hourly	1/*MTTF*	N/A	No
R. Billinton and R. N. Allan	Reliablity Evaluation of Power System 2nd edition	Yearly	Forced outage Rate	Forced outage Rate	No
Proposed model in this thesis	N/A	hourly	1/*MTTF*	Lam-p/8760^2	No

Where *MTTF* is mean time to failure for each generator and Lam-*p* is the permanent outage rate (outages/year) for each transmission line.

Comparisons of calculating outage rate in different literatures are listed in the Table D.1.

The forced outage rate (FOR) is defined as below,

$$\text{Unavailability (FOR)} = \frac{r}{m+r} = \frac{\text{Expectd Duration of Unavaiability per Year}}{\text{One Year}} \qquad \text{(D—1)}$$

Where *r* is the mean time to repair (MTTR), *m* is the mean time to failure (*MTTF*)

Expected failure rate λ is defined in (D—2)

$$\lambda = \frac{1}{MTTF} = \text{ Expected Number of Outages per Hour} \qquad \text{(D—2)}$$

One year=8760 Hours (Except the leap year), then, 8760×λ= Expected Number of Outages per Year. The proposed model in this thesis assume that all the outages are independent, and the probability of losing one unit at any particular hour will be equal to expected failure rate.

Table D.2 Generator Reliability Parameter

Unit Type	Capacity	FOR	MTTF	MTTR	Num. of Units	λ
Oil/Steam	12	0.02	2940	60	10	0.00034
Oil/CT	20	0.1	450	50	4	0.002222
Hydro	50	0.01	1980	20	10	0.000505
Coal/Steam	76	0.02	1960	40	6	0.00051
Oil/Steam	100	0.04	1200	50	5	0.000833
Coal/Steam	155	0.04	960	40	7	0.001042
Oil/Steam	197	0.05	950	50	5	0.001053
Coal/Steam	350	0.08	1150	100	2	0.00087
Nuclear	400	0.12	1100	150	3	0.000909

In Table D.2, the reliability parameters of different unit types and number of each unit type are given

Since there is no transmission reliability parameter for the IEEE 118 test system, the transmission line information from the Reliability Test System (RTS) 1996 is used to the outage rate of transmission lines in RTS96. The average value of the outage rates of RTS transmission lines is 3.91×10^{-5} and it is assumed that the probability of any single transmission line contingency in IEEE 118-bus system is 3.91×10^{-5}.

The probability that no contingency happens

$$P(0) = \prod_{i=1}^{9}(1-\lambda^i)^{NU^i} \times (1-\lambda^T)^{NU^T} = 0.9135 \qquad \text{(D—3)}$$

Where NU^i is the number of type *i* generators, and λ^i is the 1/MTTF

λ^T is the probability of single transsminon line outage, assume that all the transmission lines outage probablities are the same. NU^T is the number of non-radial transmission lines. For type *i* generator, the probability of single type *i* generator failure is

$$P(i) = P(0) \times \lambda^i/(1-\lambda^i) \quad \text{(D—4)}$$

The results of any single contingency probability is shown as below

Table D.3 Single Generator Contingency Probability

Unit Type	P(*i*)
Oil/Steam	0.00031
Oil/CT	0.00203
Hydro	0.00046
Coal/Steam	0.00047
Oil/Steam	0.00076
Coal/Steam	0.00095
Oil/Steam	0.00096
Coal/Steam	0.0008
Nuclear	0.00083

The probabilities of a single transmission line outage is: P(*Transmission*) =3.72×10^{-5}

For the N-1 reliability, it is assumed that only one contingency can happen at one time, then there are only two cases possible, normal operating condition and single generator or transmission line contingency. With this assumption, the probability of summation of normal operating state and any single contingency happened should be scaled to one. Then, the summation of the probability of normal operating state and any single contingency happened is

$$\mathrm{P}(0) + \sum_{i=1}^{9} P(i) \times NU_i + P(\mathrm{T}) \times NU^T = 0.9581 \quad \text{(D—5)}$$

Therefore, by scaling the result from (D—5) it to one, and the final probabilities of normal operating state $P(0)_{scale}$, each generator contingency $P(i)_{scale}$, and each transmission line $P(\text{Transmission})_{scale}$ are shown below.

$$P(0)_{scale} = \frac{P(0)}{0.9581} = 0.95345 \quad \text{(D—6)}$$

$$P(i)_{scale} = \frac{P(i)}{0.9581} \quad \text{(D—7)}$$

$$P(\text{Transmission})_{scale} = 3.7282 \times 10^{-5} \quad \text{(D—9)}$$

The details of each scalded generator single contingency probability are shown in Table D.4.

Table D.4 Scaled Generator Single Contingency Probability

Unit Type	$P(i)_{scale}$
Oil/Steam	0.00032
Oil/CT	0.00212
Hydro	0.00048
Coal/Steam	0.00049
Oil/Steam	0.00079
Coal/Steam	0.00099
Oil/Steam	0.00101
Coal/Steam	0.00083
Nuclear	0.00087